BED AGGRADATION EXPERIMENTS IN A SMALL RECIRCULATING FLUME EMPLOYING 40 MICRON SILT WITH SPECIAL REFERENCE TO TURBIDITY CURRENT DEPOSITIONAL STRUCTURES

by

Hugh H. Sprunt, Jr.

Submitted in Partial Fulfillment
of the Requirements for the
Degree of
Master of Science
at the
Massachusetts Institute of Technology

May 1972

Signature of Author . . . .
Department of Earth and Planetary Sciences, May 12, 1972

Certified by . . . . .
, Thesis Supervisor

Accepted by . . . . . .
Chairman, Departmental Committee
on Graduate Students

BED AGGRADATION EXPERIMENTS IN A SMALL RECIRCULATING FLUME EMPLOYING 40 MICRON SILT WITH SPECIAL REFERENCE TO TURBIDITY CURRENT DEPOSITIONAL STRUCTURES

by

Hugh H. Sprunt, Jr.

Submitted in partial fulfillment of the requirements for the degree of Master of Science at the Massachusetts Institute of Technology, May, 1972

ABSTRACT

A series of bed aggradation experiments were carried out in a small flume that recirculated both water and sediment. Of two silt fractions separated from mid-continental loess, the coarser was found to be more suitable. Dry sediment was fed into the tailbox of the flume at various aggradation rates and flow velocities, and the structures formed are described.

These structures are compared to the structures found in a series of field samples of distal turbidites gathered from the Silurian of northern Maine.

The experiments indicate that the lower the ripple-range velocity, the more distinct the internal structures are. A more rapid aggradation rate at a given velocity produces less distinct structures. In the ripple-range reducing the mean flow velocity increases the spacing of the equilibrium crests. An increase in the aggradation rate also produces an increase in ripple spacing. The height of the ripples does not change significantly with a change in the mean flow velocity. The influence of aggradation rate on ripple height is unclear; variable results were obtained.

Increasing the aggradation rate increases the size and general dominance of trough structures formed in the ripple-range of velocities. Decreasing the mean flow velocity at a given aggradation rate tends to eliminate the trough structures and favor the formation of planar structures whose linear projections on the flume sidewall are called "basal traces" in this paper.

The Bouma Model is used to interpret the laboratory results and the field samples. Bouma B, C, and D Intervals were produced in the laboratory. The limited similarity between the laboratory results and the field samples is described.

The turbidity current hypothesis and relevant experimental work is described, and the difficulties encountered in the simulation of turbidity currents in the laboratory are commented upon. Recommendations for future work are also included.

Thesis Supervisor: Dr. John B. Southard
Title: Assistant Professor of Geology

TABLE OF CONTENTS

List of Tables

List of Figures

List of Variables and Constants Employed:

Symbol	Units	Description
T	degrees C	Temperature of the flow
ΔH	inches	Manometer Height Differential
Q	cc/sec	Flow Rate in Flume
Q_S	cc/sec	Flow Rate of Dry, Unpacked Sed.
Q_B	cc/sec	Pore Water Flow Rate
$\bar{D}$	mm/hr	Rate of Bed Aggradation
$\bar{Y}$	cm	Average Flow Depth
$\bar{C}$	gm/cc	Average Concentration, sed. in H_2O
$\bar{V}_S$	cm/sec	Average Surface Velocity
$\bar{V}$	cm/sec	Average Velocity (two ways)
$\bar{V}_P$	cm/sec	Reduction Profile, Planned Vel.
$\bar{V}_A$	cm/sec	Reduction Profile, Actual Vel.
Time	hr-min-sec	Time, relative to a given point
w	cm	A Constant = Flume Width = 17.4 cm
L	cm	A Const. = Bed Length = 550 cm

Equations Employed:

$\bar{Y} = Q/\bar{V}w$, $\bar{V}$ derived from $\bar{V} = 0.85\bar{V}_S$

$\bar{V} = Q/w\bar{Y}$, $\bar{Y}$ derived from bed and water surface profiles

$\bar{D} = 0.82Q_S/wL$, 0.82 from packing co-efficient of sediment

$Q = 0.06\sqrt{\Delta H''}$ cu. ft./sec $= 1700\sqrt{\Delta H''}$ cc/sec

INTRODUCTION

In this paper I describe and then discuss the results of a series of experiments in bed aggradation specifically related to an attempt to simulate the bed aggradation structures common in distal turbidites. A comparison is made between the structures found in some Silurian turbidity deposits from northern Maine and the experimental results. The difficulties involved in simulating a turbidity current in the laboratory are described and sections on the history of field and laboratory investigations are also included. At the end of the paper there are sections on experimental error, conclusions, and recommendations for future work.

The Turbidity Current Hypothesis

Engineers have long known of density currents flowing along the bottoms of dam reservoirs carrying river sediment for miles; typically they are arrested only by the dam itself. Oceanographers, especially since World War II, have begun to map cold and warm currents in the ocean, often at depth, that preserve their identities for hundreds of miles. Indeed, one of the most recent objectives, combining the skills of the oceanographer and the civil engineer, has been the analytical and experimental study of saline wedges associated with tidal bores in river-estuary complexes and the thermal currents in rivers produced by outflow of open-circuit cooling water from commercial nuclear power plants. All of these phenomena, turbidity currents included, may be

termed density currents. The driving force is supplied by the gravitational field acting upon the mass differential of the flow with respect to the ambient fluid; the distinguishing characteristic is the cause of the density excess, be it a difference in temperature or salinity or the presence of sediment suspended by the turbulence and change in gravitational potential of the flow.

The turbidity current is unique due to the potential for inter-particle collision effects and the fact that at some point in its lifespan the turbidity current must deposit the particulate source of its density excess: the suspended sediment. The bed load may also be considered a part of the current, but recent experimental work (Kuenen, 1970) points to a lack of a traction carpet.

The suspended sediment 'rains out' of the flow as the turbulent energy and the velocity decrease (due to a lessening of the bottom gradient as the current moves down the continental slope, onto the continental rise, and finally out onto the abyssal plain) leaving a geologic record of the hydraulic conditions of the depositing flow. To the extent the relevant sedimentary structures can be linked to the characteristics of the sediment and the flow, one can better understand the dynamics of these large currents which, although acting in a highly discontinuous fashion, have deposited thousands of feet of sediment at the base of the continental slope.

Turbidity currents have become an important part of the professional literature since the 1940's and 1950's with early studies and theorizing by Knapp and Bell (1941), Phleger (1951), Natland and Kuenen (1951), Menard and Ludwick (1951), and Kuenen (1950, 1952, 1953a, 1953b). The turbidity current hypothesis was developed to explain the presence of continental-derived sediments far out onto the abyssal plains as well as the occurrence at depth of shallow water foraminifera, plant fragments, and other continental shelf debris such as molluscs, halimeda, echinoid spines, and so forth. In some cases the postulated current is capable of transporting coarse sands and conglomerates a good distance (Natland and Kuenen, 1951). The existence of submarine leveed channels at the base of the continental slope was not known to be a consequence of turbidity current action in 1951, but no one could think of a better explanation (Menard and Ludwick, 1951; Gorsline and Emery, 1959).

There is a long history in the literature of detailed descriptions of deposits felt to be turbidites as well as hypothesizing concerning the currents themselves. By the middle 1960's turbidity currents had come to be related to submarine canyons, and the question arose as to whether the currents had actually eroded the canyons or merely served as the agent which kept them remarkably clean of unconsolidated sediment (Shepard, 1951 and 1965).

There have been numerous field studies of turbidites (Enos, 1969a and 1969b; Bassett and Walton, 1960; Ballance, 1964; Allen, 1960; and van Houten, 1964) in addition to a large number of papers concerned with developing an appropriate terminology for turbidites and their related features (Crowell, 1958; Hsu, 1959; Kelling and Walton, 1957 and 1961; Kuenen, 1957; McKee, 1953 and 1957; Carozzi, 1957; Sanders, 1960; Rich, 1950; Allen, 1960; and Parkash, 1970). These papers have considered tool marks, flute casts, groove casts, flame structures, load casts, sole markings, convolute laminations, sludge casts, stratification, cross-stratification, horizontal grading, and the like.

The origin usually proposed for a turbidity current is an earthquake-triggered slump of sufficient size to become fully turbulent and adequately diluted to be a true turbidity current. This dilution takes place through turbulent interaction at the flow interface by the breaking of internal waves. The term fluxo-turbidite was employed for a while to indicate the proximal section of a turbidite (closest to the source), but some have proposed that this term be abandoned (Walker, 1967; Dzulynski et al., 1959). Other terms referring to the proximal section such as grain flow and inertia flow are falling into disuse (Stauffer, 1967; but see also Middleton, 1970). At least the nearest portions of the proximal section are thought to be some sort of pseudo-laminar flow, a transition from a disintegrating slump block to a fully developed turbidity current.

There have been objections to the turbidity current hypothesis from the beginning, and although acceptance of the idea is wide today, there are some recent detractors (Hsu, 1960 and 1964; Van der Lingen, 1969 and 1970; Hubert, 1966 and 1967). The usual argument is that a combination of high-angle faulting of flysch basins and waning oceanic bottom currents are responsible for the turbidites (see also Conolly & Ewing, 1969; Kuenen, 1970). Some have pointed out that bottom currents of the required velocities are known to exist, and that they are able to sort the available sediments. Sometimes, proposed turbidity current deposits have both parallel and interference ripples. Also, a vertical section claimed to be simply derived from a single turbidity current sometimes is thinly interbedded with shale members. Recently, bird tracks indicating a shallow water origin have been discovered in what is supposedly a turbidite (Van der Lingen, 1969).

A commonly proposed difficulty with the turbidity current hypothesis is that various indicators of the direction of flow are sometimes at right angles to the primary bottom gradient. Proponents of turbidity currents have explained this discrepancy three ways: proposing a three-dimensional flow in the head region of the current which could generate a crisscrossing of tool marks (Allen, 1971; Prentice, 1960); by the fact that a flow is not always parallel to the steepest gradient present (as in the case of water flowing down a channel with steeply inclined sides) (Potter & Pettijohn, 1963;

Dzulynski et al., 1959); and finally by proposing that certain slump folds indicating a paleoslope perpendicular to the turbidity current path can be explained by ephemeral tectonic activity (Walker, 1970).

An added difficulty is generated by some confusion regarding the terms 'flysch' and 'greywacke' in which turbidity current features often, but not exclusively (Wilson, 1969) occur (Dzulynski & Walton, 1965; Pettijohn, 1960; Boswell, 1960).

The modern interpretation of turbidity current deposition generally takes the form of the "Bouma Interval" popularized by Bouma (1962, 1964), but first proposed by Signorini in 1936 (Bouma, 1964, p. 256). The Bouma Interval is described as follows (in order of deposition):

A. Lowest Interval: sand, commonly graded, no lamination, gravel and pebbles sometimes present.
B. Interval of Parallel Lamination: a coarse sometimes faint parallel lamination in gradational contact with the A Interval.
C. Rippled Interval: ripples less than 5 cm high and 20 cm long with foreset lamination; ripples are sometimes convolute with usually a sharp contact with the B Interval below.
D. Interval of Parallel Lamination: usually fine sand to silty pelite; a sharp lower contact with sand content possibly decreasing upwards.
E. Pelitic Interval: no visible sedimentary structures, lime content may increase upwards; a very gradual contact with the D Interval below.

There is a general grading to finer sizes as one moves upward from A through E. Some horizontal variation is indicated (Bouma, 1962; Enos, 1969a). Bouma found no corelation between the direction of flow and the particles' long axes.

Although five intervals are listed above, one or more can be omitted in a given field sequence, but in the overwhelming majority of cases an interval is not skipped in a manner that would result in disordering. For example, 1) A-B-C-D-E is a possibility as is 2) C-D-E-A-B or 3) A-B-A-B-C, but intervals such as A-B-D-C-A are quite rare, even if one has two turbidity currents relatively close to each other in time with the later current doing a small amount of eroding. As the turbidity current moves away from the continent, first the A Interval is not deposited, then the B, and so on until, far out on the abyssal plain, only the D interval and the pelagic E interval are deposited.

Walker (1970) has found that of 16,000 measured turbidite deposits less than ½ of 1% differ from the Bouma model, and then the divergence usually consists of a minor reversal such as that in 3) above. One possible explanation for these minor reversals that the author has not seen elsewhere is the dependent triggering of a second turbidity current several hours after another, smaller, one. Since the larger current is hydraulically more efficient, it would override the slower smaller one which might still be depositing on a continental rise or abyssal plain thus causing

the reversal. It does not seem unlikely that on a rare occasion a slump triggered by an external source would itself trigger a second slump on the edge of the continental shelf. Some authors contend that many turbidity currents originate on the lower continental slope and on the continental rise (Conolly and Ewing, 1969). It would be interesting to discover whether or not the reversals occur primarily in turbidite intervals that are associated with currents originating near the edge of the continental shelf where the likli-hood of a first slump triggering a second seems higher.

Walker (1965) modified the Bouma Interval to seven intervals, essentially adding more detail rather than changing anything basic:

1. Graded, unlaminated interval
2. Lower interval of parallel lamination
3. Clear bed-current interface forms caused by a laminar boundary layer
4. Part of the lower parallel laminated interval re-worked into ripples
5. Ripples which cease moving at less than critical shear
6. Upper interval of parallel lamination, silt and some mud
7. Suspended mud settles out, followed by continuous oceanic sedimentation

Walker also notes that in all probability that the current is graded during its passage vertically and horizontally with the finer fractions being to the rear and further from the sea bottom. Simons' and Richardson's upper and lower flow regimes do not seem to rule out either Bouma's or Walker's Intervals.

One question which has attracted some attention is the lack of dunal structure in turbidites. Allen (1968, 1970) has written that when the power of a flow is reduced one usually gets some dunes. Walker (quoted by Allen, 1970) felt that there simply was not enough time in the dune field for them to form. Allen agreed with this and also added that for a typical turbidity current size distribution, the range of the dune field is quite small (see also, Southard, 1970). Roy in his investigation of the Silurian of northern Maine employed a Markov Chain to investigate the Bouma Model and found that the D Interval was the weakest part of the model (Roy, 1970).

The Turbidity Current Proper

The turbidity current begins as some sort of slump either on the edge of the continental shelf or further down in the lower reaches of the continental slope or upper part of the continental rise. Recently it has been proposed (Allen, 1971) that the head of the slump becomes the head of the turbidity current through a process of oppositely rotating longitudinal vortices; ambient fluid mixes with the head through 'tunnels' situated on the frontal surface, lowering the density of the slump head by introduction of the surrounding sewater, thus transforming the slump into a nascent turbidity current. Once developed, the turbidity current may cover several thousand square kilometers and

have a volume of a hundred cubic miles (Kuenen, 1964). The argument is made that a pure slump could not be responsible for turbidites generally since many tens of miles can be covered on a slope of about 1 part in a 1000. (as in the case of the famous Grand Banks Earthquake turbidity current which destroyed a series of telegraph cables, the furthest from the origin being destroyed last).

One promising suggestion which has not yet been investigated in the field (Van der Lingen, 1969) is to examine the slump produced by the 1964 Alaska earthquake to determine whether or not a turbidity current was generated. Such an earthquake should have produced a turbidity current provided there was a sufficient supply of sediment accumulated on the edge of the shelf.

As the turbidity current moves down the slope and out onto the continental rise its grain size decreases (Gorsline & Emery, 1959; & many other papers). In addition the amount of sediment deposited decreases with distance away from the shelf. Enos (1969b) has found a decrease of approximately 7% per kilometer in the distal sections of the Cloridorme formation while tracing individual beds for 7.5 km. He also notes that small pre-existing bottom irregularities can cause a large variation in bed thickness and grain size. There is some ponding of turbidity currents as the transition from continental rise to abyssal plain occurs (Belderson & Laughton, 1966). Enos finds evidence for some erosional processes caused by the passing current. Both Enos and

other authors (Parkash, 1970) have found that there may be considerable meandering or sinuosity in the course of a turbidity current, especially in the distal region.

Several authors have written that there is a hydraulic jump at the base of the continental slope causing a decrease of about 50% in the current velocity, a height increase, and a reduction in density from 5-15% depending on the initial assumption structure (Brush, 1969; Middleton, 1970; Komar, 1971). However, only the coarsest fraction of the load is dropped at the jump; the competency of the current remains high. Once the Froude number is less than one, there is little mixing at the fluid interface (Middleton, 1966). Studies in the Atlantic have shown that a lateral extent of 65 km is achieved.

It can be seen from the above that these currents are efficient transporting agents for large amounts of sediment. At least one author (Kuenen, 1971) has theorized that thin, dilute currents could not accomplish this and has proposed a density in excess of 1.16 gm/cc and noted that a current whose height from field evidence is at least a hundred meters can be sustained for two thousand kilometers on a sloping surface of 1/10% grade. He proposes a nose density of 1.1-1.2 gm/cc in an earlier paper (1966).

More recently, mathematical treatments by other authors have indicated that the 1/10% slope is the minimum that can sustain a turbidity current, even if it is composed entirely of clay-sized particles, and that a density as high as that

proposed by Kuenen is not necessary (Bye, 1971; Komar, 1970). In addition, the 1/10% slope corresponds nicely to the slope of the continental rise, giving indirect evidence that turbidity currents are slowly building a shallow wedge out onto the abyssal plains (Bye, 1971; Belderson & Laughton, 1966).

The concept of autosuspension as related to turbidity currents has been a part of the professional literature for some time (Bagnold, 1962; Knapp, 1938; Dzulynski & Walton, 1965). The autosuspension hypothesis results in a turbidity current that is not concentration-limited under certain circumstances. If the downward net movement of the current as a whole exceeds that of the settling velocity of the particle (the 'hindered' settling discussed by Knapp in which other particles in the flow hinder the settling of the given particle must be considered) then the particles themselves contribute energy to the flow as opposed to requiring the expenditure of turbulent energy for their own support. In short, where the slope angle is a few degrees or less and θ can be approximated by $\sin\theta$, the autosuspension conditions are met when

$$w < \theta u$$

where w is the hindered settling velocity, θ is the slope angle, and u is the velocity of the current (see also, Johnson, 1966; Briggs & Middleton, 1965). Bagnold gives a typical upper limit for autosuspension as 50 microns. Johnson gives 75 to 1500 microns, but he assumes higher velocities and a greater slope angle.

DESCRIPTION OF EXPERIMENTAL APPARATUS

The experiments were carried out in a small flume that reciculates both water and sediment. The inside width is 17.4 cm, the channel length is 550 cm, and the height of the channel is 33 cm. The headbox is approximately 45 cm long and the tailbox about 30 cm in length. The transparent walls of the flume were constructed of 3/8" Plexiglas. Large steel I-beams provide support. The flume is tiltable by means of two jacks approximately 2/3 the distance downstream from the headbox. Two round steel rails are mounted on the steel bracing along the top of the flume walls and aligned parallel to the flume bottom to within $\pm$ 0.01 cm. A small carriage with metal wheels is mounted on these rails to provide a convenient location for the point gage. The carriage can be clamped or allowed to move freely along the length of the flume.

A baffle consisting of close-packed lengths of stiff plastic tubing with an inside diameter of 0.7 cm and a length of 30 cm was placed between the headbox and the channel to reduce the entrance turbulence making the flow more nearly uniform. In addition, a small board 17.3 cm wide and 25 cm long, adjustable in position, was placed in contact with the water surface immediately downstream of the headbox baffle. Typically, it was tilted slightly downstream and rode just below the level of the free surface.

Two valves in the return pipe allow regulation of the rate of flow, one valve allowing coarse adjustments and the other permitting finer adjustments at reduced flow rates. The return pipe is jacketed with a second, larger, pipe in which cold water is circulated, cooling the channel flow to a minimum of 16 deg. C.

The pump in use with the flume is an Ingersoll-Rand Type 30 KRVS centrifugal pump. A 2 hp motor drives the pump by means of a geared belt. The 1750 rpm of the motor was tripled by the pulley arrangement used.

A water feed system was needed to compensate for evaporation in the longer runs and to provide water for the pore spaces of the new bed during aggradation runs. This system consisted of a bucket of several gallons capacity into which the cooling water flowed after leaving the pipe jacket. The bucket had a hole in its top from which water could drain when it was nearly full. When the experiments were in progress, this arrangement provided a constant head on a small valve attached to the bottom of the bucket. This smaller valve could be adjusted to provide a relatively constant flow rate up to several tens of cubic centimeters per minute.

A sediment-feed device was also used to introduce dry sediment into the flow at the tailbox. This apparatus consisted of the lower two-thirds of a thirty gallon drum mounted on a wooden frame and suspended over the end of the

channel. Holes of varying sizes were drilled into the bottom of the drum to provide various rates of sediment feed. All holes but the one in use were corked or taped shut. Power to produce a uniform flow of dry sediment from the drum was provided by an air-powered ball vibrator (Martin Engineering Co., Neponset, Illinois; model BDR-16, designed for prolonged continuous operation). The ball vibrator was attached securely by a bolt to the bottom of the drum a few centimeters from the various feeder holes.

A view camera was used to document each of the aggradation runs. Depending on the circumstances a series of close-ups was taken and/or a series of overlapping shots taken for three to four meters along the flume. Depending on the particular run, these shots were supplemented by overhead pictures that showed both the sediment seen through the sidewall and the bed surface. In addition, on some runs the process of aggradation and ripple advance were recorded at half-hour intervals at a given location just upstream of the tailbox.

Photo 1 shows the entire experimental apparatus except for the view camera. The main components are labeled in the photograph.

EXPERIMENTAL PROCEDURE

At the beginning of each run, whether an aggradation run or a calibration run, some or all of the sediment was added by hand to the flume, an appropriate amount of water admitted from the overhead holding tanks, the cooling system activated, and the dripper set to compensate for evaporation and/or aggradation.

It was found that a drip rate of 15 drops/min (about 1 cm^3/min) compensated for evaporation; at least no discernible change in the flow depth was noticed in a 36 hr. period.

During the calibration and aggradation runs, surface velocities were measured using a small wooden float and a standard laboratory stopwatch. The float was timed over a convenient 183 cm distance midway down the flume. Depending on the circumstances, for each desired velocity a varying number of times (4-40) were taken and their mean used to compute $\bar{V}_s$. $\bar{V}$ was then taken to be $0.85\bar{V}_s$, and $\bar{Y}$ was derived from

$$\bar{Y} = Q/w\bar{V} \quad .$$

All pipettings were taken using a 50 ml pipette. 50 ml beakers were used to contain the mixture. The net weight of sediment per 50 ml of mixture was obtained by decanting and drying in an oven. The 50 ml of water-sediment mix taken from the flume was replaced with water. A triple-beam balance was used in all cases to weigh the beakers and the sediment contained therein to within $\pm$ 0.01 gm. In the

runs longer than eight hours a method was needed to remove the fine algae/sludge (the sludge being derived from the plumbing system with time) mixture which had to be removed from the walls of the flume to obtain a view of the sediment. A thin wood sliver was used intermittently to keep the Plexiglas walls clean and disturbed the sediment only minimally.

For each aggradation run, the particular feeder hole was calibrated by averaging several test runs to obtain Q_s. After each run the sediment was dried with four infrared heat lamps. The dry sediment was then sieved through a 470 micron mesh to insure the feeder hole would not be clogged.

It was found that Q_s is a function not only of the hole size but also the distance of the hole from the ball vibrator attachment bolt and the amount of dry sediment in the drum. An increase in height of the sediment in the drum resulted in two effects, the net result of which was to decrease Q_s: the increased pressure on the hole tended to produce a higher flow rate, but this was more than compensated by the greater difficulty the ball vibrator experienced in vibrating the heavier weight, thus producing a net decrease in Q_s as the height of fill was increased from 1/3 to completely full. In addition, when the container was filled less than about 20%, the supply of dry sediment to the hole varied randomly with slumping in the container, because the hole was not completely covered at all times and therefore could not feed at a constant rate. One might think that these fluctuations would average out with time and thus would not vary the feed rate over a several

minute period, but this turned out not to be the case for reasons that are not completely clear. There was also another effect, that of packing the sediment as it was vibrated for many hours. For this reason, the vibrator was run for several hours before each aggradation experiment in an attempt to reduce the porosity to a constant value.

As a result of the decrease in Q_s caused by an increase in the height of sediment in the drum, sediment had to be added to maintain the level during each aggradation run. For the flow rates involved, this was not too inconvenient, and the level of the drum was maintained at about 50 liters $\pm$ 1 liter. The concomittant small variation of the feed depth with time seemed not to be significant and did not materially alter Q_s.

In order to estimate the amount of water needed to fill pore spaces in the aggrading bed, a small amount of sediment was packed to a reasonable density (by tapping the container on a hard surface until no change was noticed in the sediment height) and then saturated with water. This was done twice, and the required volume of water for a given volume of sediment remained essentially constant (Table 1).

A correction factor was needed as Q_s from the feeder hole was measured with reference to a relatively unpacked state (as it filled a 1000 ml graduated cylinder) and a mean flow rate calculated. This represented a feed rate determined from sediment in a fairly aerated state, whereas the water required to fill the pore spaces in a given volume of sediment was with

reference to a packed state. The 1000 ml graduated cylinder was then tamped in a manner similar to that noted above for the pore space sample, reducing the volume of sediment to 820 ml. The quantity Q_S, then, refers to a flow rate of dry sediment into a 1000 ml cylinder (or into the flow) in an unpacked state. The quantity Q_B refers to the amount of water flow required to saturate an amount of dry sediment flow equal to $0.82Q_S$.

Documentation of each experimental run was acquired as described above under the section on experimental apparatus.

Depending on the run involved a water surface profile (5 cm intervals) and a bed surface profile (2 cm intervals) were taken along the center line of the flume, allowing an independent calculation of $\bar{Y}$ (independent of the measure of surface velocity using the float). Depending on the velocity of the run, the $\bar{Y}$ value obtained from the profiles had to be increased 0.0 to 3.0 mm to compensate for the suspended sediment that settled out onto the bed when the pump was stopped.

A 20" Mercury manometer was used in conjunction with an orifice meter to obtain information on the flow rate, Q.

FINER SILT FRACTION CALIBRATION RUNS

Three calibration runs were performed with the finer fraction of the mid-continent loess; it was found to be less well-suited for the purposes of the experiment than the coarser fraction. Essentially, the difficulties were two: a relative lack of the darker particles (assumed to be plant debris) to delineate the internal sedimentary structures and, less importantly, a higher suspended concentration for a given flow velocity than the coarse fraction, resulting in greater problems in maintaining a uniform mean flow depth as the velocity was reduced.

The first calibration run consisted of a sudden drop in manometer reading from 18" to 9" in order to see how quickly the suspended concentration adjusted to the reduced velocity. The actual drop in velocity was not as much as one might think from the relationship

$$Q = 1700(\Delta H")^{\frac{1}{2}} \text{ cc/sec}$$

because of the amount of sediment that settled out thus reducing the mean flow depth at the same time Q was decreased. From measurements made at the time, the change in velocity was from 65 cm/sec to 50 cm/sec (see Table 2 and Fig. 1). The rather rapid rise in the mean concentration beginning at about eight minutes is due to the development of high-speed ripples; at the upper velocity the bed regime is planar or nearly so.

The second calibration involved two flume runs. In the first, the manometer reading was reduced by 1" every 5 min. and a pipette sample was taken for each manometer reading as it was reduced from 16" to 1". This yielded a graph of concentration versus velocity (Fig. 2 & Table 3). In the second run, larger reduction intervals were used, but an hour was allowed for the sediment to readjust to the change in manometer reading. The idea was to see how rapidly the sediment adjusted to the new equilibrium concentration for the given velocity (Table 4).

The first interpretation from the graph (Fig. 2) was that the sediment did indeed require a long time to adjust as the concentrations were systematically lower for the run in which the sediment was given an hour to adjust to each change in the flow velocity. Ideally, the desired sediment would adjust to a change in the velocity in four or five minutes; enough time for many passes through the flume, but not so long as to require extremely long aggradation runs with very small but numerous reductions in the manometer reading.

It was noticed, however, that during the run shown in Table 4, the temperature was 36 deg. C, as opposed to 22 deg. C for the run shown in Table 3. The dynamic viscosity of water is a rather strong function of temperature (Table 5 & Fig. 3) (Chemical Rubber Co., Daily and Harleman, 1966; Gibbs et al., 1971) and therefore the change in viscosity due to temperature difference would change the effective

settling diameter of the sediment, since the viscosity is a fundamental parameter of any fluid (Briggs & Middleton, 1965). Studies have shown that an increase in temperature (and thus a decrease in the viscosity) does affect the bed form as well as decrease the amount of suspended load (Hubbell & Ali, 1961).

It was decided to allow for the viscosity effect on the assumption that the viscosity and suspended concentration were linearly related in the range of this velocity and viscosity. In reality, the relationship is more complicated since a change in viscosity affects not only the effective fall diameter, but also the intensity and scale of the turbulence. Intergranular collision effects would be altered too, but this is a highly complicated problem. In this case the question was whether or not the first-order correction for viscosity would systematically do away with the discrepancies in the mean concentration as shown in Fig. 2. Taking 3 velocities from Table 4 and 3 from Table 3, that were within 1% of each other (56.0/55.5, 42.4/42.1, 49.2-49.7-49.7/49.4), a comparison of the associated mean concentrations gives the following result: three ratios are obtained (high temperature to low temperature concentrations): 0.766, 0.771, and 0.737. The ratio of high temperature (36 deg. C) to low temperature (22 deg. C) viscosities (Table 5) is 0.738. Considering the uncertainties of measurement involved (and the given 1% variance in velocities), this close an agreement is taken as proof that the finer silt could adjust to a change in velocity in five minutes or less. This was acceptable.

However, when test runs were made to examine the equilibrium sedimentary structures of the finer fraction it was found that the finer silt did not contain nearly as much dark plant debris as the coarse silt and thus would not delineate the sedimentary structures nearly as well, especially at higher velocities. A visual examination by eye and by binocular microscope did not reveal this difference.

COARSER SILT CALIBRATION RUNS

Similar calibration runs were conducted with the coarser silt except that the one-hour adjustment was omitted since it was known that the finer silt did not require this much time. But just to be certain, in the run in which the manometer reading was decreased one inch at a time, a half-hour interval was used.

In the calibration run in which the manometer reading was reduced abruptly from 18" to 9" the net weight of suspended sediment per cubic centimeter was roughly half what it was for the finer fraction (Table 6 & Fig. 4). As can be seen from Fig.4, the sediment reacts fully to the change in velocity in about four minutes. As with the fine fraction the concentration rises sharply after the four minutes and then oscillates about an equilibrium level once ripples have begun forming.

The apparently sinusoidal variation of mean concentration with time is evident from Fig.4, and to a lesser extent in Fig. 1. The cause of this sinuous variation is unknown. The pipettings were taken from the tailbox about 8-10 cm beneath the free surface and about 20 cm from the downstream end of the channel. The fluid in the tailbox is well-mixed and should reflect an average of upstream conditions, such as bed roughness. If the ripples were slowly growing during the measurement period, one would expect the concentration to climb slowly, perhaps still oscillating in the process. However, after the

first few minutes this does not occur. There were no fluctuations in the flow rate through the pump, and the suggestion that the average concentration varied with time depending on whether a trough or a crest was immediately upstream of the tailbox is unattractive, given the characteristics of either the coarser or finer fractions. It seems that the averaging process mentioned above must take place, so that no single terminal feature could affect sediment concentration in the tailbox. In addition, it must be remembered that in all likelihood at a given instant the terminal feature just upstream of the tailbox is part crest and part trough because the bed features are to some degree three-dimensional. Of course, one cannot be sure that the variation is of the period indicated by the Figures; the low rate of sampling does not allow a full description of the variation with time.

In Fig. 5 and Table 7 the results of the mean concentration versus velocity run are depicted. The increase in mean concentration with velocity is nearly linear in the velocity range investigated. A test run to view the equilibrium ripples and other structures showed that the coarser silt contained a considerably higher concentration of dark plant debris than did the finer fraction and would therefore be more suited for the experimental study. In addition the lower suspended-sediment concentration of the coarser fraction makes it easier to provide for a uniform mean flow depth in the aggradation experiments in which velocity changes with time.

A knowledge of the equilibrium concentration of sediment at a given velocity would provide an idea how much sediment would drop out of the flow as the speed was reduced, thus allowing one to corrent for the decrease in flow depth by adding water over and above that required to compensate for evaporation and the pore spaces of the aggrading bed. However, ideally this water would have to be added in analog fashion, the rate derived from the curve of Fig. 5. This presents some additional simulation problems which are discussed below in the conclusions.

Run 1

Run 1 was a preliminary run to test the entire system (Table 8 and Figs. 6 & 7). A planned velocity-reduction program was carried out while the bed aggraded at a relatively high rate. Q_s was 2.23 ml/sec, which, given the area of the flume bottom, aggraded 5.9 cm of sediment over the 420 min of the run, a rate of 6.8 mm/hr. It was thought before the run that this rate of aggradation was appropriate in terms of the thickness of distal turbidites and what was felt to be a reasonable duration of current flow (5-10 hrs.).

The run produced structures that bore little resemblance to the known appearance of equilibrium ripples in the sediment (Photos 2-5): their spacing was up to 30 cm, and their average height was about 3 cm. Fairly distinct foreset laminations were obtained, as well as parallel laminations of the Bouma D Interval.

The velocity was held high (plane-bed conditions) for two hours in an attempt to aggrade a B Interval. Remains of a faint B Interval can be seen in some of the photographs, but the record of the B Interval was generally destroyed by the erosive action of the C Interval ripples that followed. This is in contrast to statements in the literature to the effect that there is no truncation of backset laminae (Enos, 1969a; Sanders, 1963). Even with this rate of aggradation, both the B Interval and much of the earlier portions of the interval of ripple-drift cross lamination

were eroded away by subsequent ripples movement. Enos states that the rate of aggradation must be high in order for the laminae not to be eroded, but he does not say how high. Sanders (1963, p. 177) gives a sketch of ripples whose internal laminae are not truncated because of the rate of "sand fallout". The sketch shows some ripples moving under equilibrium conditions without aggradation as well, but the spacing of the equilibrium and the aggraded ripples is the same.

According to Enos, the angle of climb generated by a rate of aggradation high enough to avoid truncation is about 15 deg. In two of the accompanying photographs in which the angle of climb is most readily determined from the structures the angle is $11\pm\frac{1}{2}$ deg. Thus, it seems contradictory that almost all the B Interval and early C Interval were truncated by the C Interval itself with time. But higher aggradation rates would undoubtedly produce structures with greater spacing than the ones recorded in Run 1.

An odd structure can be seen in the Photographs 4 and 5: it appears to be a reverse ripple moving from right to left. No other reverse ripples were seen in any of the runs that approached this in size.

When interpreting the photographs one must realize that the top most sedimentary layer (typically shaded a little darker than the D Interval immediately below it) is composed of fine sludge and possibly brown algae that were generated within the system with time. It forms a non-laminated interval that could be taken to be an E Interval for the sake of

completeness, except for the fact that it settled out in the few minutes after the run was stopped rather than over many years, as is the case with the true E Interval of pelagic sediment.

As can be seen from a comparison of Figs. 5 & 7, under this aggradation rate the concentration of sediment is typically two to three times higher for a given velocity than under equilibrium conditions. Curiously, there is a decrease in sediment concentration in Run 1 for velocities above about 54 cm/sec; the only reason I can give is that it took a couple of hours in the high turbulence above 54 cm/sec for the sediment to reach its maximum concentration. The run was begun with the flow saturated with sediment; an average thickness for the bed at the highest velocity was perhaps ½ cm along the flume channel. Apparently, highly turbulent flows can suspend sediment loads over and above their customary equilibrium concentrations for quite some time during the aggradation process. This is to be contrasted with the calibration runs in which the sediment reacted in a few minutes to a change in velocity. But it must be remembered that in the latter cases, there was no sediment being added to the flow.

This additional suspension created some difficulties with regard to uniform flow depth. In this run no "extra" water was added to make up for the loss in flow depth due to sediment dropped from suspension as the velocity was

reduced. This was intentional in order to get an idea of the magnitude of the problem. Not only was there a good bit of suspended sediment to rain out when the velocity was reduced, but there was little deposition of sediment during the first two hours; most of it stayed suspended along with the small amount of pore water that was also being added.

Since little sediment settled out during the first two hours (and most of what did, the B Interval, was destroyed by truncation later in the run), the discharge had to be increased in an attempt to maintain a constant velocity for that period. When it came time to actually reduce the velocity according to the pre-planned curve, much sediment fell from suspension, reducing the flow depth, and thus requiring further reductions in the discharge to continue the velocity reduction, which in turn caused more sediment to settle out, etc.

An examination of Table 8 shows the variation of $\bar{Y}$ with time for Run 1; much of the variation can be explained by the concentration of suspended sediment in the original 6.3 cm of flow depth. In addition, the extremely rapid aggradation rate during the 210-270 minute interval (over 4 cm/hr.) quite possibly formed a bed with more water than a normal bed moving under equilibrium conditions. It could be that the calculations derived from Table 1 provide too little water for pore spaces because the sediment was packed too tightly; however, several probes by hand of the bed

in the flume and the sediment measured in Table 1 indicated a similarly packed condition (the sediment was quite firm).

Because of the difficulties cited above, a decision was made to study bed forms at two different velocities in the ripple field to see the effects of varying the aggradation rate.

RUN 2

Run 2 was conducted at what is thought to be a reasonable minimum rate of aggradation for a distal turbidity current. About 4.8 cm of sediment was aggraded on a pre-existing bed, which had progressed at the same speed at equilibrium for 22 hrs., by 27½ hrs. of dry sediment feeding into the tailbox. This is an aggradation rate over the area of the channel bottom of 1.2 mm/hr.

The pipetted samples were allowed to settle for 2 min. in 50 ml beakers and then the liquid was poured off. An examination of the clarity of the liquid showed little change after 1-2 mins. indicating that small or low density particles were present, probably brown algae. After 2 min. in a test case, little change was noticed during the third minute of settling. It was decided that in Run 2 and in future runs the fluid could be decanted any time in the 2-3 min. range and still allow most of the algae to be removed. Since more algae was produced as the run went on, this prevented the later pipette samples from being biased to a higher weight.

At the end of Run 2 a water-surface profile was taken for about 3 m along the flume (spacing interval: 5 cm) with the pump running, and after the run was completed a bed-surface profile was taken over the same distance at 2 cm intervals. A careful examination had previously shown that no rail correction was necessary as the rails were parallel

to the flume bottom within ± 0.01 cm, the precision of the point gage. These two profiles allowed $\bar{Y}$ to be calculated directly and then a $\bar{V}$ can be calculated from the equation

$$\bar{V} = Q/w\bar{Y},$$

or one can take a series of measurements of surface velocity with a stopwatch and a small float, computing $\bar{V}$ from the assumption that the mean velocity is 0.85 the surface velocity, a relationship that has proved reasonable for flow over beds in the experimental flume in the past.

That the two methods of determining $\bar{V}$ differ in results is evident from the table. Although a large number of measurements of $\bar{V}_s$ were made, reducing the chances for error there, in all likelihood there is a systematic error in assuming that the mean velocity is 85% of the surface velocity (there is probably a functional dependence on flow depth and bed profile that is not considered) so the $\bar{V}$ generated through use of the surface-profiles and the discharge equation is the more accurate.

It was noticed during this run that there appeared to be areas of net deposition and erosion on a scale larger than the ripple spacing. This produced a gently undulating bed varying in thickness considerably over the length of the channel, the spacing of these larger undulations being about 75 cm.

Measurements were taken from photographs of the 4 m of bed immediately upstream of the tailbox for both the

equilibrium and the aggraded ripples. It was found that the spacing of the equilibrium ripples has a mean value of 10 cm, and the mean spacing for the aggraded ripples was about 12 cm. The heights were more difficult to compare since roughly 3 mm of sediment rained out of the flow when the power was shut down, but it appears that the height of the aggraded ripples is less than that of the equilibrium ripples. Measurements over 30-40 crests give 1.4 cm for the equilibrium ripples and 1.1 cm for the aggraded ripples. The argument could be made that the 0.3 cm of mantling sediment made up the difference but it must be remembered that the mantling sediment rained out on both crests and troughs; certainly not the entire 0.3 cm of "fallout" was deposited in the troughs. Although the change in ripple height can be argued, the increase in ripple spacing seems to be nearly certain.

The values for height and spacing above have been corrected for systematic error: the meter stick that appears in the photographs had to be placed outside the Plexiglas for clarity and convenience, thus placing the meter stick nearer the camera by its own thickness plus that of the Plexiglas. Pictures taken of two meter sticks at this viewing distance, one offset from the other by the displacement distance above, and then enlarged for accuracy of measurement, indicate a 6% reduction factor caused by this effect. Eight different measurements were taken to compute

the correction factor, and all of them produced a correction of $6\pm\frac{1}{2}\%$. Similar corrections were taken for the other expermental runs, the amount of the factor being larger in the relatively close-up photographs.

The average suspended concentration varied with time as it had in the previous calibration runs. Pipettes 11 and 12 (Table 9) were taken within a minute of each other, indicating that the variation in concentration either has a high frequency or that the pipette error is about 2%; the latter is probably the better choice. Again there is no general increase in the mean suspended concentration with time, the minimum and maximum suspended concentrations (#14 and #16) being fairly close to each other in time.

A certain planar feature whose linear projection can be seen through the Plexiglas are evident in both the equilibrium and the aggradational ripples. This feature represents the locus of the transition between the lee slope and trough of a ripple and will be called the "Basal Trace". Photographs 6-13 depict basal traces and other features described in the accompanying captions.

Basal traces in the equilibrium ripples indicate that in some cases they are climbing (positively inclined to the horizontal), but that in other cases they are negatively inclined; the result being a net climb angle of zero degrees. The aggraded ripples show positively inclined basal traces generally, although they show some horizontal ones.

The aggraded ripples show some large trough structures which may or may not be related to the occasional boil-like structures that appear on the bed surface (Photos 12 and 13). Further, the rather distantly spaced (75 cm) undulating trough-crest pattern mentioned above could be a result of the boil structures. The inter-relationship among these three features, if any, is not at all clear.

An examination of the basal traces for the equilibrium and the aggraded ripples shows that one must examine more than a few basal traces in the field before making a generalization as to whether or not true ripple drift cross-lamination (aggradation) is taking place; a basal trace may be horizontal in an aggrading bed just as equilibrium ripples can produce an occasional climbing basal trace. Only an average angle of inclination computed over several tens of basal traces can indicate what is taking place. Perhaps in a bed that is slowly being eroded by a flow in the ripple regime the average angle of inclination of the basal traces would be negative. In any case since there are areas of relative scour and deposition along the length of the bed surface, it is the average angle of inclination that must be considered.

RUN 3

Run 3 was conducted at the same mean velocity and mean flow depth as Run 2, or as nearly so as possible (Table 10). The value of Q_s in Run 3 was 2¼ times that in Run 2, however. Thus one would expect the main differences between the two runs to be a consequence of the increase in the dry sediment feed rate. The velocities (by averaging the two methods) were 39.0 cm/sec ± 3%, and the mean flow depth was 9.95 cm ± 6%. Considering the limited effect of a small variation in flow depth and the fairly good control on velocity, the large difference in aggradation rates should explain any changes in the spacing, height, and internal structures observed.

In the equilibrium run for Run 3 the mean spacing was 10 cm and the mean height was 1.3 cm. Thus, compared to the equilibrium ripples of Run 2 (the conditions were the same) there was no change in spacing and only a 7% decrease in amplitude.

During the aggraded interval of Run 3 pictures were taken at half-hour spacings at a given sidewall station just upstream from the tailbox in order to ascertain more clearly how the aggradation proceeded. These pictures make possible a second estimate of the spacing and height of the aggraded ripples in addition to the estimates from photographs taken of the bed after aggradation was complete. To allow time for the bed to adjust to the aggrading process, only the

last seven hours of the aggradation photographs were used to compute mean spacing and height. The average spacing computed from measurements along the aggraded bed was 17 cm. The average spacing computed from single station measurements was 16 cm. The mean heights respectively were 1.0 and 1.6 cm.

In the equilibrium run, the measurements were made over 25-30 ripples in a manner similar to that for Run 2. The spacing for the aggraded ripples is nearly the same for the two methods, but there is a large difference between the 1.0 and 1.6 cm values for the ripple heights. The amplitudes generated by the single-site measurements do not decrease with time, ruling out the possibility that the bed is very slowly adjusting to its equilibrium form under aggradation.

Accepting the 1.0 cm value for the ripple height which was obtained in the same manner as the aggraded ripple height was reached in Run 2, it can be seen that the ripple height decreases with increasing aggradation rate, using either the equilibrium height (zero aggradation) or the reduced aggradation rate of Run 2 as a basis for comparison. The mean spacing of the aggraded ripples obviously increases from the mean aggraded spacing in Run 2 where the aggradation rate was less.

Run 3 is seen as a transition between Runs 1 and 2, even though Run 1 involved a velocity reduction profile. The trough structures apparent in Run 2 have become more dominant

in Run 3 (Photos 14-17) and the internal structures are less distinct than in Run 2. If one looks at the structures produced in Run 1 at about this velocity, one sees that they are even less distinct than in Run 3. It seems that at the higher aggradation rates the flow does not have sufficient time to sort the sediment and therefore produces less distinct sedimentary structures. One can see a contrast between the lower portions of the bed in Run 3 which are the remains of equilibirum ripples and the upper part of the bed where the internal structure is much less distinct.

As the aggradation rate increases the ripple spacing increases. As the aggradation rate increases, the height of the ripples decreases (to a point; in Run 1, which also had the changing mean velocity, the height increased producing the long bar-like profiles).

In contrast with Run 2, there appear to be no obvious basal traces in Run 3; it is believed that these structures were not produced: the trough structures were produced instead.

The average concentration of suspended sediment again varies over time, but in this case there is a general increase in $\bar{C}$ with time which cannot be explained; indeed, with the decrease in the amplitude of the ripples, a general decrease in the suspended sediment concentration would have been more expected.

RUN 4

Run 4 was made at the same rate of dry sediment feed as Run 3, but with the mean flow velocity about 30% less. An equilibrium run was made as well; the main difference being that the time allowed for the ripples to come to equilibrium was doubled, since the flow velocity had been reduced. There are a variety of comparisons that can be made with Run 3. (Table 11).

In Run 4 the equilibrium ripples had a spacing of 12 cm, about 20% greater than the spacings in Run 3. The height in the equilibrium phase of Run 4 was 1.3 cm, the same as it was for the equilibrium phase of Run 3. The 20% increase in spacing is especially significant in that the equilibrium ripples in Runs 2 and 3 had the same spacing to within a millimeter (though the data are probably only good to two figures: 10 cm).

As with all these runs there is a slight shift in the viscosity of the water with a shift in temperature of one or two deg. C. This is believed not to be significant, since a two degree shift affects the dynamic viscosity of pure water only 5% (and the necessarily higher viscosity of sediment laden water even less).

The aggraded ripples showed a spacing of 15 cm and a height of 1.7 cm on the average. The increase in spacing with aggradation has been noted before. However, in comparison to Run 3, in which the shift was 60%, in Run 4 with a reduced velocity, the increase was only about 30%.

An attempt to measure spacing and height from the single station photographs that were taken during aggradation failed since the scale of the photographs did not allow the longest wavelengths to be measured from the single picture.

A comparison of the heights of the aggraded ripples between Run 3 and Run 4 shows that the Ripples in Run 4 have noticeably greater heights, either compared to the equilibrium height in Run 4 or to the aggraded height in Run 3. Run 4 also produced internal structures which are more distinct than those of Run 3. Thus it appears that the more intense turbulence at the higher velocity is a poorer creator of sedimentary structures for a given rate of aggradation.

In the aggradation ripples of Run 4, the trough structures do not appear to be as dominant as they were in Run 3 (see Photos 18-23). They appear to be more similar to those in Run 2 where the velocity was higher but the aggradation rate lower. In Run 4 there is also clearer evidence of the ripple-drift-cross-lamination in that the basal traces are again present after not being produced in Run 3. As in Run 2, the basal traces are generally inclined positively to the horizontal.

In short, from Run 4 it has been seen that a drop in the velocity (while still in the ripple field) tends to increase spacing, have little effect on the height of equilibrium ripples while increasing that of the aggraded ripples, and to increase the distinctness of the structures produced.

In addition, at the lower velocity of Run 4, the tendency for small ripples to form on the backs of larger ones and eventually grow in size while overtaking the larger ripple is more pronounced. This holds for both equilibrium ripples and aggradaing ripples (Photos 19 and 20).

The variation of the mean suspended concentration of sediment is still present in Run 4; again there seems to be a general increase in the values with time. The only explanation readily available is that all of the algae is not being caught in the decanting process, however the variation is too irregular for this to be a good explanation.

RUN 5

Run 5 was essentially a duplicate of Run 1 but with a lower aggradation rate, 1.2mm/hr. as opposed to the 6.9 mm/hr in Run 1. The velocity reduction profile was lengthened to 30 hrs. from 7 hrs. Table 12 and Fig. 8 show the results of Run 5. The shape of the velocity reduction profile is similar to that in Run 1 except for the longer period of time and the fact that the early period of constant velocity was omitted.

A decision was made six hours into the run to increase the flow depth to about 9 cm to lessen the effects of the free surface. This did not alter any of the previously deposited sedimentary record since the ripples present were scouring to the bottom of the flume. This destruction of previously deposited sedimentary structures was even more thorough in Run 5 since the aggradation rate was much less than in Run 1.

Water was added from the holding tanks during the last 24 hours of the run in an effort to keep the flow depth more nearly constant than it had been in Run 1 where the largest value for mean flow depth was nearly three times the smallest value. In Run 5 after the decision to increase the flow depth, it slowly decreased with time despite the additions of water from outside the system such that after 30 hours it was only 70% of the six hour value.

This 30% decrease was surprising since several measurements along the sidewall were used to get a value for the mean flow depth. It is felt that the relatively low downstream component of motion in the troughs makes it difficult to estimate a mean flow depth by measuring the average distance from the bed surface to the free surface. In other words 6 cm of actual mean flow depth will look like 8 or 9 cm of mean flow depth if the ripples have a height of 3 cm.

The water flowing in the flume was loaded to capacity with sediment and a half-hour was allowed to pass before the aggradation began at Time = 0. The concentration of suspended sediment increased from its pre-aggradational value and continued to climb until the flow depth was increased at 6 hours. It then dropped for 6 hours and except for a slight rise at 15 hours (probably due to the increasing height of the ripples being formed), continued to drop as the velocity was reduced. A comparison with Fig. 5 or Table 6 shows the suspended concentration in Run 5 to be substantially higher than the equilibrium concentrations for the given velocities. This is to be expected when the addition of extra sediment to the flow loads it beyond its equilibrium capacity.

In order to maximize the amount of dry sediment available in Run 5 for aggradation most of the sediment used to saturate the pre-aggradation flow came from another flume not then in use that contained identical sediment. This sediment was responsible for a very large amount of brown algae growth, much more than in any of the previous runs. The pipetted

samples showed more and more of this growth with time. The unsettled portions of the pipetted samples were decanted from their beakers after two minutes of settling and the decanted portions later examined by eye to determine that the growth was progressing. At 21 hours an algacide was added to the flow in an attempt to reduce the growth rate (primarily to make it easier to keep the inside wall of the Plexiglas free of algae). The algacide was found to work pretty well although some cleaning of the sidewall was still necessary to cope with the dead algae still present in the flow. It is difficult to make a quantitative estimate of the volume percent of algae present, but careful probings of the bed immediately upstream from the tailbox revealed it to be much softer than usual as well as more cohesive.

As in the previous Run 1, the sedimentary structures became more distinct as the velocity was reduced. This can be seen in the photographs 24 and 25; the top four or five centimeters of the aggraded bed show distinct structures wheras the lower one-half to one-third of the bed shows little if any structure.

The height and spacing of the ripples could not be determined accurately enough for a close comparison with Run 1 due to the highly irregular nature of the ripples and to the relatively small number available (since their spacing was large). Very roughly, the height appears to be about 3 cm and the spacing about 20 cm.

Photograph 24 indicates the irregular nature of the ripples involved. The ripple on the left is a long shallow one; the ripple in the center is a steep-sided large one; and the two small ripples on the right are small with finer scaled scour features. Generally in Run 5 the ripples are markedly symmetric, the foreset and backslopes are of approximately equal length and angle.

Photograph 25 shows several parallel laminations (beneath the 68-84 cm mark on the meter stick) upon which ripples later advanced even though the velocity was being continually reduced. Thus, one may make the hypothesis that the boundary between ripple- and parallel- lamination, that is between the C and the D Intervals, is not precise. Upstream conditions such as the rate of ripple advance and rates of net deposition and erosion might be responsible for the broadening of the boundary into a transition region in velocity space.

Photograph 26 shows a small (about 1.5 cm across) slump on the foreslope of a ripple located about 30 cm upstream from the tailbox. During the run occasional slumps could be seen on the foreslopes of various ripples, slumps that were quite pronounced and much larger than the intermittent slumping that ordinarily occurs during ripple migration. To the right and to the rear in the photograph are gully-like structures which bear a certain resemblance to the sub-aerial erosion of a bluff by water. It is felt that the presence of the algae was

primarily responsible for these new features by increasing both the cohesiveness and the water content of the bed. Perhaps the presence of clay would not have a totally dissimilar effect. It is difficult to imagine what other variable change could be responsible for this; most likely not the different aggradation rate or the lengthened velocity reduction profile.

CONCLUDING REMARKS

Experimental Difficulties

There are many difficulties associated with simulating turbidity current depositional features in the laboratory. Several experimental methods have been tried in the past. One can hold a slurry in suspension and then let it slide down a flume bottom, depositing as it goes (Middleton, 1966a, 1966b, 1967), but then one has drastic scale problems at least (Bagnold, 1962). One could choose to use a circular flume, which would allow the sediment particles to come to "equilibrium" with the turbulence, as Kuenen (1965, 1966) has done, but there are two concomitant difficulties: the unwanted effect of centripetal acceleration caused by the curvature of the flume and the continuous distortion of the natural turbulence due to the obligatory paddlewheels used to power the flow. Kuenen used a circular flume primarily to counter opponents of the turbidity current hypothesis who claimed that pulsations in current were necessary to produce horizontal laminations. Kuenen also states, (Kuenen, 1965, p. 51),

> "If one were to attempt to feed sediment into a gradually decelerating current in a straight flume, there would be no guarantee that the amount of each grain size were already adjusted to both competency and capacity after a few meters of selective transportation."

It is difficult to say how many meters are necessary for a given sediment size and a given state of turbulence. It was noticed in the present series of experimental runs

that there was no discernible difference in the structures formed downstream of a point about one meter from the headbox. This does not prove that Kuenen is wrong; the structures could well change if another 10 or 100m of flume were available to allow the flow to reach equilibrium. One would have to know a great deal about the frequency and strength of turbulent eddies in order to decide how long a flume is necessary for a given sediment size. The smaller the particle, the longer the distance, but it is difficult to be quantitative about it. One could also make the argument that if the scale of the turbulent eddies were small and their frequency high, it would take less distance for the adjustment. It must be remembered as well that the slower velocity in this set of experiments (Run 4) produced the best apparent capability to produce distinct sedimentary structures (for a given aggradation rate).

It is nonetheless true that the pump and flow entrance section recreate a disequilibrium situation continuously which partially sorts itself out as the flow moves toward the tailbox; the question is, how much distance is needed? Any small-scale experiment will suffer from this difficulty to the extent that it is present; the experimental flow must be powered by a motor and pump and not the activity of a gravity field on a density differential if one is to have laboratory currents lasting more than a few seconds.

Another difficulty with turbidity current simulation in a flume is that the air-water interface is a distinct upward limit on the amount of upward diffusion of sediment

that doesn't exist in the field. The rate of vertical diffusion due to turbulence is a basic property of any sediment laden fluid flow (Briggs and Middleton, 1965), and distorting it artificially with a water surface poses a problem.

Further, one would expect that the temppprature of the water involved in a turbidity current would be perhaps 2-5 deg. C., as opposed to the 16-18 deg. C. possible in this experiment. The viscosity of the water is altered substantially by a fifteen degree change in temperature (Handbook, Chemical Rubber Co.). Also, since the turbidity currents under investigation occur in the ocean, there are additional density and viscosity effects caused by the presence of about 30 parts per 1000 of dissolved salts.

One must make some sort of guess as to the time-dependence of velocity for the typical turbidity current. The velocity must begin at zero and end at zero, when the turbidity current is fully dissipated far out onto the abyssal plain, so there must be a period of increasing velocity and then a decrease, perhaps separated by a longish period of relatively constant velocity. In simulating the distal portion of a turbidity current, the author chose to start out with a relatively high value of velocity (for the flume) and then to decrease it approximately linearly. The rise from zero velocity to a maximum (at a given point on the path) is probably nearly a velocity spike anyway. Additionally, the velocities of several meters a second which are almost certain to occur in the field are not matched by the 60-70 cm/sec obtainable in the flume.

One final difficulty is caused by the lack of a clay fraction. This fraction was removed from the sediment in order that it could be handled more easily, especially in the drying process. Had the clay been present, the sediment would have dried into hard adobe-like blocks which would have required many hours of crushing before they could be used in the sediment feeder to produce a uniform feed rate.

There have been numerous experimental studies showing that the effect of suspended clay on a current composed of silt or sand is non-trivial (Kuenen, 1951; Hauschild, et al., 1961; Kuenen, 1970; Riddell, 1969). The effect on competence and capacity of the flow is substantial, and it has been shown that the presence or lack of a clay fraction in the flume alters the structures that are laid down (Hauschild, et al., 1961).

It is difficult to imagine a current that suspends and transports cubic kilometers of sediment for hundreds of kilometers along the ocean bottom, a current tens of meters tall moving as fast as ten or fifteen meters a second. Even in the most distal sections of interest in this experimental series, the scale will be much larger than that afforded by the average laboratory flume.

In the light of all the above objections, it must be remembered that there is little that can be done experimentally that nears dynamic similitude. Facing the lack of a general theory of turbulence which appears to be several tens of years in the future (and basic to many fields of scientific endeavor), this sort of laboratory experimentation is all

that can be done other than hypothesizing from field evidence to explain the processes that created the field evidence.

Conclusions From The Experiments and Field Samples

Error, Accuracy, and Precision

The estimates of spacing and height for the ripples are accurate to two significant figures. It must be remembered that only 4 m of bed was available for measurement, the 1½ m immediately downstream from the headbox being discounted. The value for the dry sediment feed rate is accurate to two figures and possibly three: for example in Run 3 the times measured to fill a 1000 ml graduated cylinder were 1116, 1110, 1114, and 1115 seconds. The value for the water feed rate is good to two significant figures largely because of uncertainties in the compensation for evaporation (another, different sort of error exists in the estimate of bed porosity).

The value for the discharge is accurate to two significant figures except at the lower values where the ± 1/10" accuracy in reading the manometer becomes relatively more significant. All of the other derived quantities such as mean rate of aggradation, mean flow depth, mean velocity, etc., are good to two significant figures. Of the two methods of determining the mean velocity, the value calculated using the discharge relationship and the point gage profiles is the more accurate. However, the wooden surface float could be used while the flume was running to obtain a value for the mean velocity.

The Field Samples

The field samples differ from the experimental results primarily in the C Interval. The C Interval in the field samples is often convoluted and often incorporates in fine detail the pelagic interval deposited prior to the arrival of the turbidity current. Perhaps the large scale of the true current and the presence of clay are responsible for this. One difficulty noted in the experiments was the tendency of the ripples to destroy the B Interval and to generally rework earlier ripples as they advance. Perhaps with high (several cm/hr) aggradation rates this would be less of a problem, but the experiments have also shown that there is an increase in spacing associated with high aggradation rates. The B (before it was wiped out through truncation) and the D Intervals in the experiments are generally coarser than the corresponding intervals in the samples, perhaps for the reasons mentioned above.

The Experimental Results

The flume experiments indicate that the lower the velocity (provided it is still sufficinet to maintain ripples), the more distinctly the internal structures are delineated by the plant debris. A rapid aggradation rate at a given velocity produces less distinct structures. In the ripple range, reducing the speed increases the spacing of the equilibrium crests. An increase in the aggradation rate also produces an increase in ripple spacing. The height of the ripples does not seem to vary significantly

with a change in velocity for the speed range investigated, and the influence of aggradation rate on ripple height is unclear: at the higher speed of Run 3 the height of the aggraded ripples was less than at the lower mean flow velocity of Run 4, both runs having the same aggradation rate. In Run 3, the height of the aggraded ripples was less than the height of the equilibrium ripples; in Run 4, the aggraded ripples increased in height.

Increasing the aggradation rate increases the size and the general dominance of the trough structures formed in the rippled interval and tends to suppress the formation of the basal trace. Decreasing the speed at a given aggradation rate tends to eliminate the trough structures and favor the basal trace.

Run 5 poses serious questions. The aggradation rate was the same as in Run 2, and the velocity was reduced with time in a generally similar manner (as far as the preserved sedimentary record is concerned). An examination of the photographs of Run 5 show that at no point were structures produced that have much in common with those in Run 2. The ripples were of approximately the same height and spacing (this could only be roughly determined), but their shapes were greatly different. Perhaps the presence of algae was responsible for this, but it could be that the velocity reduction itself coupled with the rate of velocity decrease and the aggradation rate produces the difference since the ripples are never fully in equilibrium with the flow velocity. Run 1 with its long bar-like forms and lack of similarity with Runs 2-4

again points out this possibility.

In future experiments runs should be made with higher aggradation rates (2-10 times those in this study) and the velocity range from 15 to 15 cm/sec investigated at various aggradation rates. A more powerful motor and pump would be of use in performing the velocity reduction runs since it would then be possible to have a 60-75 cm/sec mean velocity with a flow depth much greater than the 6-7 cm now possible. Velocity reduction profiles that begin at 4045 cm/sec and terminate at 10-15 cm/sec should produce interesting results at various aggradation rates.

Appendices

APPENDIX I

Film and Processing Data

The film employed to document the aggradation runs and to photograph the field samples was Kodak Plus-X Pan Professional Film (4147 Estar Thick Base) having an ASA of 125.

The negatives were developed in Kodak developer, HC-110 Dilution A, and the prints were made using Kodabromide F-4 and F-5 high contrast paper and Kodak Dektol developer.

In all cases the subject was underexposed one-half an f-stop and then the negative was developed to achieve the maximum contrast (approximately 8 mins. in HC-110A at 68 deg. F).

This choice of film and developing technique was chosen since it provided a high contrast print as well as the capability for a good amount of enlargement without loss of detail.

APPENDIX II

Description of the Silt Fractions Derived from the Loess

The loess is of Wisconsin Age and was obtained from bluffs near the west bank of the Illinois River west of Springfield, Illinois. It was sieved clean of coarse plant debris, calcareous concretions, and snail shells and was then processed in a large tank. Most of the clay was separated and drained off, and the remaining sediment was separated hydraulically into two size fractions, termed coarser silt and finer silt. The silt coarse fraction which was used in the majority of experimental runs has a mean size of 38 microns, and the finer fraction has a mean size of 30 microns. When used in the flume, each fractions was further cleaned of clay by draining off those particles still in suspension about five minutes of settling in 10 cm of water.

The sediment is composed of highly angular quartz, sub-rounded finely crystalline calcite, and some dolomite rhombs, with minor muscovite, some fine grained heavy minerals, and a small percentage of fine plant detritus which is the dark material that reveals the laminated primary structures in the experimental runs.

APPENDIX III

Description of Fieldwork and Samples

The fieldwork was carried out in the general area of Ashland, Maine, over a two-week period in May and June of 1971. The sample localities are situated in the following quadrangles: Van Buren, Square Lake, Stockholm, Portage, Caribou, Presque Isle, and Ashland. Copies of these quadrangle maps are appended. The sites labelled on the maps are those found to be the best for sampling distal turbidites. Although in a few cases a promising sample was removed from the outcrop, the float rock generally provided the samples.

Although most samples were taken from the Silurian Jemtland formation, the Madawaska Lake, Fogelin Hill, Frenchville, and Aroostook River formations were also sampled. For a detailed account of the geology of the area, see Roy, 1970.

In the laboratory the samples were cleaned for the photographs and, depending on the particular sample, they were sometimes sawed and leached with a weak solution of hydrochloric acid to heighten the contrast of the structures, the acid dissolving some of the carbonate that was usually present. One sample was polished with #600 grit on a wheel and then leached to bring out its fine scaled features. It was found that photographing the samples with the sawed surface wet enhanced the contrast so this was usually done. In some photographs a specimen of the weathered rock is included.

The sample from locality 7 (Photo 32) consists of several D Intervals. The thinning of a D Interval over a slight rise in the bottom can be seen. The parallel laminations stand out well; in some cases one can see a short thin E Interval of pelagix sediment between two D Intervals. In some cases the E Interval is better than ½ cm thick, probably indicating several thousand years of oceanic sedimentation. Sometimes the depositing D Interval produces small incipient flame structures in the E Interval just below. The right-hand block was sawed, leached, and photographed wet. The left-hand block shows the natural surface of the same rock.

The first sample from locality 4 (Photo 31) has, from the bottom up, an E Interval, a D Interval, possibly a thin E Interval, a small slump deposit of some sort, another probable E Interval, truncated by the next feature, a large slump or mudslide with the obvious hump feature. After the slide there came an E Interval, a D Interval, another E, a D, an E, a D, another E, and then another slump similar to the previous one. Then another possible thin E, partially truncated by another small slump, then an E, a weak D, an E, and at the top of the block what appears to be another slump. Thus the sequence is E-D-E(?)-slump-E(?)-slump-E-D-E-D-E-D-E-slump-E(?)-slump-E-D-E-slump. The major slump visible had a good carbonate content and could once have been a limey mud. From the change in the D Interval immediately after the major slump, it appears that the flow had a right to left

component (the D Interval involved is more diffuse to the left of the hump, as it would be after passing over the hump). The photograph shows the natural joint face of the sample, although it was wetted for the photograph.

The first sample from locality 11 (Photo 28) has the following sequence, top to bottom; a series of alternating small D and E Intervals, then what appears to be a C Interval (convoluted instead of rippled, possibly due to a large clay fraction and the cohesivity of the particles), followed by an E Interval that was disturbed by a similar C Interval (this C Interval destroyed the preceeding B Interval, although traces of it can still be seen) which penetrated to the highly water-saturated E and C Intervals below. Above this second C many D Intervals can be seen faintly (if the photograph were not slightly over-exposed they would be clearer). They are so thin and numerous (at least 12 in 2 cm) that one wonders if they are all individual D's separated by small E's or whether they are all related genetically related to the large C Interval. This sample was sawed, leached, and photographed wet.

The second sample from locality 11 (Photo 33) shows two views of some sort of ripple laminated interval. They do not resemble the laboratory aggraded ripples, however, as there are feathery thin laminations of E Interval within the C. Considering that the thin E laminations within the C are truncated it is probably better to consider them as part of

an E that was liad down earlier and then delicately integrated into the C Interval. Following the C Interval there is little or no D before the subsequent E. This is perhaps the most difficult sample to explain in the series. Flow was apparently with a right-to-left component in the top block and a left-to-right component in the bottom one. Perhaps some sort of gentle crumpling could have created these structures, though at first glance, they do appear to be some sort of current rippling. These samples were sawed, leached, and photographed wet.

The second sample from locality 4 (Photo 34) is somewhat similar. The central region is apparently a C Interval with a B Interval below and a D Interval above. One can see other D and E Intervals in the sample. This sample was unsawed, leached, and photographed wet. It must be rememered in all cases that the sawn or joint surface is probably not parallel to the direction of flow, although in most cases there apparently is a large component of the velocity field parallel to the sample face.

The sample from locality 13 (Photo 27) is shown unsawed, leached, and wet. It consists of an A Interval followed by a B, then a crumpled pseudo-rippled C Interval, and then a D Interval. The main difficulty with this sample is the nearly continuous dark band near the center portion. Was this a short E Interval? The grading in the A Interval shows up nicely. The small trough under the "4" and "5" on the scale could be the result of being laid down on a ripple's

back or could be from penecontemporaneous crumpling of some sort.

The first sample from locality 3 (Photo 30) shows from top to bottom an A Interval in which the grading seems to pulsate, a B Interval, a C Interval of convolute lamination, then a D Interval, and finally an E Interval. But again, some sort of darker material (partially cohesive?) is caught up in the convoluted interval. Was it from the previous E Interval? This is hard to believe in the presence of the A Interval. The thin D Interval near the top of the lower block could well be from a separate current (note the partially truncated E Interval below it), but this is hard to say. The upper block shows the rock in its natural state. The lower block was sawed, leached, and photographed wet.

The second sample from locality 3 is the most interesting. There is a sequence of small A Intervals beginning near the bottom. In between them are at least two different types of muddy intervals that could be slumps. Perhaps there were two or three original sources for this deposit; but the change in color of the mud could be accomplished by varying the carbonate content, or by a change in the oxydation potential of the basin. The muddy material is disturbed by the A Interval (see the nascent flame structures). Higher in the sample there is an A Interval similar to the other A's that dies out in the middle of the sample at a fairly steep angle for no apparent reason. Above the A is a faintly

laminated B Interval, a small C Interval that seems to be partially pulled apart, then a D, and finally an E Interval. This sample was sawed, polished on a grinding wheel with #600 grit, then leached with hydrochloric acid, and photographed wet. The small circle in the lower A Interval on the lower right is a fault in the negative; it does not appear in the sample.

The major impression from the samples is one of delicacy and fineness of detail: the small flame structures, the feathery features, the thin E Intervals that have been incorporated within a C Interval, and so on. The incorprroration of part of an E Interval within a C should generate a new descriptive term since the "E" Interval in this case was uprooted and shifted relatively intact by the C Interval.

Tables and Figures

TABLE 1

H_2O REQUIRED BY BED POROSITY

1. 31 ML PACKED SED REQUIRES

   10.9 ML H_2O TO FILL PORES → .35 ML/ML

2. 30 ML PACKED SED REQUIRES

   10.8 ML H_2O TO FILL PORES → 36 ML/ML

AVERAGE → 0.355 ML H_2O/ML SED

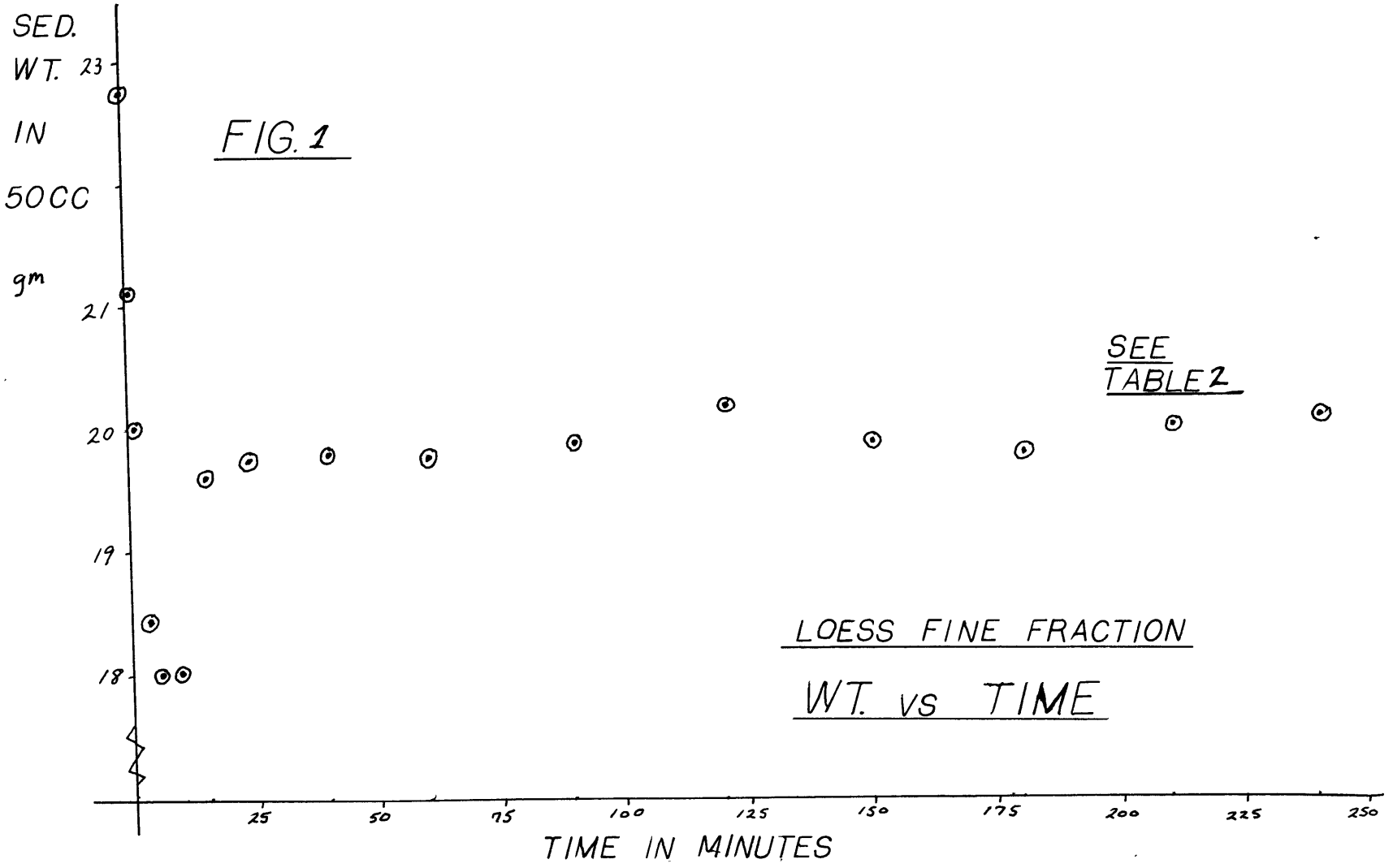

FIG. 1

SEE TABLE 2

LOESS FINE FRACTION

WT. VS TIME

TABLE 2 — LOESS FINE FRACTION

50CC ±.2cc

PIPETTE ANALYSIS — ΔH: 18" → 9" AT TIME = 0

#	TIME	GROSS	TARE	NET WT.*
1	000 min	50.01 gm	27.26 gm	22.75 gm ±.02
2	001	50.21	29.09	21.12
3	002	49.02	29.02	20.00
4	004	47.97	29.53	18.44
5	006	55.69	37.67	18.02
6	010	46.52	28.49	18.03
7	015	48.90	29.30	19.60
8	025	49.87	30.13	19.74
9	040	48.72	28.91	19.81
10	060	49.01	29.22	19.79
11	090	48.88	28.97	19.91
12	120	49.53	29.33	20.20
13	150	47.90	28.01	19.89
14	180	48.74	28.95	19.79
15	210	50.58	30.54	20.04
16	240 min	49.28	29.16	20.12
17				

T = 22°C 80 MINS. RUN AT 18" *DRY

TOTAL DEPTH = 6.5 CM SEE FIG. 1

TABLE 3 — LOESS FRACTION, FINE

50CC ±.2cc
PIPETTE ANALYSIS

#	GROSS	TARE	NET wt.*	$\bar{C}$	$\Delta H''$	$\bar{V}$	$\bar{Y}$
1	56.50gm	27.26gm	29.24gm ±.02	0.586 $\frac{gm}{cc}$	16 ±.1"	59.2 cm/sec	6.65cm
2	58.17	29.09	29.08	.583	15	57.6	6.54
3	57.92	29.02	28.90	.578	14	55.5	6.53
4	58.43	29.53	28.90	.578	13	55.5	6.29
5	66.22	37.67	28.55	.571	12	54.3	6.29
6	56.85	28.49	28.36	.567	11	52.4	6.20
7	57.08	29.30	27.78	.555	10	49.7	6.20
8	57.29	30.13	27.16	.543	9	49.7	5.89
9	55.67	28.91	26.76	.535	8	49.2	5.66
10	49.25	29.22	(25.02)	(.502)	(7-6)	46.2	5.64
11	58.97	28.97	(25.02)	(.502)	(7-6)	46.2	5.21
12	54.20	29.33	24.87	.498	5	44.5	4.91
13	51.70	28.01	23.69	.475	4	45.4	4.36
14	50.96	28.95	22.01	.442	3	42.1	4.03
15	49.48	30.54	18.94	.379	2	35.4	3.95
16	41.19gm	29.16gm	12.03gm	.240 $\frac{gm}{cc}$	1	29.6 cm/sec	3.25
17							

$T = 22°C$

$\bar{V} = V_s \cdot 85$

$Q = 7\sqrt{\Delta H''} \cdot 0.06$ CFS

$\bar{Y} = Q/\bar{V} \cdot w$

Flow kept AT GRADE

( ) → #10 & #11 WERE mixed to get AN AVERAGE - VALUE Suspect

SEE FIG. 2

*DRY

ΔH dropped 1" AT 5 min INTERVALS

V_s gotten FROM AN AVERAGE OF 3 times OVER 183 cm dist ±.1 Sec → $\bar{V}$ good to 1 part IN 50 AT worst (IF $\bar{V} = V_s \cdot 85$ is ASSumed TRUE)

TABLE 4 — LOESS FINE FRACTION

50CC ±.2cc

PIPETTE ANALYSIS

#	GROSS	TARE	NET wt.	$\bar{C}$	ΔH	$\bar{V}$	$\bar{Y}$
1	51.34 gm	27.26 gm	24.08 gm ±.02	0.484 gm/cc	18" ±.1"	64.8 cm/sec	6.4 cm
2	51.55	29.09	22.46	0.451	12	56.0	6.07
3	50.00	29.02	20.98	0.419	8	49.4	5.61
4	47.51	29.53	17.88	0.358	6	46.7	5.13
5	53.99	37.67	16.32	0.326	4	42.4	4.56
6	37.63	28.49	9.14	0.183	2	36.8	3.76
7	33.45 gm	29.30 gm	4.15 gm	0.083 gm/cc	1"	32.9 cm/sec	2.96 cm
8							

Flow kept At Grade.

$Q = \sqrt{\Delta H"} \cdot 0.06$ cfs

$\bar{y} = Q/\bar{v}w$

$\bar{V} = V_s \cdot 0.85$

1 Hr. Run At EACH ΔH → Samples taken 46 mins into EACH HR.

$T = 36°C$

SEE FIG. 2

FIG 2

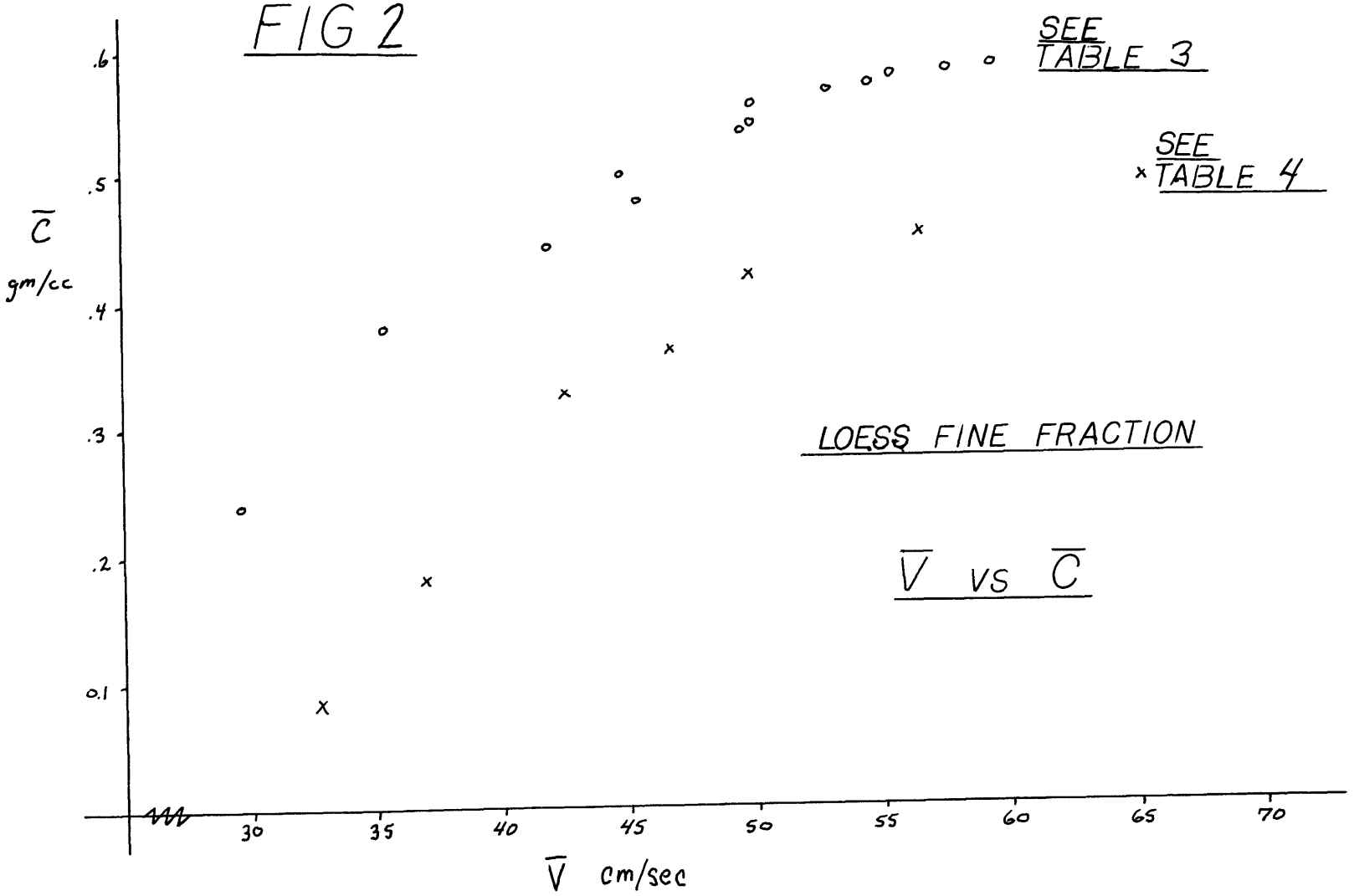
SEE TABLE 3
SEE TABLE 4
LOESS FINE FRACTION
$\overline{V}$ VS $\overline{C}$
$\overline{C}$ gm/cc
.6
.5
.4
.3
.2
0.1
30
35
40
45
50
55
60
65
70
$\overline{V}$ cm/sec

FIG 3

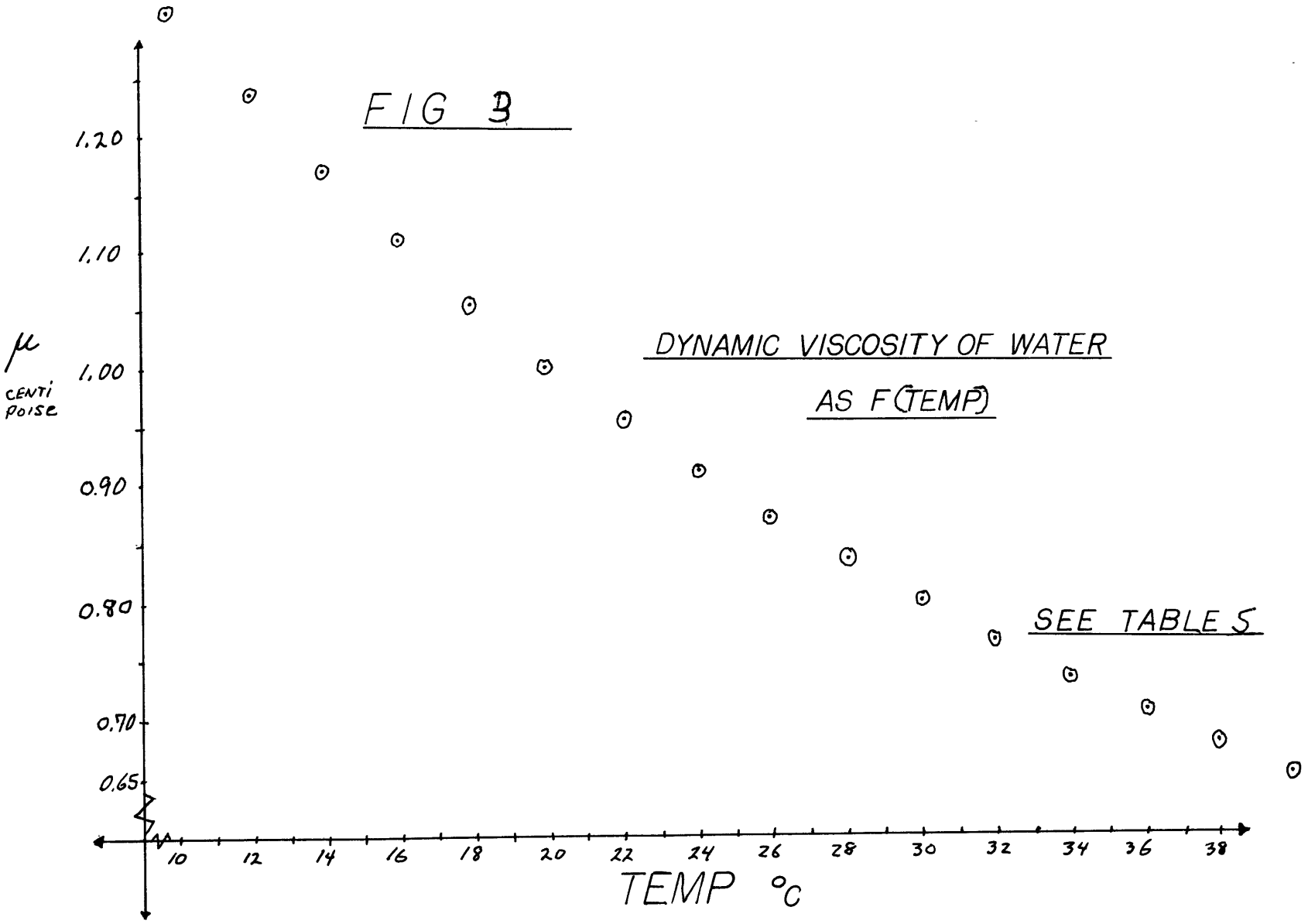
DYNAMIC VISCOSITY OF WATER
AS F(TEMP)
SEE TABLE 5
μ
CENTI POISE
1.20
1.10
1.00
0.90
0.80
0.70
0.65
10
12
14
16
18
20
22
24
26
28
30
32
34
36
38
TEMP °C

TABLE 5

H_2O DYNAMIC VISCOSITY AS F(TEMP)

TEMP °C	μ CENTI-POISE
10	1.307
12	1.235
14	1.169
16	1.109
18	1.053
20	1.002
22	0.9548
24	0.9111
26	0.8705
28	0.8327
30	0.7975
32	0.7647
34	0.7340
36.	0.7052
38	0.6783
40	0.6529

SEE FIG 4

FIG 4

LOESS COARSE FRACTION

$\overline{C}$ vs TIME

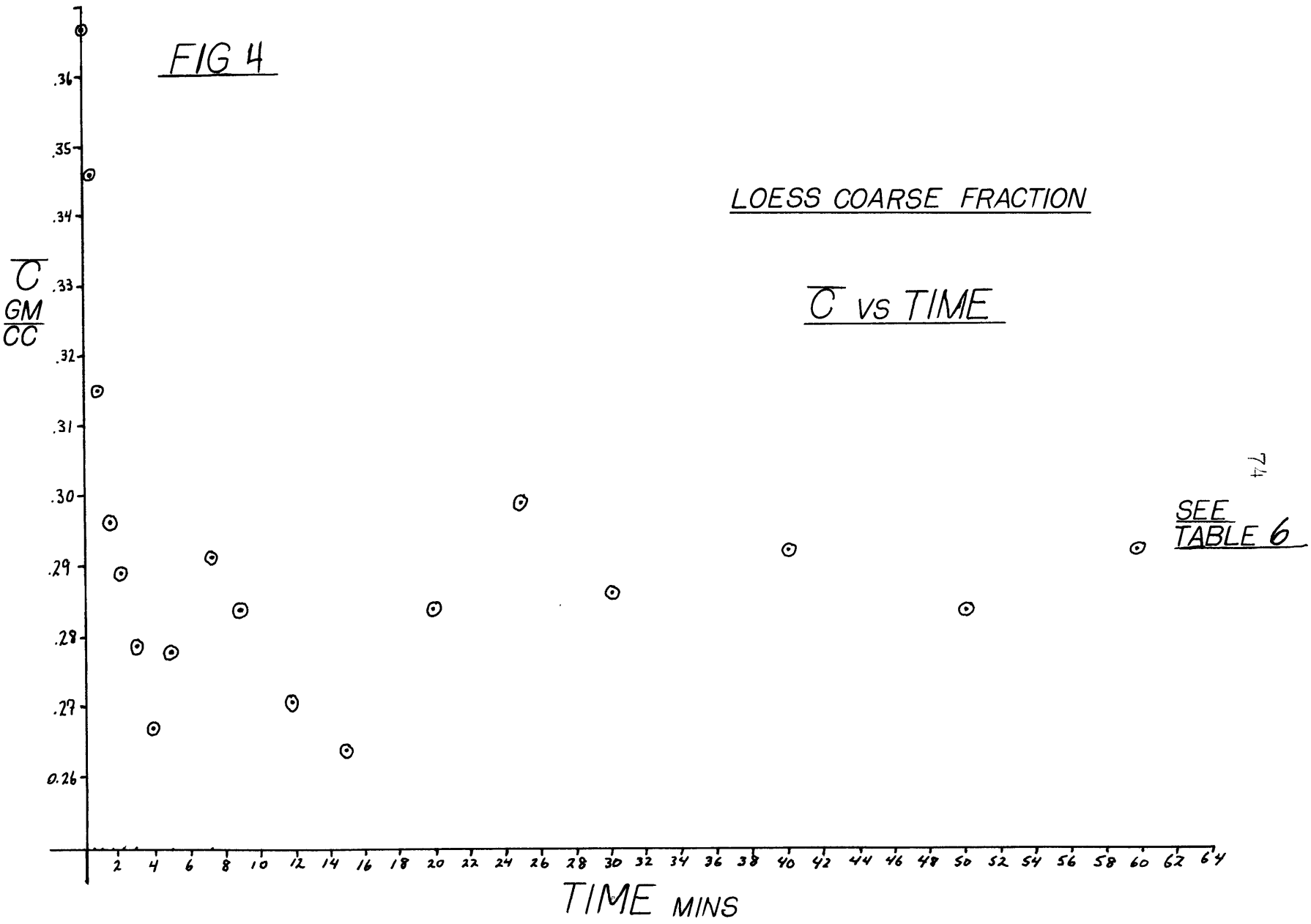

SEE TABLE 6

TABLE 6

50CC ±.2cc

PIPETTE ANALYSIS

LOESS COARSE FRACTION

ΔH: 18" → 9" At TIME = 00 MINS

50 MINS At 18" PRIOR to drop.

#	TIME	GROSS	TARE	NET WT.	$\overline{C}$
1	00.0 MIN	45.62 gm	27.29 gm	18.33 gm ±.02	0.367 gm/cc
2	0.50	46.43	29.11	17.32	.346
3	1.10	44.67	29.05	15.64	.314
4	1.75	44.36	29.55	14.81	.296
5	2.33	52.12	37.71	14.41	.289
6	3.0	42.43	28.50	13.93	.279
7	4.0	40.33	27.02	13.31	.267
8	5.0	43.14	29.26	13.88	.278
9	7.25	41.57	27.00	14.57	.291
10	9.0	41.24	27.10	14.14	.283
11	12.0	39.96	26.47	13.49	.270
12	15.0	39.73	26.62	13.11	.263
13	20.0	41.62	27.49	14.13	.283
14	25.0	42.11	27.27	14.84	.298
15	30.33	40.70	26.45	14.25	.286
16	40.0	41.27	26.68	14.59	.292
17	50.0	43.73	29.60	14.13	.283
18	60.0 MIN	43.32 gm	28.71 gm	14.61 gm	.292
19					

T = 17°C FLOW AT GRADE. SED. + H_2O = 6.7 cm.

SEE FIG 5

TABLE 7

LOESS COARSE FRACTION

50CC ±.2cc

PIPETTE ANALYSIS

#	GROSS	TARE	NET wt.*	$\bar{C}$	$\Delta H''$	$\bar{V}$	$\bar{y}$
1	40.54gm	26.67gm	13.87gm ±.02	0.278 gm/cc	16" ±.1	62.2 cm/sec	6.30cm
2	41.03	26.92	14.11gm ±.02	0.282	15	58.4	6.62
3	40.63	27.21	13.42	0.268	14	57.6	6.34
4	40.56	27.80	12.76	0.255	13	57.6	6.12
5	38.78	26.74	12.04	0.241	12	56.4	6.03
6	39.52	28.11	11.41	0.228	11	52.9	6.11
7	37.73	26.70	11.03	0.221	10	52.5	5.90
8	38.45	27.52	10.93	0.218	9	49.4	5.96
9	35.70	26.03	9.67	0.193	8	49.1	5.65
10	35.72	26.47	9.25	0.185	7	48.9	5.31
11	35.73	27.86	7.87	0.157	6	46.0	5.23
12	33.63	26.42	7.21	0.144	5	44.4	4.93
13	31.20	26.08	5.12	0.102	4	42.6	4.61
14	30.54	26.89	3.65	0.0731	3	35.2	4.82
15	27.92	26.50	1.42	0.0284	2	30.8	4.51
16	27.55gm	27.32gm	0.23 ±.02	0.00462	1	22.9	4.27
17							

$Q = \sqrt{\Delta H''} \cdot 0.06$ c.f.s. $T = 18°C$

$\bar{V} = V_s \cdot 0.85$ $\bar{y} = Q/\bar{V}w$

FLOW kept AT GRADE

1 Sample EACH 30 MINS. Just beFORE 1" ΔH drop.

Run At 16" FOR 60 MINS beFORE FIRST drop.

*DRY

SEE FIG. 5

SEE TABLE 7

FIG. 5

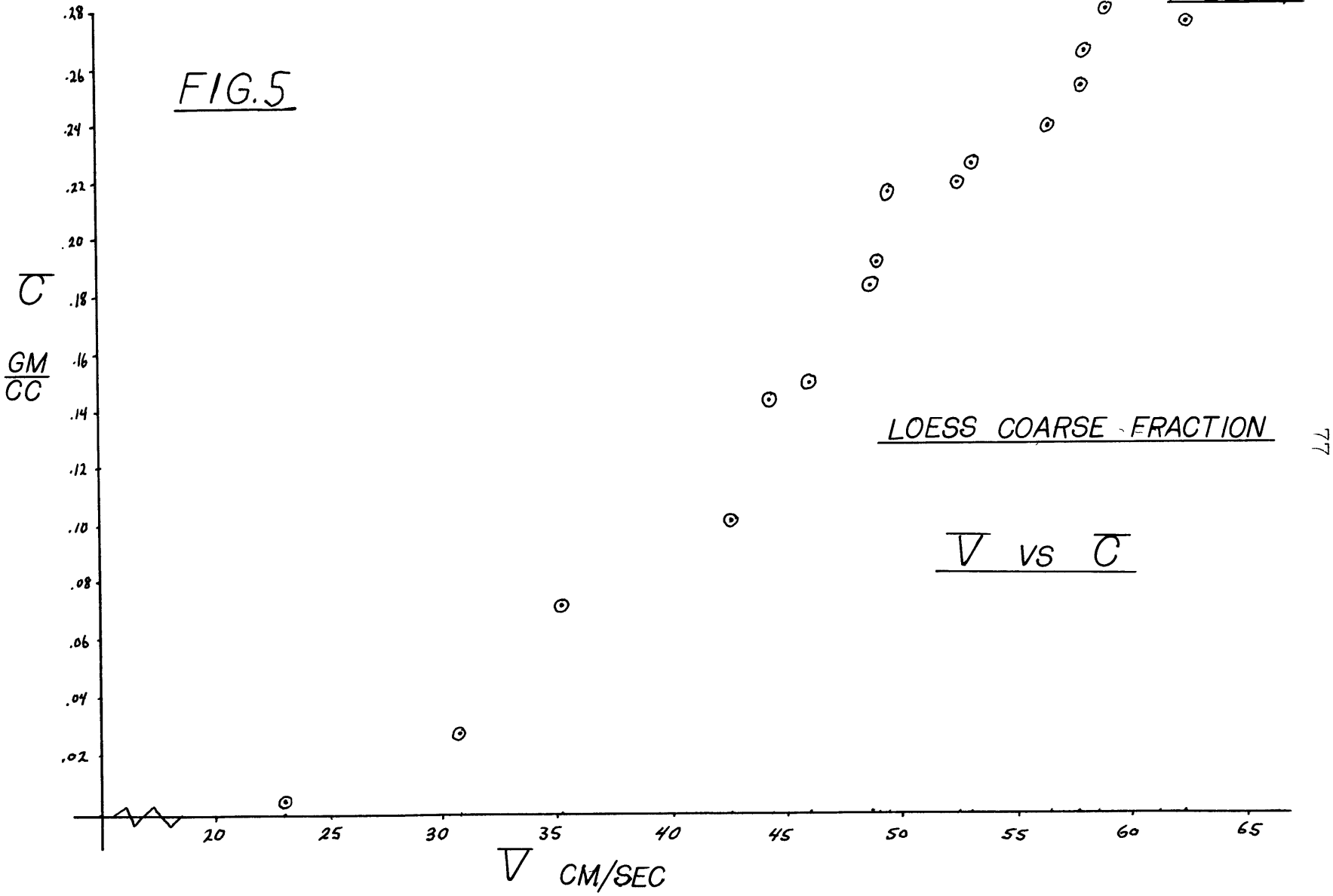

LOESS COARSE FRACTION

$\overline{V}$ VS $\overline{C}$

TABLE 8

RUN ONE +

50CC

PIPETTE ANALYSIS

LOESS COARSE FRACTION

Q_S = 2.23 ML/SEC $\bar{D}$ = 6.9 mm/hr.

Q_B = 0.64 ML/SEC

#	GROSS	TARE	NET WT.	ΔH	TIME	$\overline{V_A}$	$\overline{V_P}$	$\overline{C}$	$\overline{Y}$
1	41.46 gm	26.94 gm	14.52 gm ±.02	16" ±.1	00 mins	62.2 cm/sec	62.2	.291 gm/cc	6.30 cm
2	42.57	27.18	15.39	17.0	30	61.4	62.2	.308	6.56
3	43.05	26.80	16.25	18.0	60	62.2	62.2	.326	6.58
4	44.66	26.01	18.65	18.0	90	57.6	62.2	.374	7.18
5	46.15	26.72	19.43	18.0"	120	56.2	62.2	.389	7.37
6	50.71	30.07	20.64	18 3/4	150	51.8	53.6	.413	8.18
7	48.26	26.87	21.39	(16)	180	47.5	47.2	.428	8.23
8	40.81	26.60	14.21	12.0	210	42.3	42.0	.284	8.02
9	38.22	28.88	9.34	3.2	240	38.1	37.9	.187	4.60
10	33.91	29.21	4.70	1.7	270	32.9	34.6	.094	3.87
11	30.92	28.96	1.96	1.1	300	31.2	31.7	.039	3.30
12	30.21	29.28	0.93	0.8	330	29.2	29.4	.019	3.00
13	28.67	27.99	0.68	0.7"	360	27.7	27.3	.014	2.94
14	29.65 gm	28.94	0.71 gm	07"	390	24.7	25.5	.014	3.31
15	—	26.16 gm			420 mins	11.9 cm/sec	23.9		
16									

SEE FIG 6

SEE FIG 7

T = 17.9°C

FLOW AT GRADE

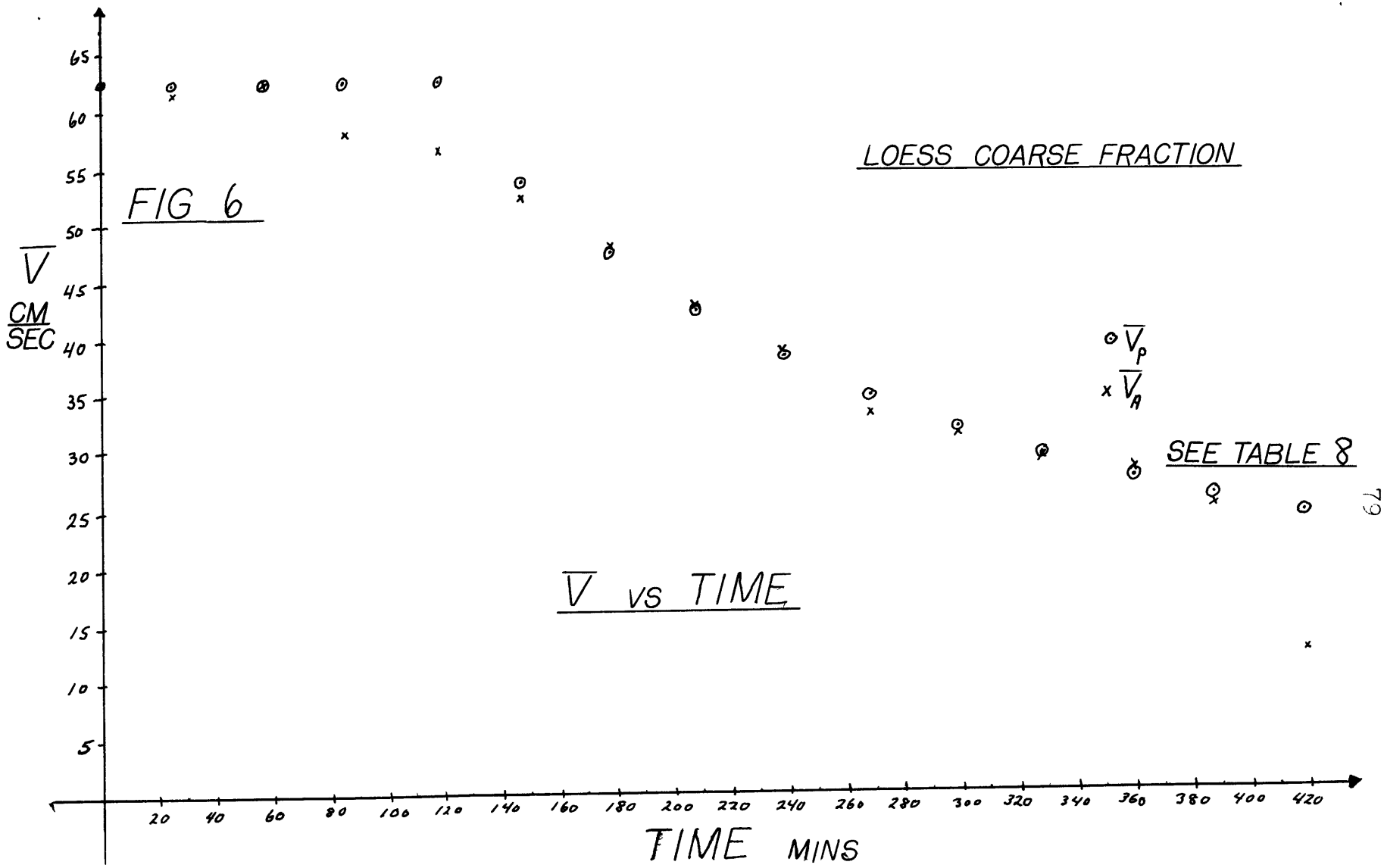
FIG 6
LOESS COARSE FRACTION
$\overline{V}$ CM/SEC
65
60
55
50
45
40
35
30
25
20
15
10
5
$\overline{V}_P$
$\overline{V}_A$
SEE TABLE 8
$\overline{V}$ VS TIME
20 40 60 80 100 120 140 160 180 200 220 240 260 280 300 320 340 360 380 400 420
TIME MINS

FIG 7

LOESS COARSE FRACTION

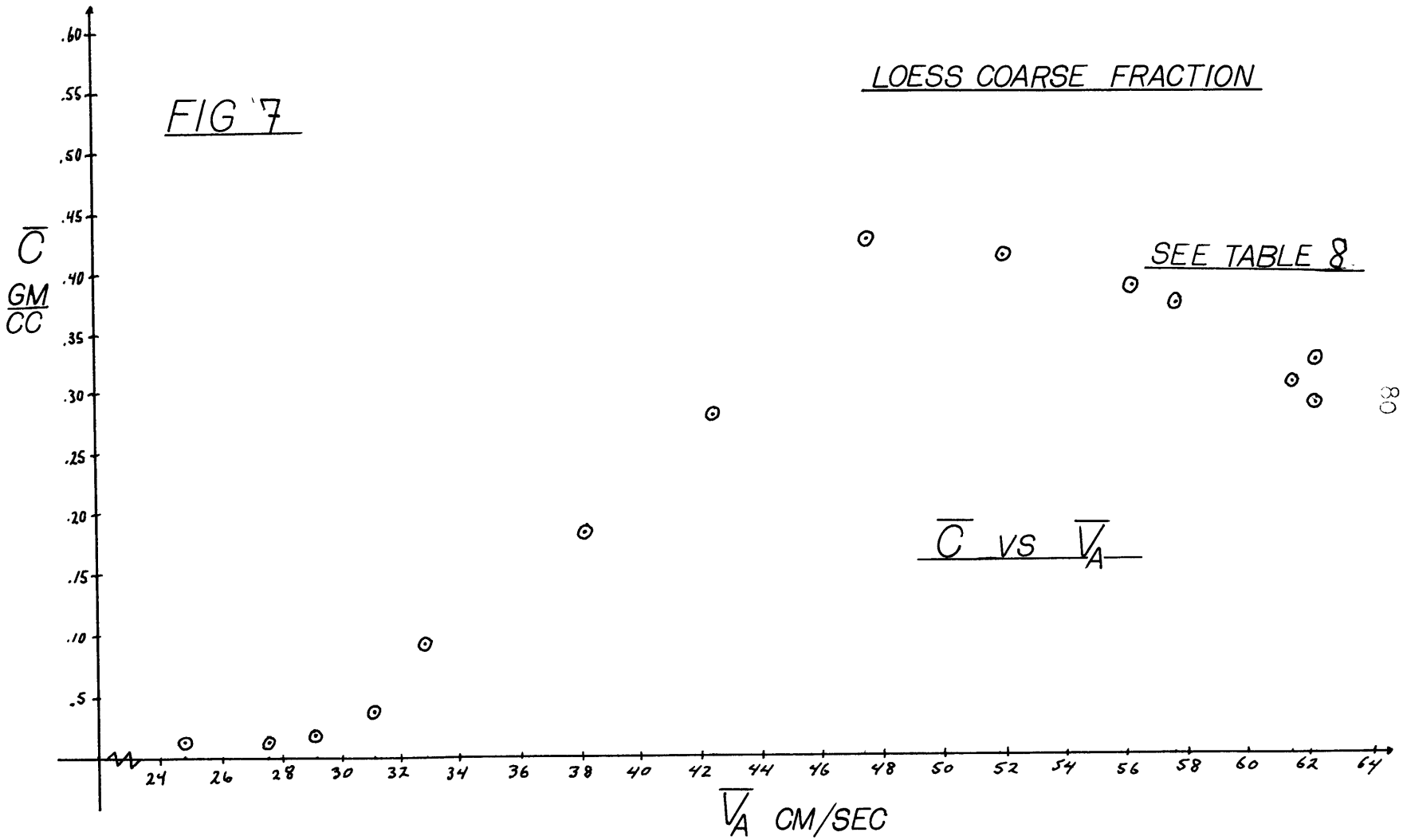

SEE TABLE 8

$\overline{C}$ VS $\overline{V_A}$

TABLE 9 LOESS COARSE FRACTION

RUN TWO +
50CC ±.2cc
PIPETTE ANALYSIS

#	GROSS	TARE	NET WT	TIME	$\overline{C}$
1	28.37 gm	26.94 gm	1.43 gm ±.02	00 min	gm/cc .0286
2	28.44	27.18	1.26	120	.0252
3	28.08	26.80	1.28	210	.0256
4	27.41	26.01	1.40	360	.0280
5	28.04	26.72	1.32	465	.0264
6	31.37	30.07	1.30	585	.0260
7	28.14	26.87	1.27	705	.0254
8	28.14	26.80	1.34	825	.0268
9	30.58	28.88	1.70	945	.0340
10	30.71	29.21	1.50	1065	.0300
11	29.35	27.86	1.49	1135	.0298
12	30.81	29.28	1.53	1136	.0306
13	29.53	27.99	1.54	1200	.0308
14	30.17	28.94	1.23	1340	.0246
15	28.13	26.39	1.74	1445	.0348
16	29.17 gm	27.32 gm	1.85	1545	.0371
17					

Q_S = 0.400 cc/sec

Q_B = 0.116 cc/sec

$\Delta H = \begin{matrix} 14.2 \\ 14.2 \\ 14.6 \end{matrix}\} 14.33$"

TEMP = 16°C

SED FEED: 27½ hrs

EQUIL RUN: 22 hrs

Q = 6430 cc/sec

W = 17.4 cm

$\overline{Y}$ (FROM PROFILES) = 10.48 cm

$\overline{V}$ = 40.4 (FROM AU OF 43 V_s MEASUREMENTS)

$\overline{V}$ = 35.4 (FROM PROFILES & CALCULATIONS) cm/sec.

$Q/\omega\overline{Y} = \overline{V}$

$\dot{D}$ = 1.2 mm/hr.

TABLE 10 LOESS COARSE FRACTION

RUN THREE +

50CC ±.2cc

PIPETTE ANALYSIS

#	GROSS	TARE	NET WT	TIME	$\bar{C}$
1	28.09gm	26.94gm	1.15gm ±.02	00 min	.0230 gm/cc
2	28.60	27.18	1.42	60	.0284
3	28.44	26.80	1.64	120	.0328
4	27.87	26.01	1.86	180	.0372
5	28.52	26.72	1.80	182	.0360
6	32.02	30.07	1.95	240	.0390
7	28.74	26.87	1.87	300	.0374
8	28.52	26.47	2.05	360	.0410
9	31.63	28.88	2.75	420	.0550
10	31.50	29.21	2.29	480	.0458
11	32.54	28.96	3.58	540	.0716
12	32.65	29.28	3.27	600	.0654
13	31.73	27.45	4.28	660	.0856
14	32.50	28.94	3.56	820	.0713
15	30.25gm	26.40	3.85gm	880 min	.0772 gm/cc
16	-	27.32gm	-	-	-
17					

Q_S = 0.897 ml/sec

Q_B = 0.263 ml/sec

ΔH = 15.67"

TEMP = 18°

SED FEED = 14½ hrs

EQUIL RUN = 19 hrs

Q = 6720 cc/sec

W = 17.4 cm

$\bar{Y}$ (FROM PROFILES) = 9.37 cm

$\bar{V}$ = 39.7 cm/sec (AV OF 43 V_S'S)

$\bar{V}$ = 40.7 cm/sec (FROM PROFILES + CALCS)

$Q/w\bar{y} = \bar{V}$

$\bar{D}$ = 2.8 mm/hr

TABLE II
RUN FOUR

LOESS COARSE FRACTION

50CC ±.2cc
PIPETTE ANALYSIS

#	GROSS	TARE	NET WT	TIME	$\overline{C}$
1	27.00 ±.01 gm	26.93 ±.01 gm	0.07 ±.02 gm	−1470 min	.0014 gm/cc
2	27.27	27.17	0.10	−1170½	.0020
3	26.12	26.04	0.08	−1170	.0016
4	29.61	29.54	0.09	−330	.0018
5	28.20	28.10	0.10	00	.0020
6	27.11	27.00	0.11	+10	.0022
7	26.86	26.60	0.26	60	.0052
8	26.30	26.02	0.28	120	.0056
9	29.47	29.22	0.25	180	.005
10	28.19	27.86	0.33	240	.0066
11	26.95	26.62	0.33	300	.0066
12	26.42	26.07	0.35	360	.007
13	28.17	27.79	0.38	420	.0076
14	27.14	26.74	0.40	480	.0080
15	27.71	27.11	0.60 ?	540	.0120
16	29.72	29.54	0.18 ?	600	.0036
17	29.09	28.74	0.35	750	.007

Q_S = 0.897 ml/sec

Q_B = 0.263 ml/sec

ΔH = 6.9"

TEMP = 17°C

SED FEED = 13 1/6 hrs

EQUIL RUN = 38 hrs.

Q_w = 4460 cc/sec

W = 17.4cm

$\bar{Y}$ (From Profiles) = 10.08cm

$\bar{V}$ = (From time meas., 31) = 29.0 cm/sec

$\bar{V}$ = (From Profiles) = 25.5 cm/sec

$Q/w\bar{y} = \bar{V}$

$\bar{D}$ = 2.8 mm/hr.

TABLE 12

RUN FIVE +

50 CC

PIPETTE ANALYSIS

LOESS COARSE FRACTION

Q_S = 0.400 ML/sec

Q_B = —

$\bar{D}$ = 1.2 mm/hr

#	GROSS	TARE	NET WT	H	TIME	$\bar{V}_A$	$\bar{V}_P$	$\bar{C}$	$\bar{Y}$
1	42.68 gm	26.46 gm	16.22 ±.02 gm	12.3"	00' mins	64.8 cm/sec	62.2	0.324 gm/cc	5.30 cm
2	44.66	27.15	17.51	9.6	180	56.2	55.5	.351	5.38
3	47.07	27.16	19.91	8.2	360	50.6	50.2	.398	5.58
4	45.25	26.65	18.60	18.0	540	46.2	45.7	.372	9.00
5	49.17	37.67	11.50	12.5	720	42.0	42.0	.230	8.22
6	41.03	28.08	12.95	10.1	900	38.2	38.9	.259	8.08
7	39.79	26.99	12.80	8.0	1080	36.2	36.2	.256	7.65
8	33.97	26.58	7.39	6.8	1260	33.8	33.8	.148	7.55
9	30.63	26.42	4.21	4.2	1440	31.9	31.7	.084	6.77
10	31.80	29.20	2.60	3.5	1620	29.8	29.8	.052	6.16
11	30.59	28.69	1.90	2.8	1800	28.2	28.2	.038	5.80
12				=					

See Fig. 8

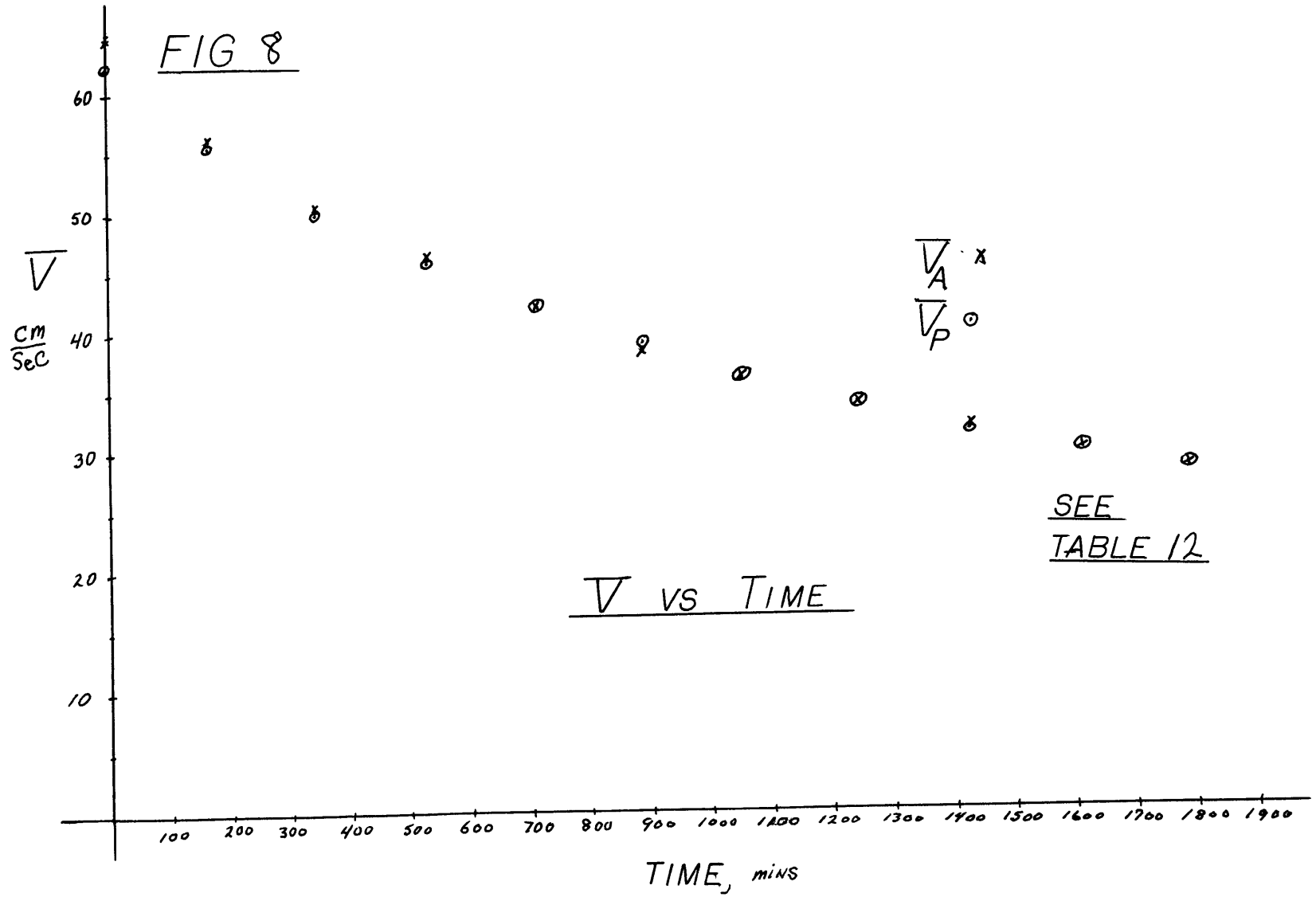
FIG 8
60
50
40
30
20
10
$\overline{V}$
cm/sec
$\overline{V}_A$
$\overline{V}_P$
SEE TABLE 12
$\overline{V}$ VS TIME
100 200 300 400 500 600 700 800 900 1000 1100 1200 1300 1400 1500 1600 1700 1800 1900
TIME, mins

TABLE 13 LIST OF EXPERIMENTAL RUNS

RUN #	Q	Q_B	Q_S	$\bar{D}$	$\bar{Y}$ PROFILES	$\bar{V}$ PROFILES / $\bar{V}$ TIMES	TEMP	ΔH	Aggradation Time	EQUILIBRIUM Run Time
1	VARIES	0.64 ml/sec	2.23 ml/sec	6.9 mm/hr	VARIES	VARIES / VARIES	17.9°C	0.7→18.75"	420 MINS	0 MINS
2	6430 cc/sec	0.116	0.400	1.2 mm/hr	10.48 cm	35.4 cm/sec / 40.4 cm/sec	16.0	14.3	1645	1320
3	6720	0.263	0.897	2.8 mm/hr	9.37	48.7 / 39.7	18.0	15.7	870	1140
4	4460	0.263	0.897	2.8 mm/hr	10.08	25.5 / 29.0	17.0	6.9	790	2240
5	Varies	NONE	0.400	1.2 mm/hr	VARIES	VARIES / VARIES	20.0°C	2.8→18"	1800	0

$$\bar{D} = \left[\frac{\Phi_s}{\omega L}\right] 0.82$$

Bibliography:

Allen, J.R.L., 1960, The mam tor sandstone: J. Sediment. Petrology, v. 30, p. 193-208.

———, 1968, The nature and origin of bed form hierarchies: Sedimentology, v. 10, p. 161-182.

———, 1970, The sequence of sedimentary structures in turbidites with special reference to dunes: Scot. J. Geol., v. 6, no. 2, p. 146-161.

———, 1971, Mixing at turbidity current heads: J. Sediment. Petrology, v. 41, p. 97-113.

Bagnold, R.A., 1966, An approach to the sediment transport problem from general physics: U.S. Geol. Surv. Prof. Pap. 422-I.

———, 1962, Auto-suspension of transported sediments; turbidity currents: Proc. Roy. Soc. London Ser. A, v. 265, p. 315-319.

Ballance, R.F., 1964, The sedimentology of the waitemata group in the takapuna section, Auckland: N.Z. J. Geol. Geophys., v. 7, p. 466-499.

Bassett & Walton, 1960, The hell's mouth grits: Quart. J. Geol. Soc. London, v. 116, p. 85-110.

Belderson, R.H. & Laughton, A.S., 1966, Correlation of some Atlantic turbidity currents: Sedimentology, v. 7, p. 110-116.

Boswell, P.G.H., 1960, The term greywacke: J. Sediment. Petrology, v. 30, p.,154-157.

Bouma, A.H., 1962, Sedimentology of some flysch deposits, Elsevier, Amsterdam & New York.

———, 1964, Turbidites, in Developments in sedimentology, v. 3, Elsevier, Amsterdam & New York.

Briggs, L.I. & Middleton, G.V., 1965, Hydromechanical principles of sediment structure formation, in Primary sedimentary structures and their hydraulic interpretation: Soc. Econ. Paleontol. Mineral. Spec. Pub. 12, p. 5-16.

Brush, L.M., 1959, Absence of cross-stratification in the bed regimes of density underflows (abs.): Geol. Soc. Amer. Bull., v. 70, p. 1576.

Bye, J.A.T., 1971, The slope of abyssal plains: J. Geophys. Research, v. 76, no. 18, p. 4188-4194.

Carozzi, A., 1957, Tracing turbidity current deposits down the slope of an alpine basin: J. Sediment. Petrology, v. 27, p. 271-281.

Chemical Rubber Company, 1970, Handbook of chemistry and physics, 50th edition, Cleveland, Ohio, p. F-36.

Conolly, J.R. & Ewing, M., 1969, Redeposition of pelagic sediments by turbidity currents; a common process for building abyssal plains: Amer. Ass. Petrol. Geol. Bull. v. 53, no. 9, p. 2034.

Crowell, J.C., 1968, Sole markings: J. Geol., v. 66, p. 333-335.

Daily, J.W. & Harleman, D.R.F., 1966, Fluid dynamics, Addison-Wesley, Reading, Massachusetts, p. 33.

Dzulynski, S., Ksiazkiewicz, M., & Kuenen, Ph.H., 1959, Turbidites in flysch of the Polish Carpathian Mountains, Geol. Soc. Amer. Bull., v. 70, p. 1089-1118.

Dzulynski, S. & Walton, E.K., 1965, Sedimentary features of flysch and greywackes, Developments in sedimentology, v. 7, Elsevier, Amsterdam & New York.

Enos, P., 1969, The cloridorme formation, Geol. Soc. Amer. Spec. Pap. 117.

———, 1969, Anatomy of a flysch: J. Sediment. Petrology, v. 39, p. 680-723.

Gibbs, R.J., Matthews, M.D., & Link, D.A., 1971, The relationship between sphere size and settling velocity: J. Sediment. Petrology, v. 41, p. 7-18.

Gorsline, D.S. & Emery, K.O., 1959, Turbidity current deposits: Geol. Soc. Amer. Bull., v. 70, p. 279-290.

Harms, J.C. & Fahnestock, R.K., 1965, Stratification, bed forms, and flow phenomena (with an example from the Rio Grande); in Primary sedimentary structures and their hydraulic interpretation, Soc. Econ. Paleontol. Mineral. Spec. Pub. 12, p. 84-115.

Hauschild, W.L., Simons, D.B., & Richardson, E.V., 1961, The significance of the fall velocity and effective fall diameter of bed materials: U.S. Geol. Surv. Prof. Pap. 424-D, Art. 300, p. D17-D20.

Hsu, K.J., 1959, Flute and groove casts in the pre-alpine flysch, Switzerland: Amer. J. Sci., v. 257, p. 529-536.

———, 1960, Paleocurrent structures: Geol. Soc. Amer. Bull., v. 71, p. 577-610.

———, 1964, Cross laminations in graded bed sequences: J. Sediment. Petrology, v. 34, p. 379-388.

Hubbell, D.W., & Ali, K. A₇-S., 1961, Qualitative effects of temperature on flow phenomena in alluvial channels: U.S. Geol. Surv. Prof. Pap. 424-D, Art. 301., p. D21-D23.

Hubert, J.F., 1967, Sedimentology of pre-alpine flysch sequences, Switzerland; J. Sediment. Petrology, v. 37, p. 885-907.

Johnson, M.A., 1966, Application of theory to an atlantic turbidity current path: Sedimentology, v. 7, p. 117-129.

Kelling, G., & Wlaton, E.K., 1961, Flow structures in sedimentary rocks: J. Geol., v. 69, p. 224-225.

Knapp, R.T., 1938, Energy Balance in stream flows carrying a suspended load: Trans. Ameri Geophys. Union, v. 19, p. 501-505.

Knapp, R.T., & Bell, H.S., 1941, Density currents: Trans. Amer. Geophys. Union, v. 22, p. 257-261.

Komar, P.D., 1970, The competence of turbidity current flow: Geol. Soc. Amer. Bull., v. 81, p. 1555-1562.

———, 1971, Hydraulic jumps in turbidity currents: Geol. Soc. Amer. Bull., v. 82, p. 1477-1487.

Kuenen, Ph. H., 1950, Turbidity currents as a cause of graded bedding: J. Geol., v. 58, p. 91-127.

———, 1951, Properties of turbidity currents of high density: in Turbidity currents, Soc. Econ. Paleontol. Mineral. Spec. Pub. 2, p. 13-14.

———, 1952, Turbidity currents, graded and non-graded deposits: J. Sediment. Petrol., v. 22, p. 83-96.

Kuenen, Ph. H., 1953, Turbidity currents and sliding in geosynclinal basins in the alps: J. Geol., v. 61, p. 363-373.

———, 1953, Significant features of graded bedding; Amer. Ass. Petrol. Geol. Bull., v. 37, p. 1044-1066.

———, 1957, Sole markings: J. Geol., v. 65, p. 321-258.

———, 1964, Deep sea sands and ancient turbidites, in Turbidites, Developments in Sedimentology, v. 3, Bouma & Brouwer, eds., Elsevier, Amsterdam & New York.

———, 1965, Experiments in connection with turbidity currents and clay suspensions, in Submarine geology and geophysics, Butterworth's, London, p. 47-74.

———, 1966, Experimental turbidite lamination in a circular flume; J. Geol., v. 74, p. 523-545.

———, 1966, Matrix of turbidites — an experimental approach: Sedimentology, v. 7, p. 267-297.

———, 1970, Experimental marine suspension currents: Geol. Mijnbouw, v. 49, p. 89-118.

———, 1970, A reply to van der Lingen: N.Z. J. Geol. Geophys., v. 13, p. 852-857.

———, 1971, Tentative data on flow resistance in turbidity currents: Geol. Mijnbouw, v. 50, p. 429-442.

Menard, H.W.,& Ludwick, J.C., 1951, Applications of hydraulics to the study of marine turbidity currents: in Turbidity currents, Soc. Econ. Paleontol. Mineral. Spec. Pub. 2., p. 2-13.

McKee, E.D.& Weir, G.W., 1953, Terminology for stratification and cross-stratification in sedimentary rocks: Geol. Soc. Amer. Bull., v. 64, p. 381-390.

McKee, E.D., 1957, Flume experiments on the production of stratification and cross-stratification: J. Sediment. Petrology, v. 27, p. 129-134.

———, 1957, Primary structures in recent sediments: Amer. Ass. Petrol. Geol. Bull., v. 41, p. 1704-1747.

Middleton, G.V., 1966, Experiments on density and turbidity currents I, Motion of the head: Can. J. Earth Sci., v. 3, p. 523-546.

Middleton, G.V., 1966, Turbidity current experiments: Amer. Assoc. Petrol. Geol. Bull., v. 50, p. 627.

———, 1966, Experiments on density and turbidity currents II, Uniform flow of density currents: Can. J. Earth Sci., v. 3, p. 627-637.

———, 1967, Experiments on density and turbidity currents, III, Deposition of sediment: Can J. Earth Sci., v. 4, p. 475-504.

———, 1970, Experimental studies related to problems of flysch sedimentation: in Geol. Ass. Can. Spec. Pap. 7, Flysch sedimentology in North America, p. 253-272.

Natland & Kuenen, Ph.H., 1951, Sedimentary history of the Ventura Basin, California: in Soc. Econ. Paleontol. Mineral. Spec. Pub. 2, Turbidity currents, p. 76-107.

Parkash, B., 1970, Downcurrent changes in sedimentary structures in ordovician turbidite greywaches: J. Sediment. Petrology, v. 40, p. 572-590.

Pettijohn, F.J., 1960, Greywacke: J. Sediment. Petrology, v. 30, p. 627.

Phleger, F.B., 1951, Displaced foraminifera faunas: in Soc. Econ. Paleontol. Mineral Spec. Pub. 2, Turbidity Currents, p. 66-75.

Potter & Pettijohn, F.J., 1963, Paleocurrents and basin analysis, Springer-Verlag, Berlin, p. 131-132.

Prentice, J.E., 1960, Flow structures in sedimentary rocks: J. Geol. v. 68, p. 217-225.

Rich, J.L., 1950, Flow markings, groovings, and intrastratal crumplings as criteria for recognition of slope deposits, with illustrations from the silurian rocks of Wales: Amer. Ass. Petrol. Geol. Bull., v. 34, p. 717-741.

Riddell, J.F., 1969, A laboratory study of suspension effect density currents: Can. J. Earth Sci., v. 6, p. 231-246.

Roy, D.C., 1970, The silurian of northern Aroostook County, Maine, M.I.T. Ph.D. Thesis, Dept. of Earth and Planetary Sciences.

Sanders, J.E., 1960, Origin of convoluted laminae; Geol. Mag., v. 97, p. 409-421.

Shepard, F.P., 1951, Transport of sand into deep water: in Soc. Econ. Paleontol. Mineral. Spec. Pub. 2, Turbidity Currents, p. 53-65.

Shepard, F.P., 1965, in Progress in Ocenogrpahy, v. 3, Sears, ed., Pergamon Press, p. 331-332.

Simons, D.B. & Richardson, E.V., Forms of Bed Roughness in alluvial channels; Amer. Soc. Civil Engrs., J. Hydraul. Division, v. 87, p. 87-105.

Southard, J.B., 1971, Representation of bed configurations in depth-velocity-size diagrams: J. Sediment. Petrology, v. 41, p. 903-915.

Stauffer, P.H., 1967, Grain flow deposits and their implications, Santa Ynez Mountains, California: J. Sediment. Petrology, v. 37, p. 487-508.

Van der Lingen, 1969, The turbidite problem: N.Z. J. Geol. Geophys., v. 12, p. 7-50.

———, 1970, The turbidite problem — a reply to Kuenen? N.Z. J. Geol. Geophys. v. 13, p. 858-872.

Van Houten, F.B., 1964, Sedimentary features of martinsburg slate, Northwestern New Jersey: Geol. Soc. Amer. Bull., v. 65, p. 813-818.

Walker, R.G., 1965, The origin and significance of the internal structures of turbidites: Proc. Yorkshire Geol. Soc., v. 35, p. 1-32.

———, 1967, Turbidite sedimentary structures and their relationship to proximal and distal depositional environments: J. Sediment. Petrol. v. 37, p. 25-43.

———, 1970, Review of the geometry and facies organization of turbidites and turbidite bearing basins: in Geol. Ass. Can. Spec. Pap. 7, Flysch sedimentation in North America, p. 219-251.

Wilson, J.L., 1969, Microfacies and sedimentary structures in 'deeper water' limestones: in Soc. Econ. Paleontol. Mineral. Spec. Pub. 14, Depositional Environments in Carbonate Rocks, p. 4-16.

Photographs

Photo 1

Photograph of Experimental Apparatus

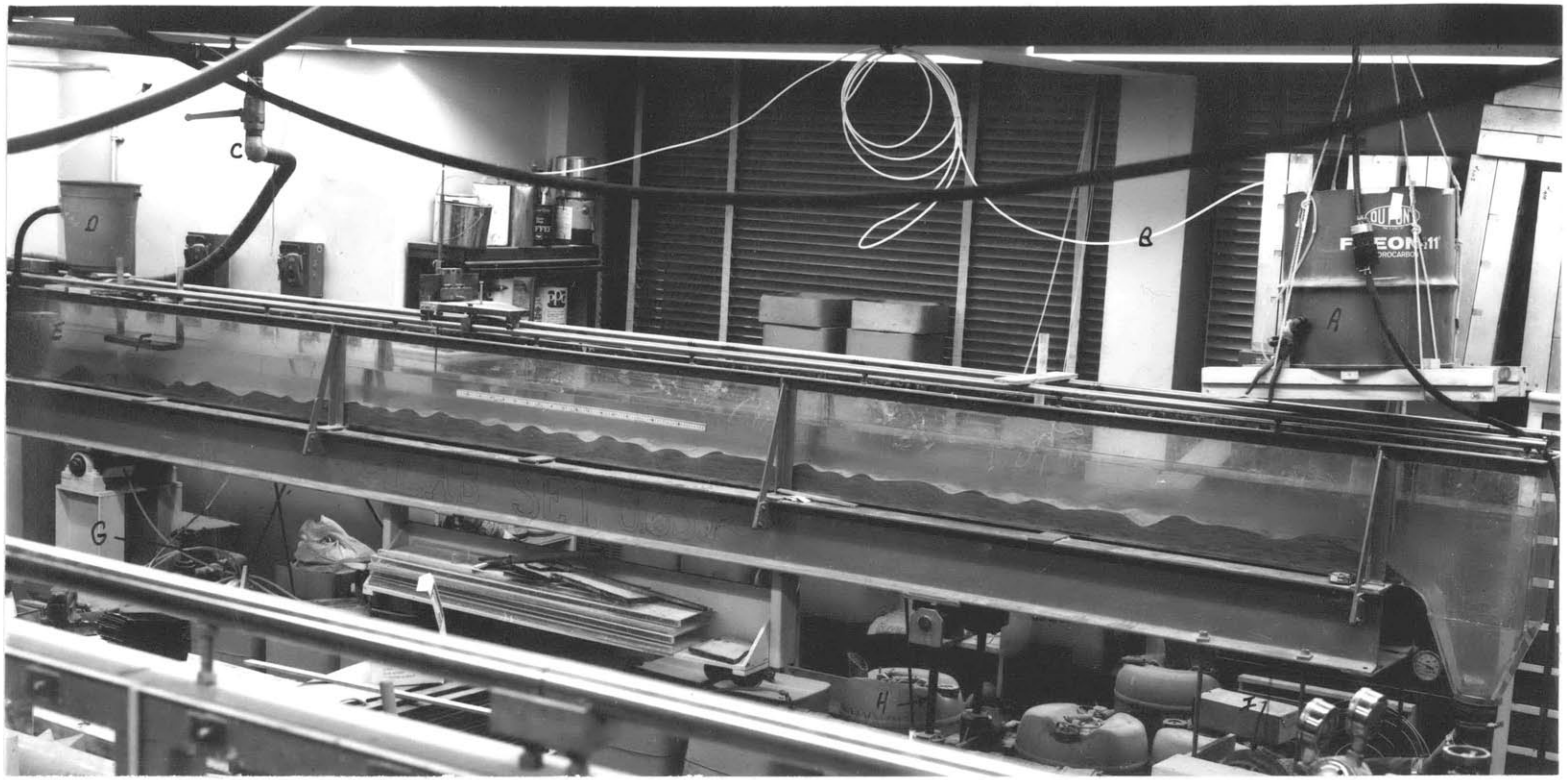

Photo

Photograph of Experimental Apparatus

A. Dry Sediment Bin

B. Air Tubing to Ball Vibrator

C. Pipe from Overhead Filling Tanks

D. Pore Water Feed Bucket

E. Turbulence Diffusers

F. Plank to Damp Surface Waves

G. Orifice Meter and Tubing

H. Jacks for Tilting Flume

I. Pump Housing

Photographs of Experimental Runs

Unless otherwise noted, the direction of flow is from left to right

Photo 2

Run 1

Post-Aggradation

Ripple foreset laminae overriding fainter forset laminae from an earlier ripple

Note lack of structure in the lower 2 cm of the deposit (the higher velocity of flow during the earlier phase of aggradation did not leave leave as distinct a record as did the slower velocities higher in the section)

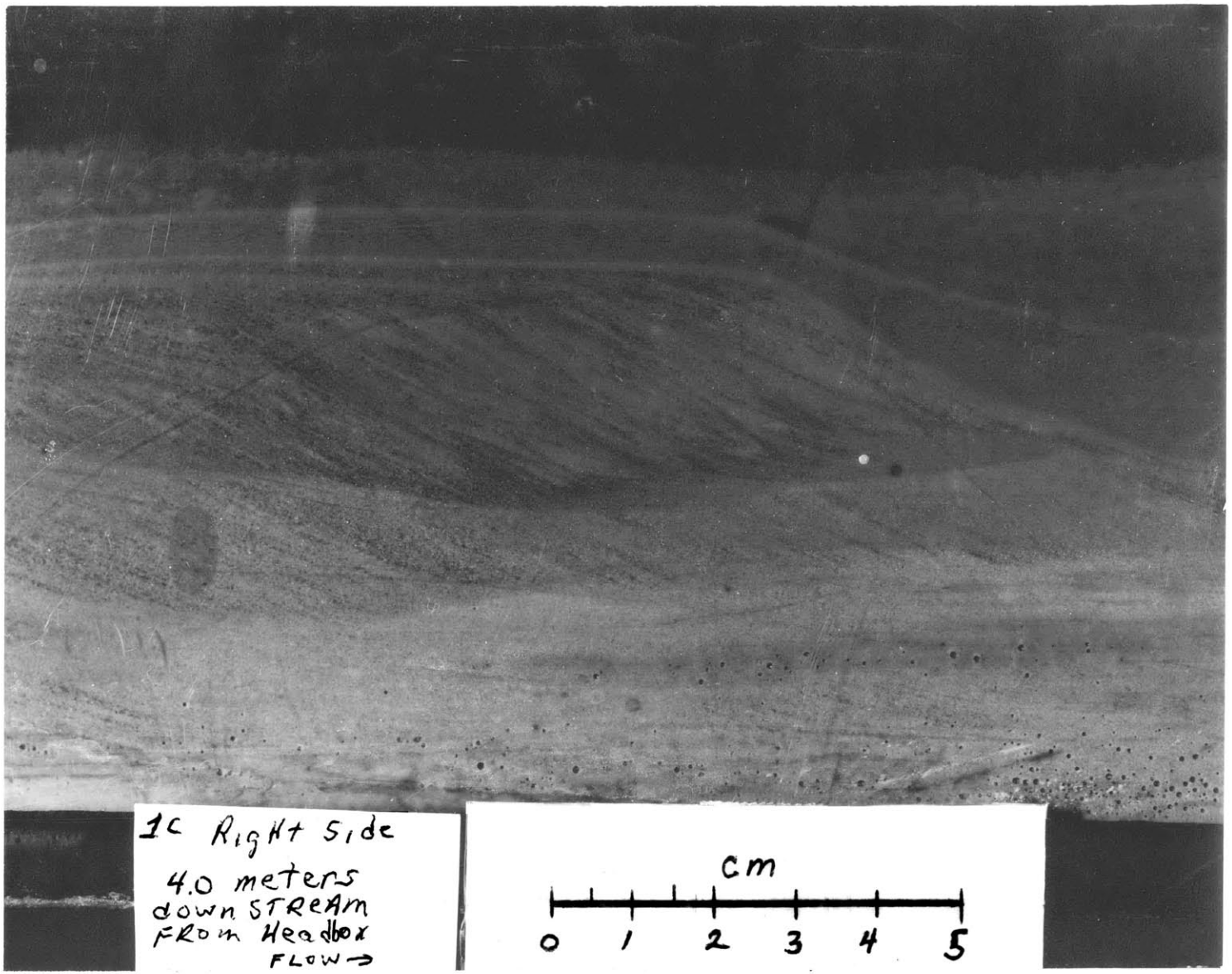
1c Right Side
4.0 meters
down STREAM
FROM Headbox
FLOW →
cm
0 1 2 3 4 5

Photo 3

Run 1

Ripple foreset laminae
grading upwards into
an interval of parallel
lamination

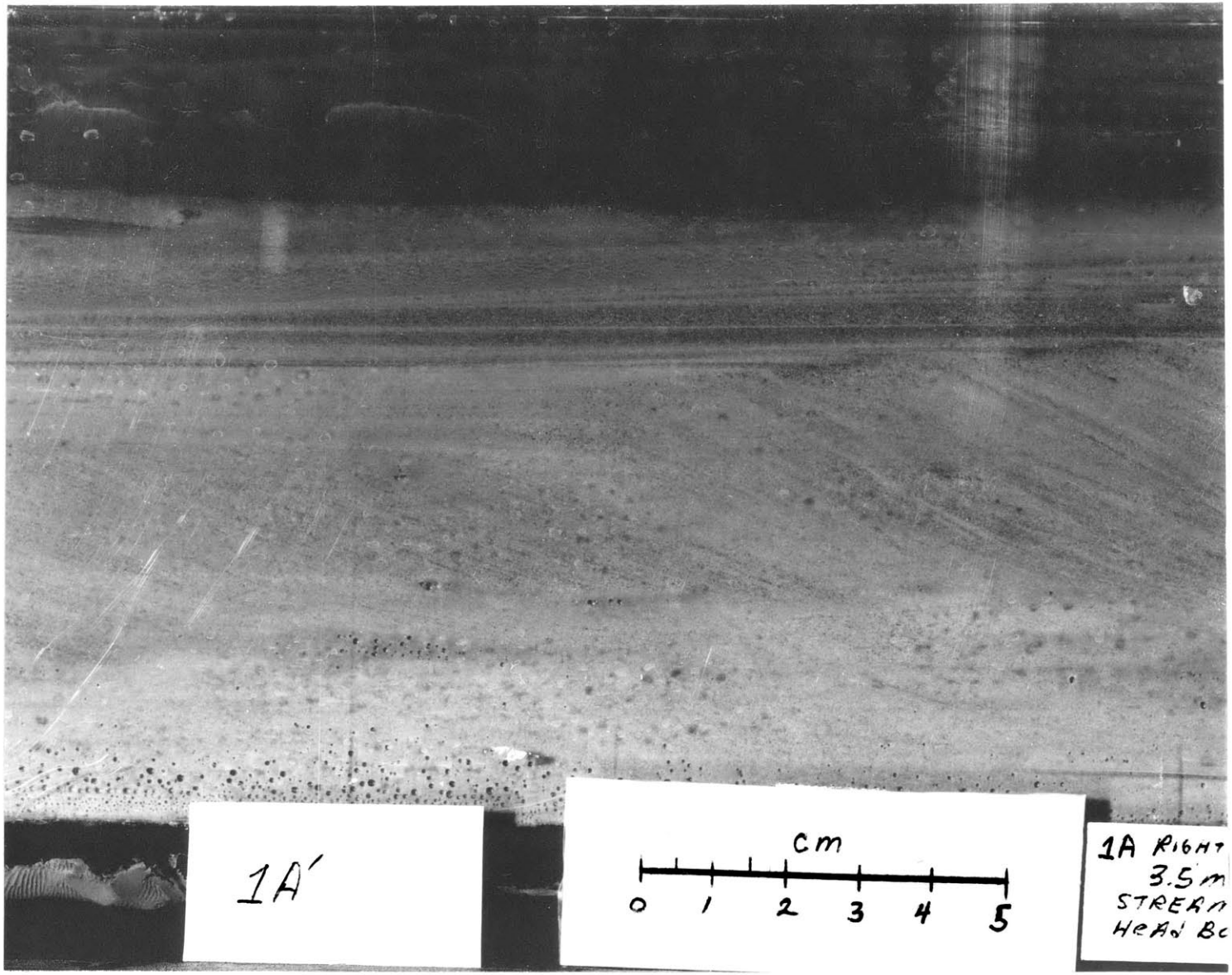

001

Photo 4

Run 1

Faint ripple foreset laminae

Some indication that the higher speed ripples lower in the section (right hand side about 2 cm from flume bottom) may have had their stoss slopes inclined at a lower angle than the ripples higher in the section

Faint trace of reverse ripple on top left

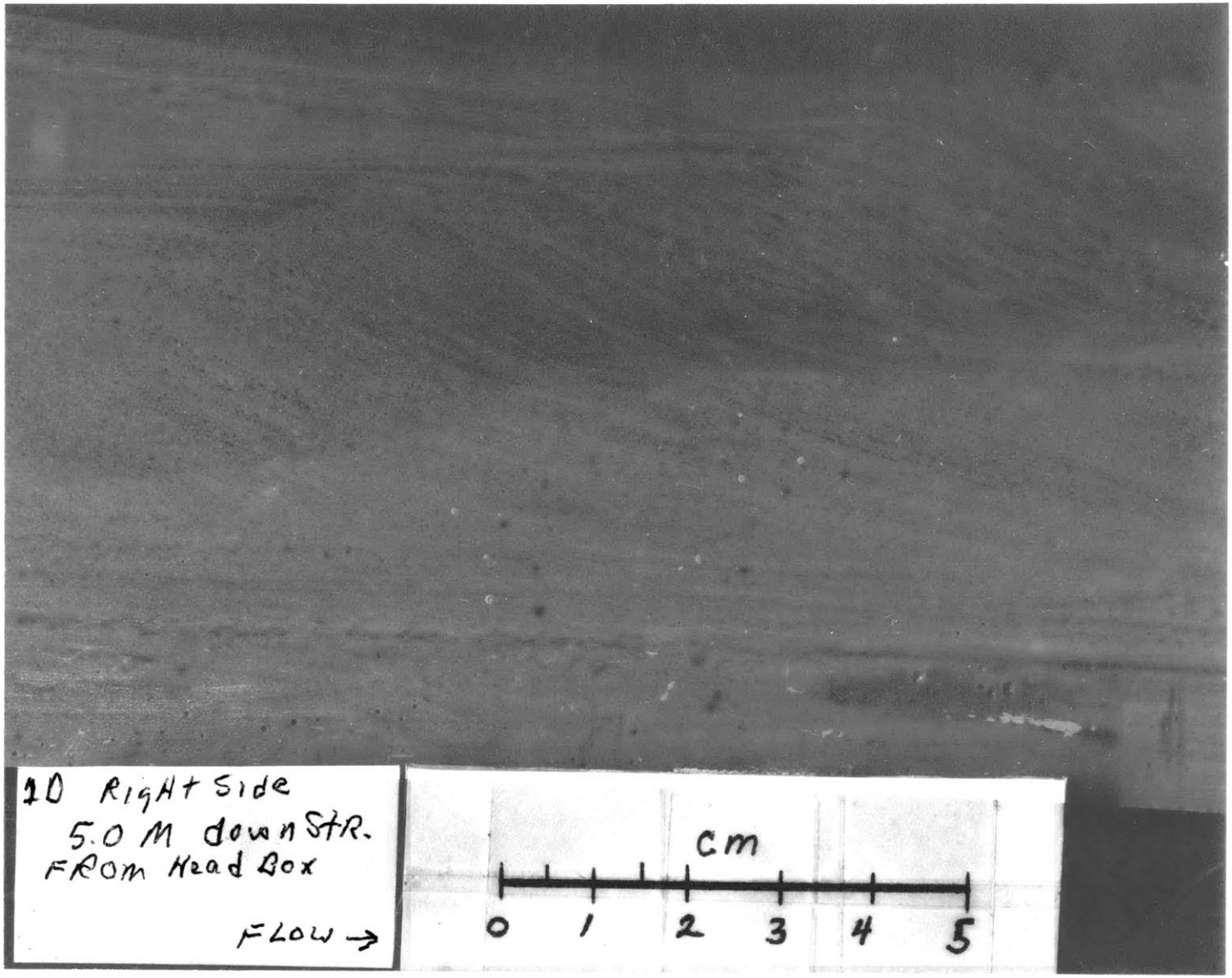
1D Right Side
5.0 M downSTR.
FROM Head Box
FLOW →
cm
0 1 2 3 4 5

Photo 5

Run 1

Upstream continuation
of reverse ripple from
Photo

Indistinct "B" Interval
laminations destroyed
by advancing aggrading
ripples; faint foreset
laminae reaching nearly to
flume bottom

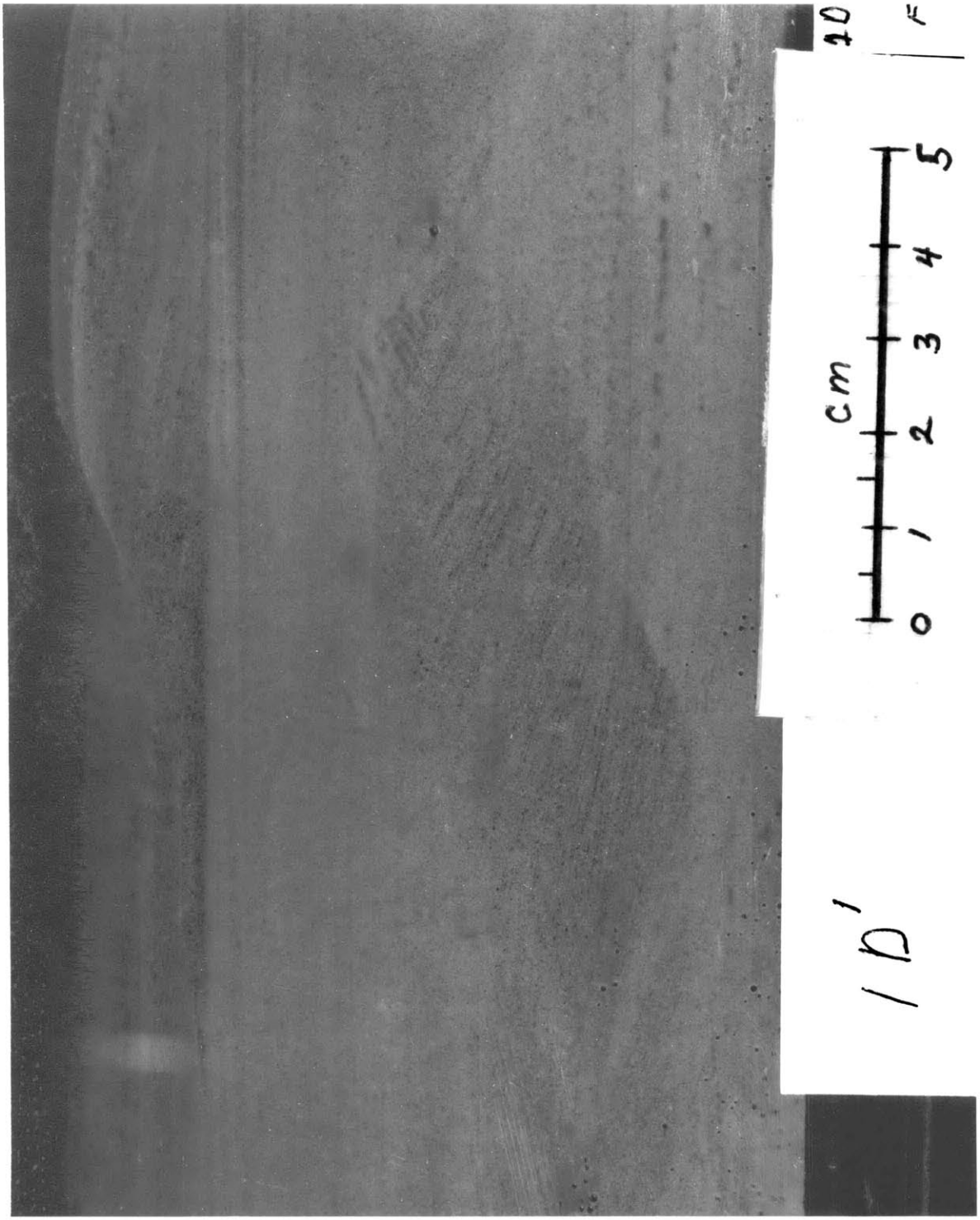
1D'
cm
0 1 2 3 4 5
10

Photo 6

Run 2

Typical Equilibrium Ripples
for this run

Faint generally horizontal
Basal Traces seen in left
third of photograph

Foresets inclined about
25 deg. to horizontal

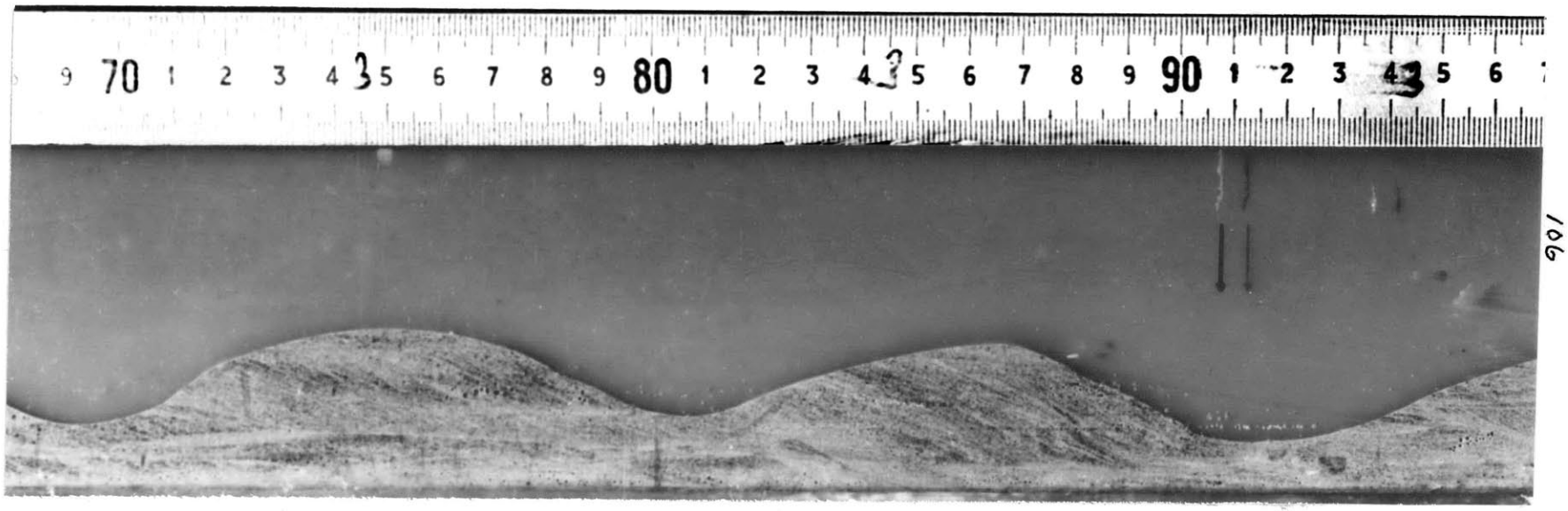

106

Photo 7

Run 2

A shot immediately upstream
of Photo

Two clear Basal Traces;
one climbing at 2-3 deg.
and the other descending
and finally climbing (on
the right side)

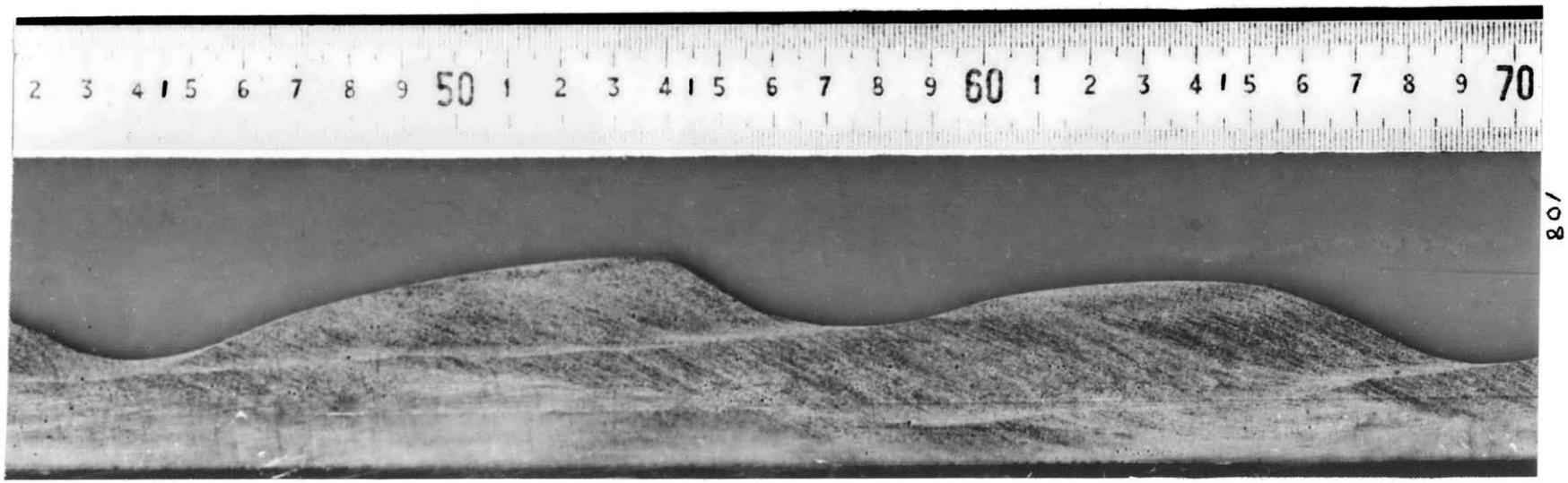
2 3 4 5 6 7 8 9 50 1 2 3 4 5 6 7 8 9 60 1 2 3 4 5 6 7 8 9 70
801

Photo 8

Run 2

Photo immediately upstream of Photo

One horizontal Basal Trace and one descending Basal Trace

Upstream slope of central ripple being rapidly eroded

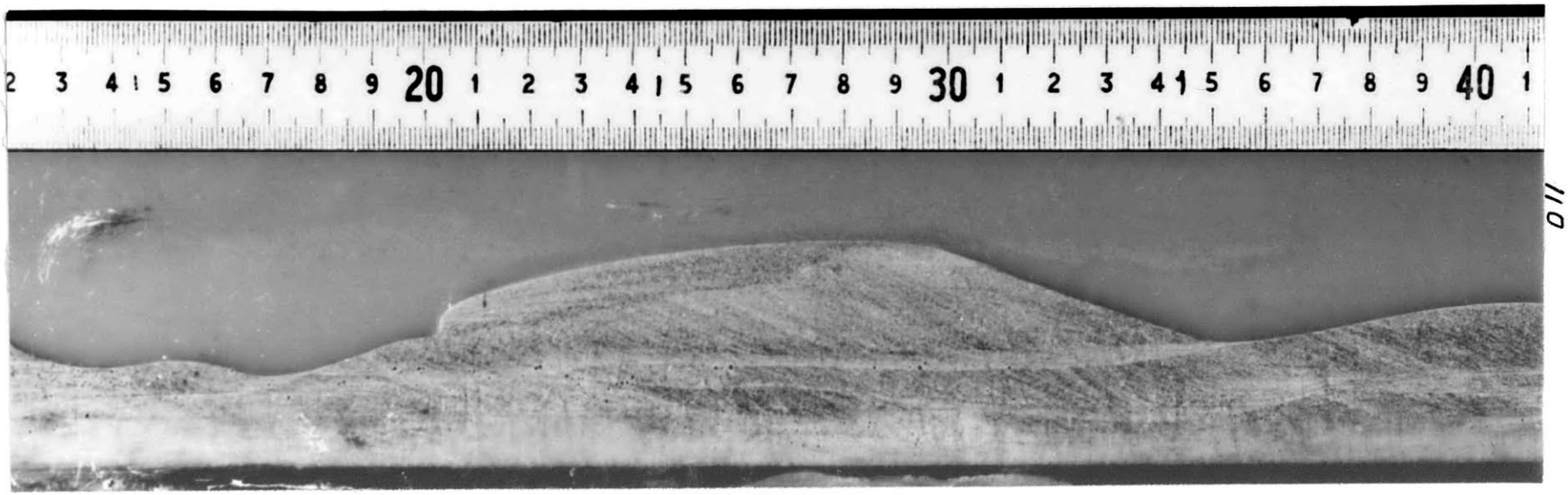

110

Photo 9

Run 2

Post-Aggradation

Small Trough Structures
and small Truncated Basal
Traces

Long horizontal Basal Trace
extending 18 cm in top left

Thin mantling of sediment
fell from suspension when
flow stopped

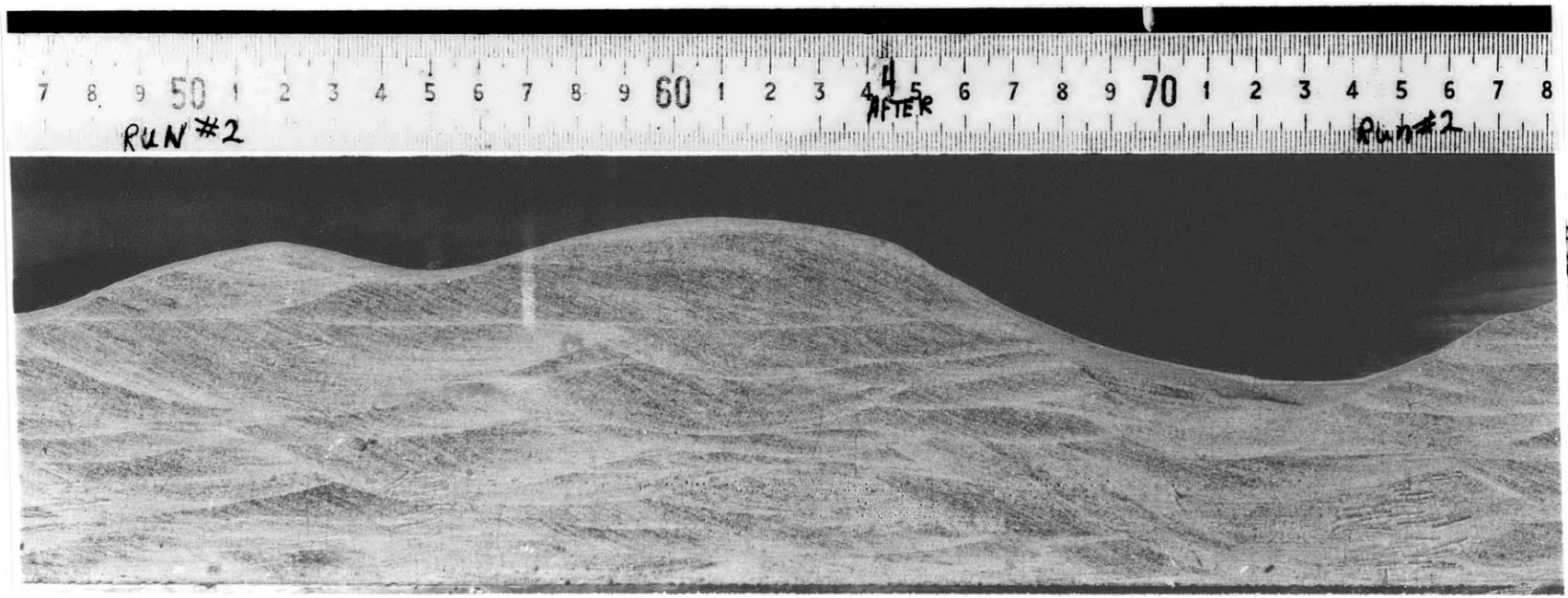
RUN #2
AFTER
Run #2

Photo 10

Run 2

Two long (10 & 30 cm)
Basal Traces in upper
part of section; climbing
at about 2 deg.

Trough Structures also
evident in the section

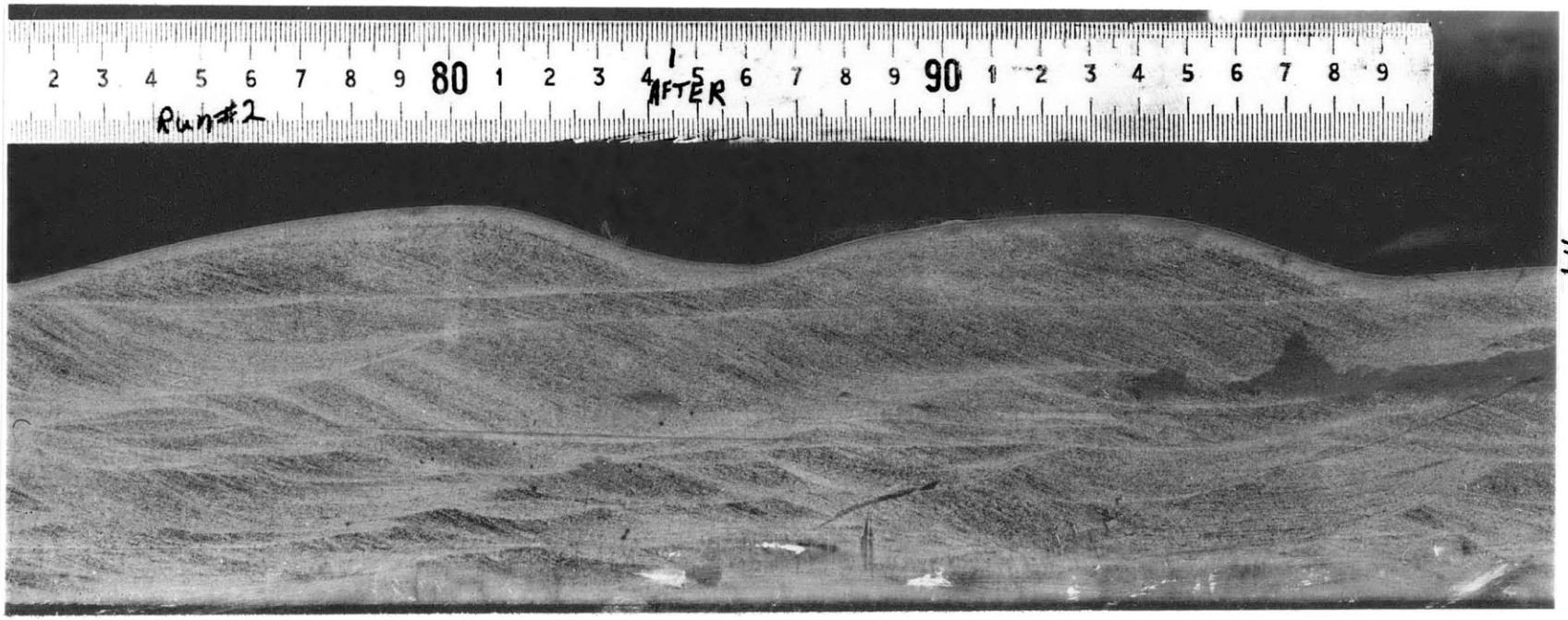
Run #2
AFTER

Photo 11

Run 2

Large overlapping Trough Structures

Trough Structures Reach to Bottom of flume at some points

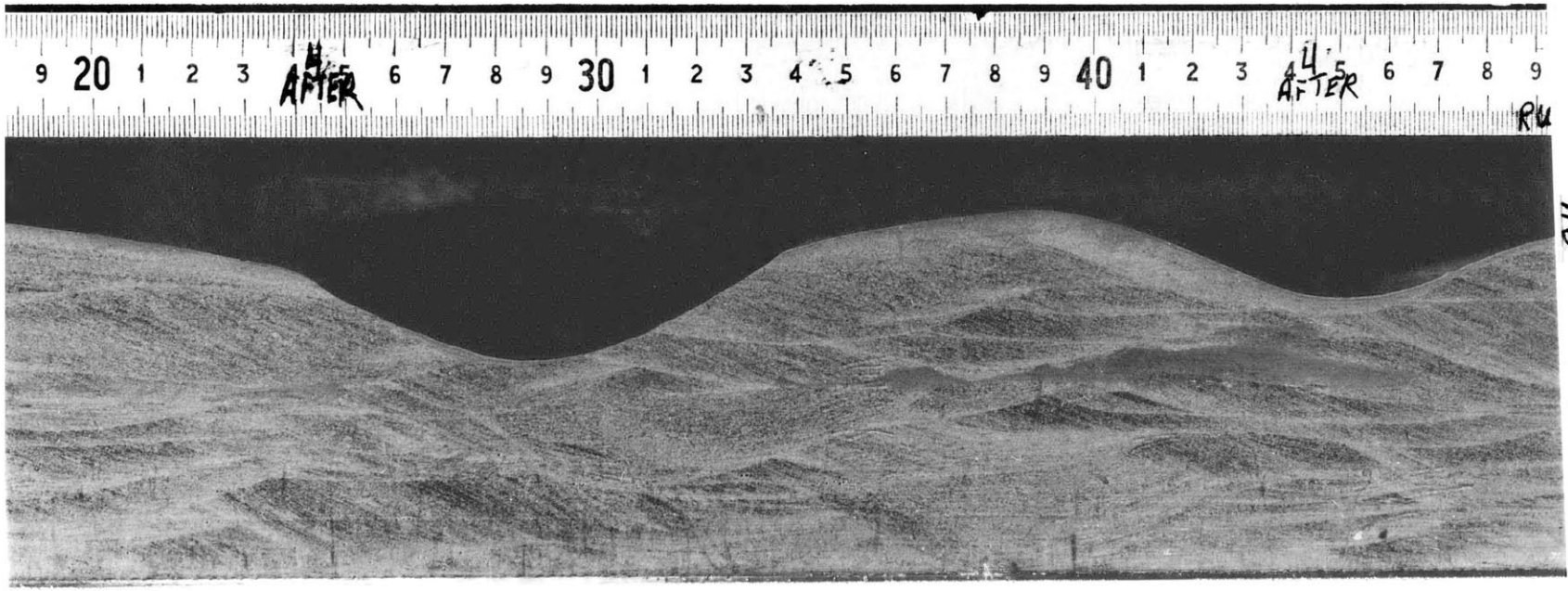

116

Photo 12

Run 2

Photograph showing Bed Surface

A typical length of bed surface after aggradation

Distinctness of features dependent on rate of net deposition and advance


cm
1
2
3
4
5

Photo 13

Run 2

Post-Aggradation Bed Surface

Large boil structure in center of photograph; these occured approximately every 2 m along the flume

Scale is suspended in water along flume centerline


cm
5
4
3
2
1
0

Photo 14

Run 3

Post-Aggradation

Distinctness of structure decreases as rise in section

Scale increases as rise in the section

Remains of equilibrium and early post-equilibrium structure can be seen at the base of the section

Trough Structures replace a combination of trough structure and basal trace seen in Run 2

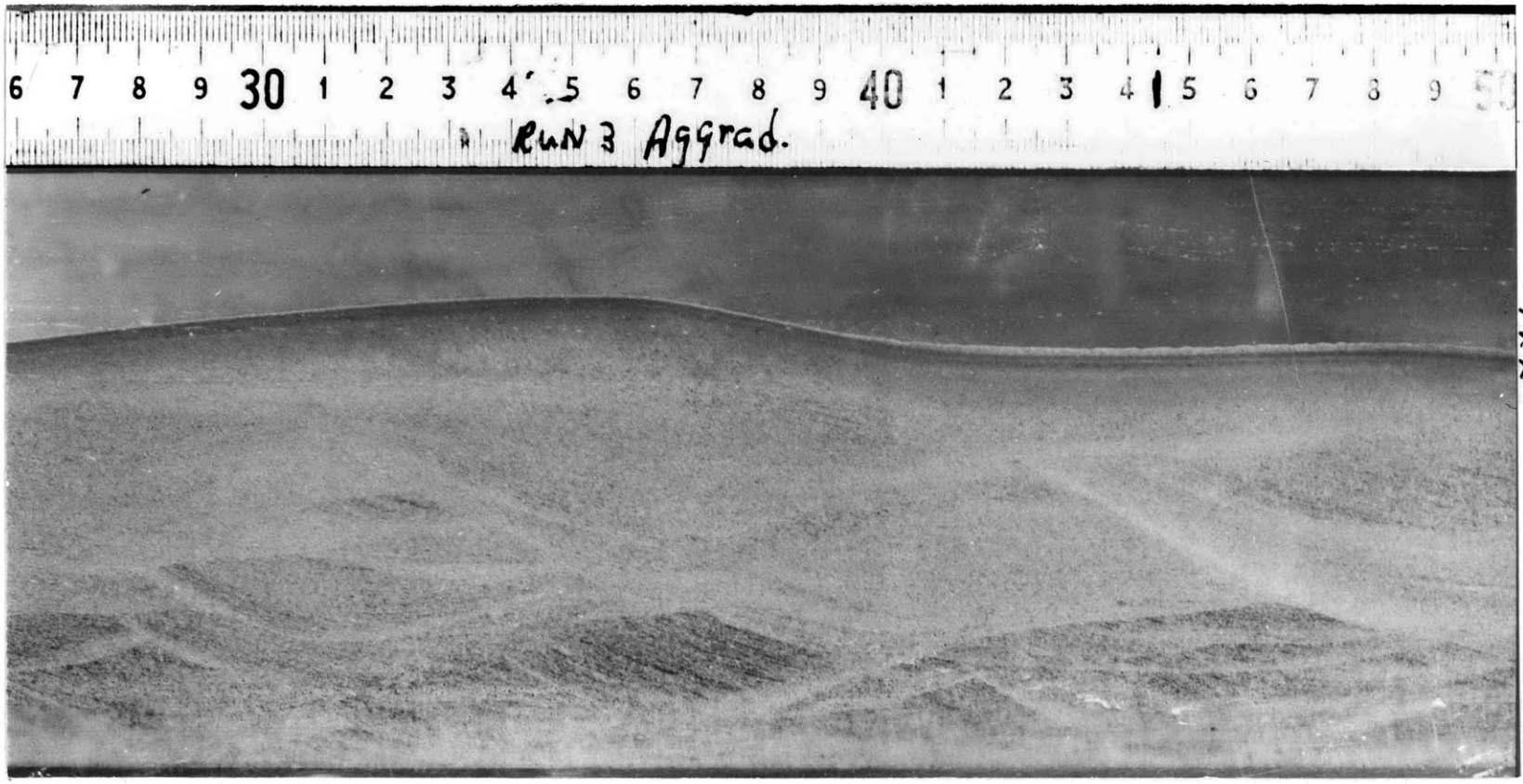
6 7 8 9 30 1 2 3 4 5 6 7 8 9 40 1 2 3 4 5 6 7 8 9
Run 3 Aggrad.

Photo 15

Run 3

Post-Aggradation

A reduction in ripple height with aggradation

Ripple spacing increases as well

(Compare to Run 2 Equilibrium Ripples; Equilibrium Ripples for Run 3 were identical)

Decreasing distinctness of structure with aggradation

Almost all remains of the equilibrium ripples have been truncated by the trough structures

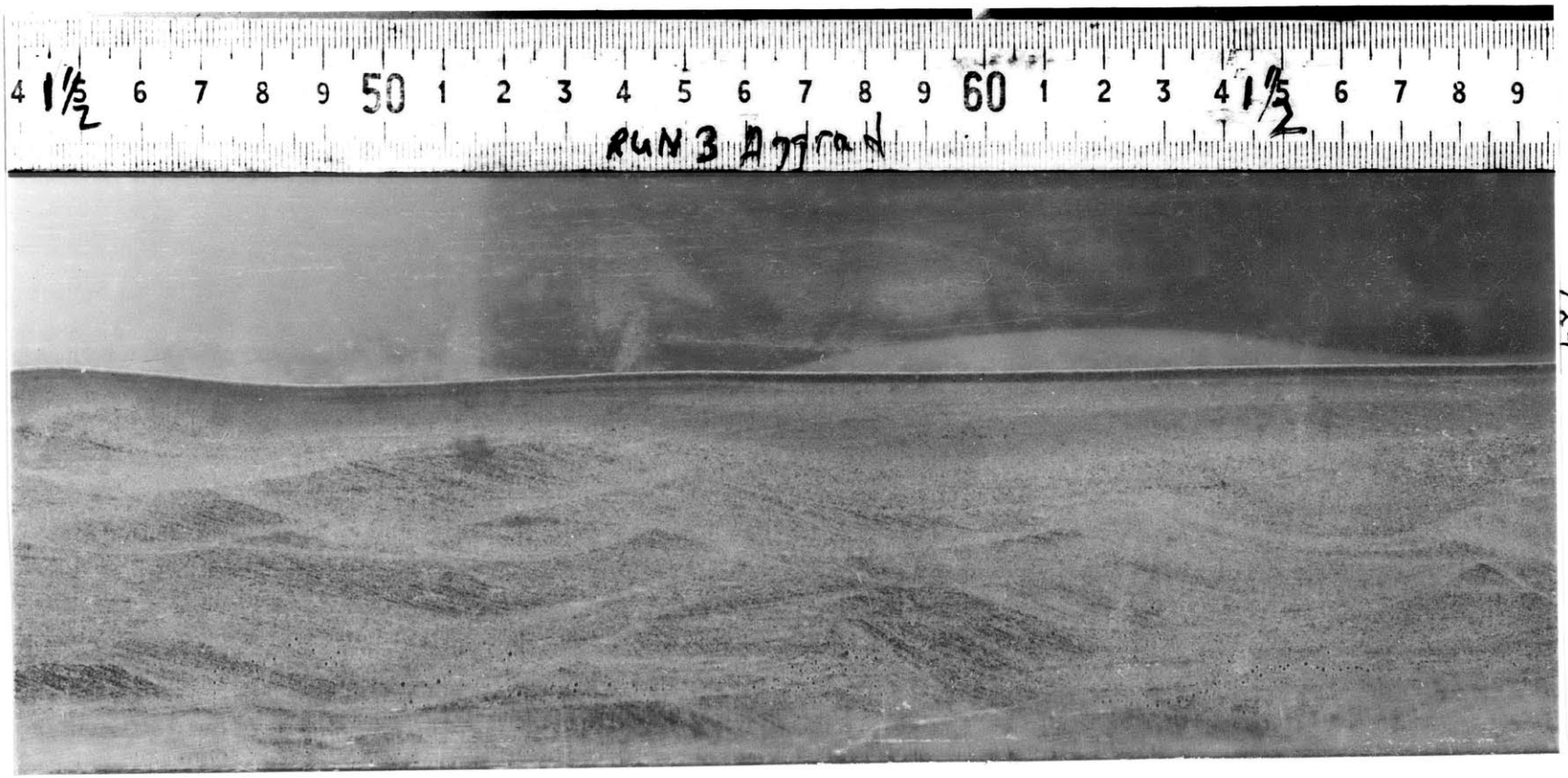
4 1½ 6 7 8 9 50 1 2 3 4 5 6 7 8 9 60 1 2 3 4 1½ 6 7 8 9
RUN 3 Aground

Photo 16

Run 3

Syn-Aggradational

Photograph taken 3 hrs.
into aggradation process

Basal traces still clear
and generally rising

Trough Structures evident,
but are distinct and small

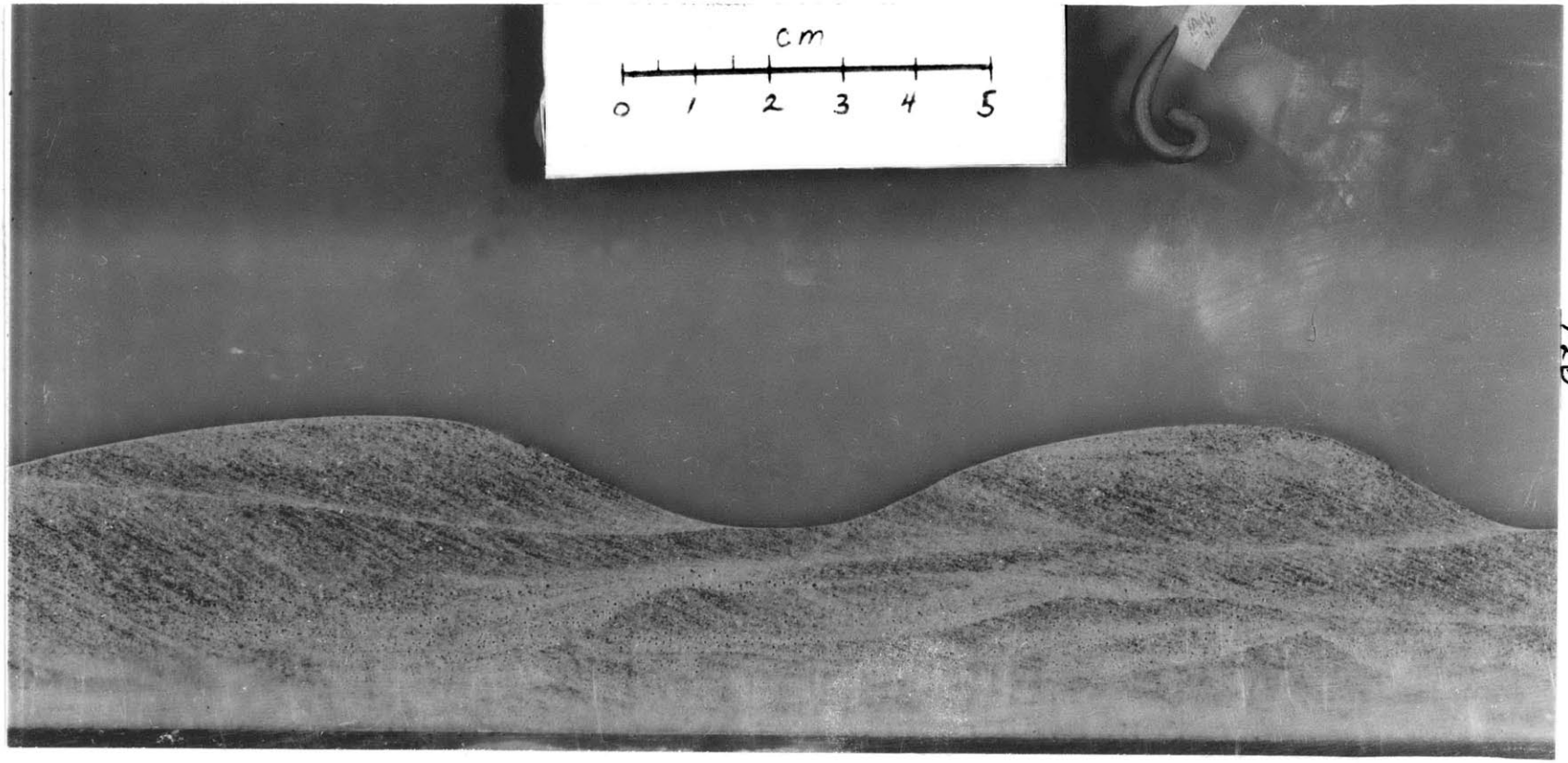
cm
0 1 2 3 4 5

Photo 17

Run 3

Syn-Aggradational

Photograph taken 13½ hrs.
into aggradational process

Decreasing distinctness of
structure as aggradation
proceeds

Trough Structures come to strongly
dominate Basal Traces

Foreset Laminae are very faint

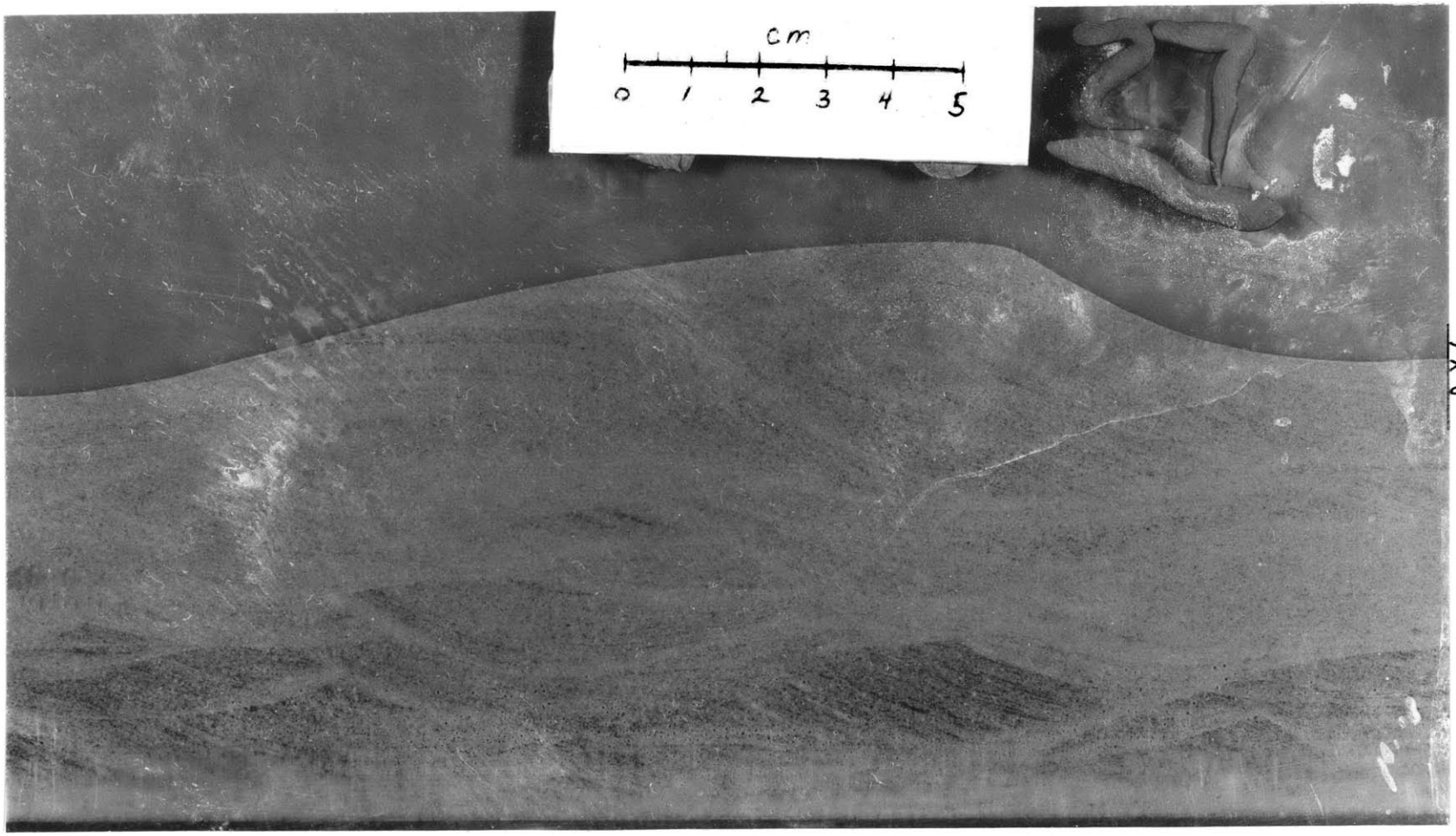

128

Photo 18

Run 4

Equilibrium Ripples

Typical Equilibrium Ripples
at the lower velocity of
Run 4 (compared to #2 & #3)

Remains of unworked sediment
on flume bottom to extreme right

Basal Traces generally negatively
inclined

130

Photo 19

Run 4

Equilibrium Ripples

Photograph immediately
upstream of Photo

A prism of unworked sediment
to left on flume bottom

A small ripple advancing on
a larger ripple, forming its
Basal Trace in the process;
compare this small ripple to
the ripple in Photo
Both are dark incidcating a
concentration of plant debris
and both are advancing on a
larger, slower moving ripple

The foreset laminae of the larger
ripple are clearly less distinct
than is typical, so rate of advance
is not the only factor influencing
the distinctness of structures

132

Photo 20

Run 4

Syn-Aggradational

Photograph taken 7½ hrs.
into the aggradation process

Small Ripple advancing on
the back of a larger one
forming a basal trace as it
does so.

Clearly the larger ripple is
much above the equilibrium ripple
spacing

Basal traces still dominate
Trough Structures

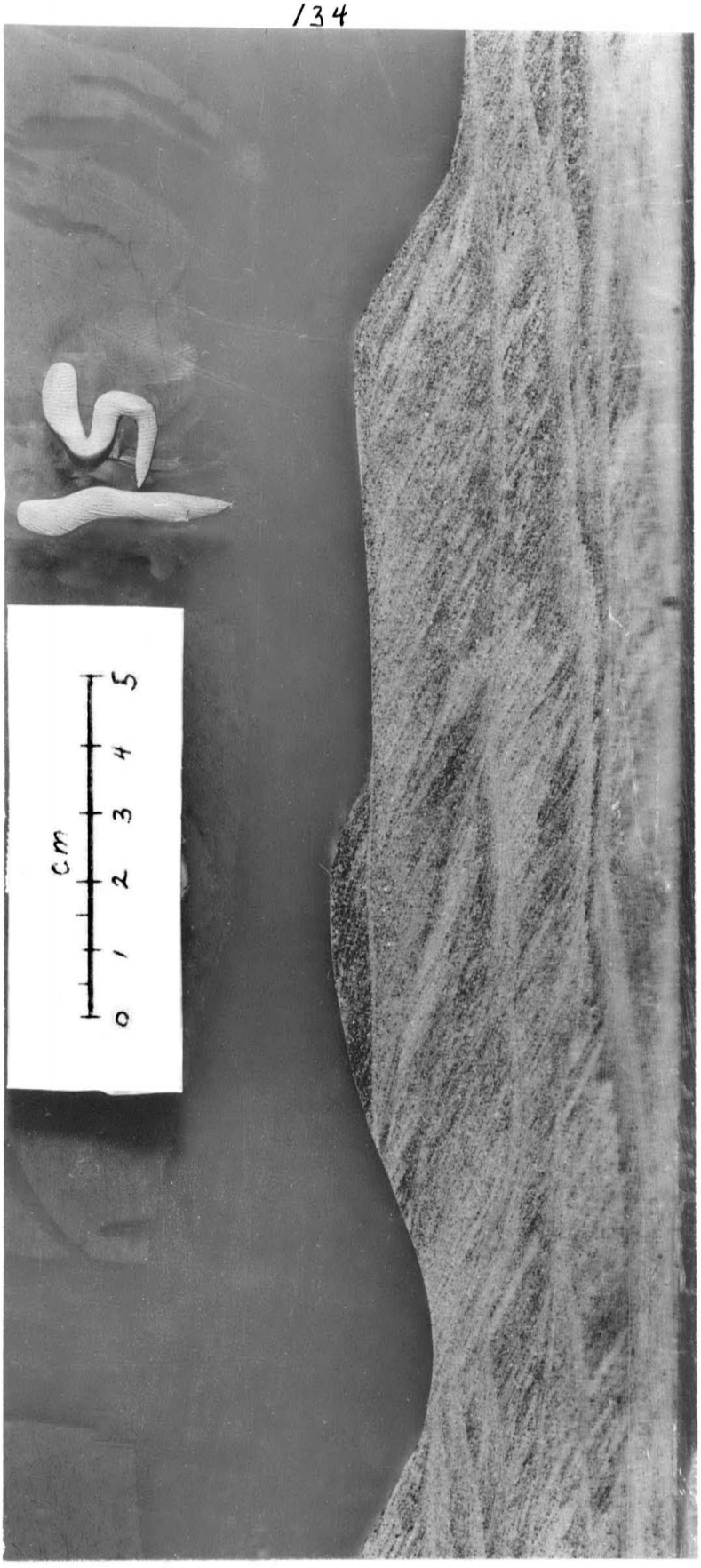
cm
0 1 2 3 4 5

Photo 21

Run 4

Syn-Aggradational

Photograph taken 9 hrs.
into aggradational process

Basal Traces inclined
positively

Upstream slope of ripple on
extreme right undergoing
rapid erosion

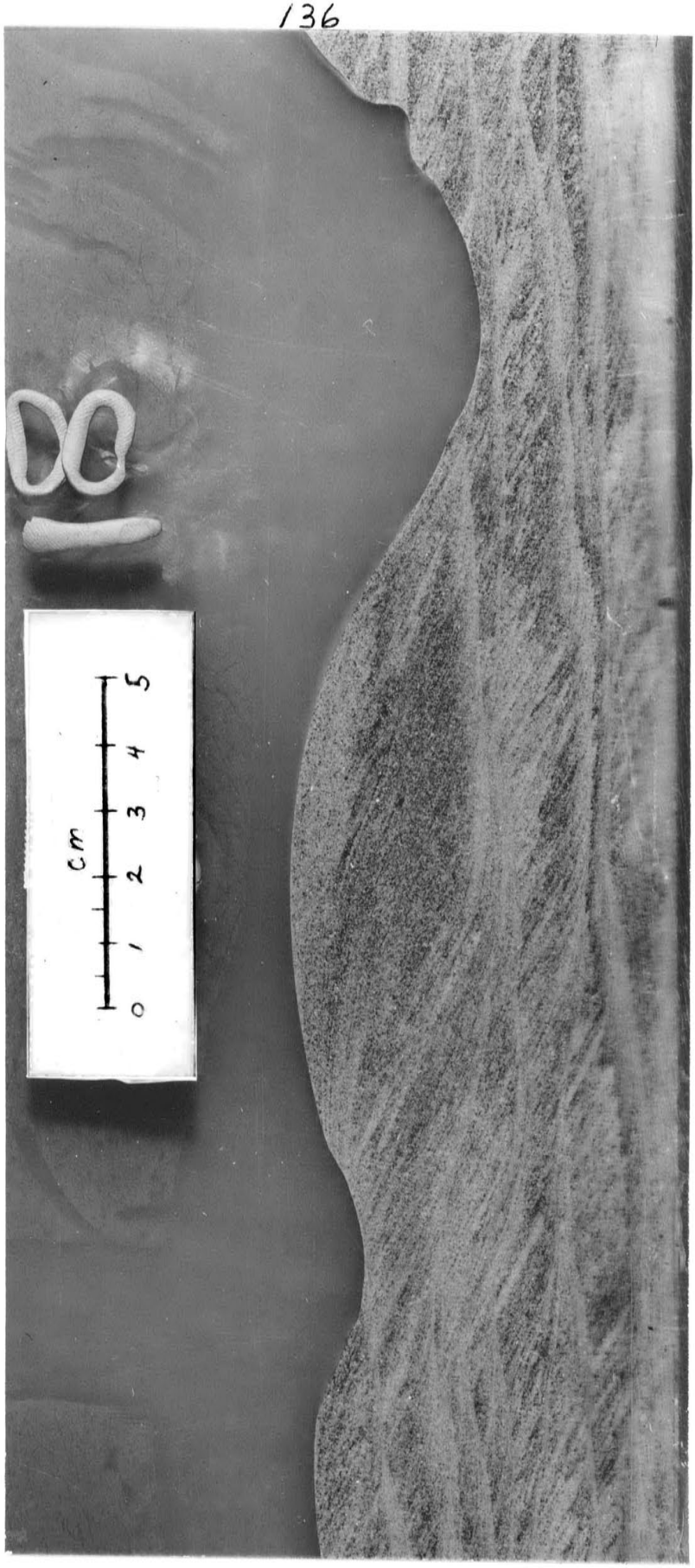
cm
0 1 2 3 4 5

Photo 22

Run 4

Post-Aggradational

Basal Traces generally positively inclined

Some trough structure present but they do not dominate (Compare with Run 3)

No change in distinctness of structure as rise in section

A lens of undisturbed sediment not worked by equilibrium ripples at lower right


RUN 4 Aboard

Photo 23

Run 4

Post-Aggradational

Do get an increase in mean ripple spacing with aggradation

Trough structures are present, but Basal Traces dominate at least in this photograph

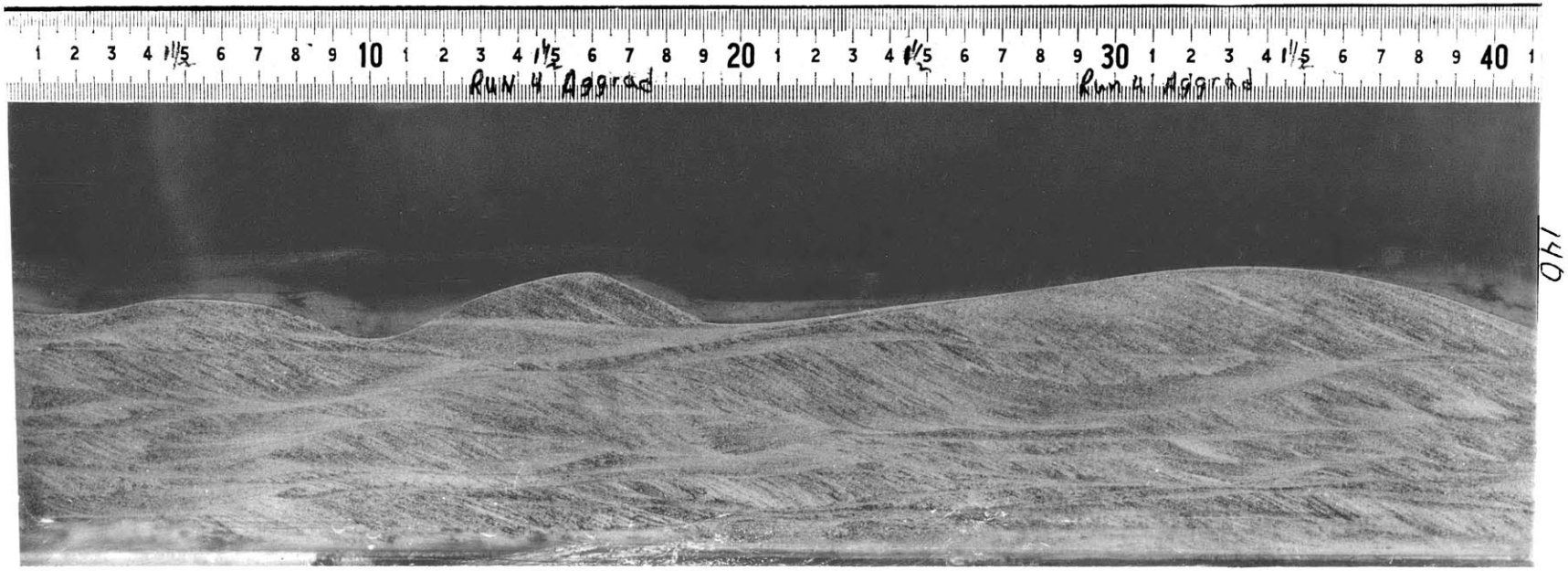

140

Photo 24

Run 5

Post-Aggradational

Flow is from Right to Left

Note increasing distinctness of structure with decreasing velocity (as move higher in section); similar to Run 1

Ripples are highly irregular and vary greatly in size; are rather steep and hummocky (central ripple) or low and smooth

Ripple cross-sections generally symmetric as compared to previous ripples

Weak Basal Traces, but Trough Structures predominate

Note very small scale irregular bumps on ripple faces (due to relatively high percentage of brown algae present?)

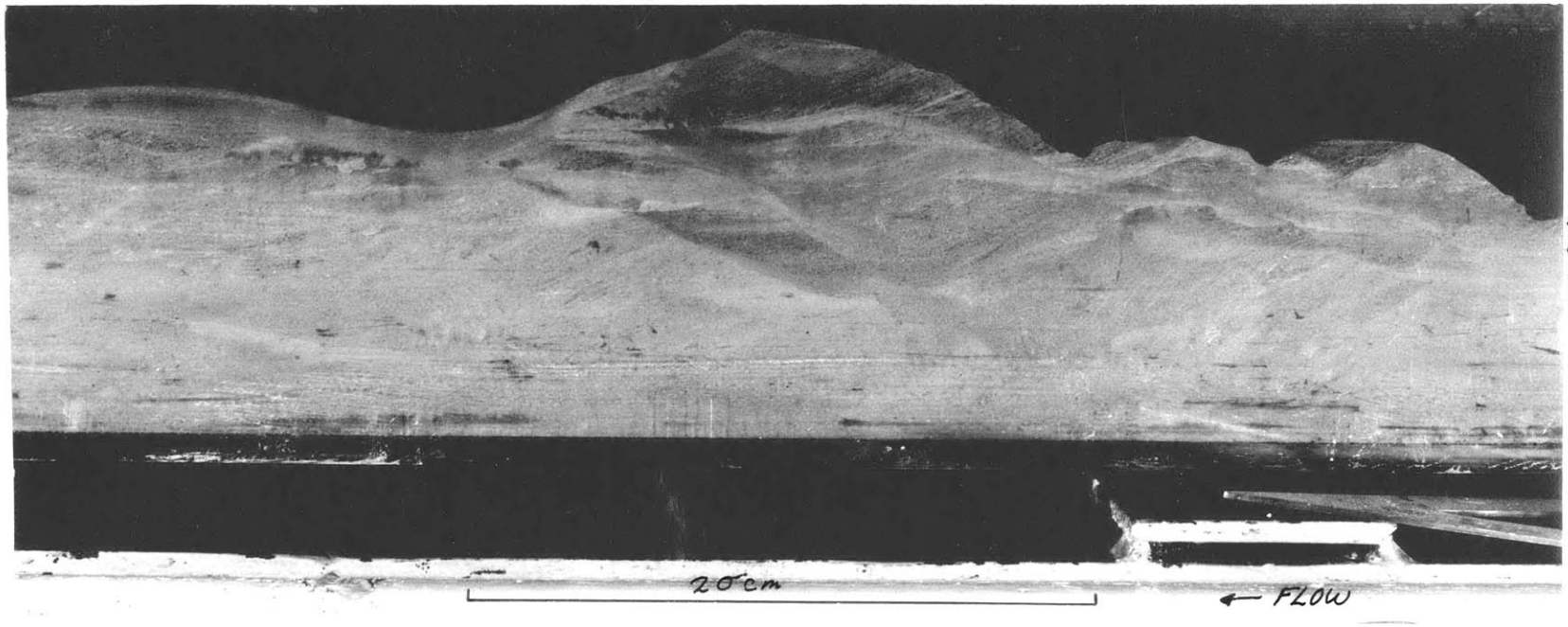
20cm
FLOW

Photo 25

Run 5

Post-Aggradational

Ripples generally symmetric

Note interval of parallel lamination ("D" Interval) with ripples above it in section despite fact that velocity reduced continuously

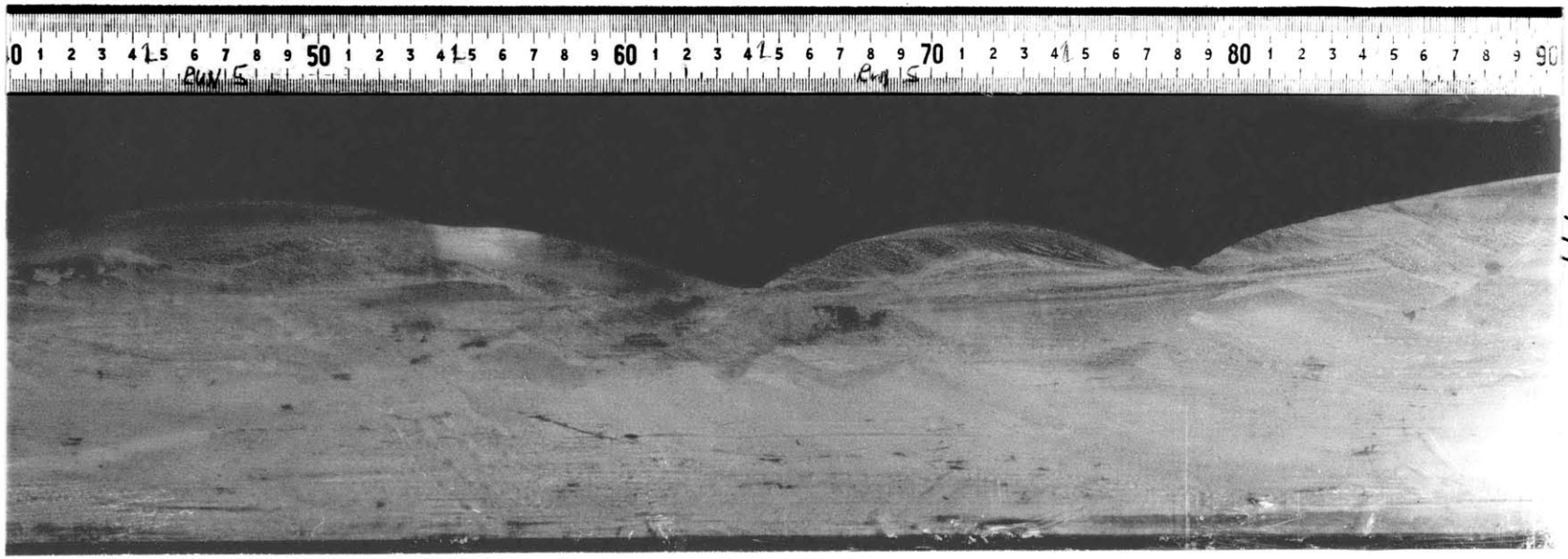
0 1 2 3 4 5 6 7 8 9 50 1 2 3 4 5 6 7 8 9 60 1 2 3 4 5 6 7 8 9 70 1 2 3 4 5 6 7 8 9 80 1 2 3 4 5 6 7 8 9 90
Avg 5
Avg 5

144

Photo 26

Run 5

Post-Aggradational

A detail of a ripple foreslope appears in the photograph

A small slump appears on the lower left

Note strange 'erosional' features of foreslope; attributable to the presence of brown algae (an increase in cohesivity?)?

Features such as this were seen occasionally along the length of the flume


1.5 cm

Photographs of Field Samples

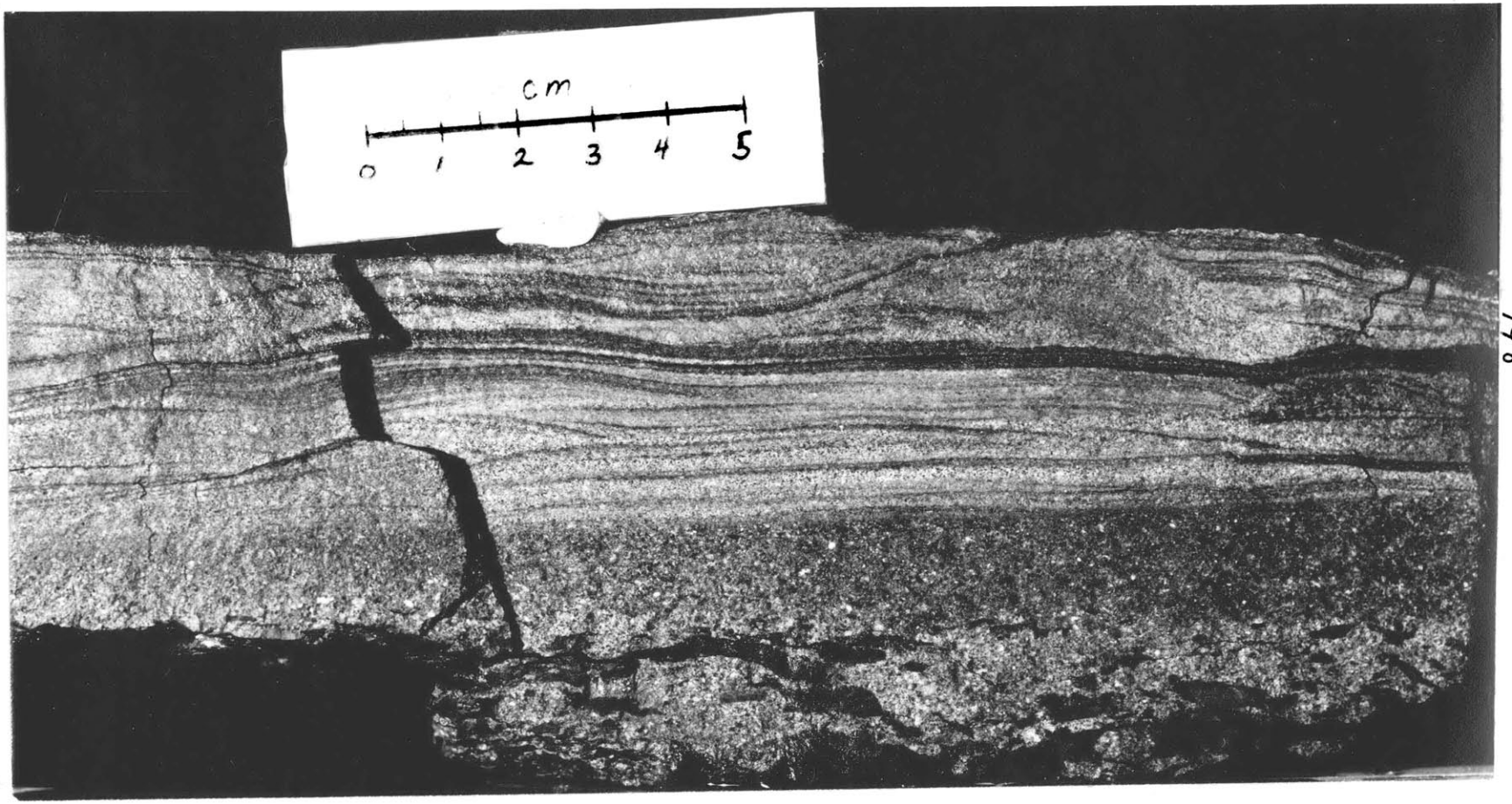

Photo 27

Field Sample From Locality 13

Photo 28

Field Sample 1 Locality 11

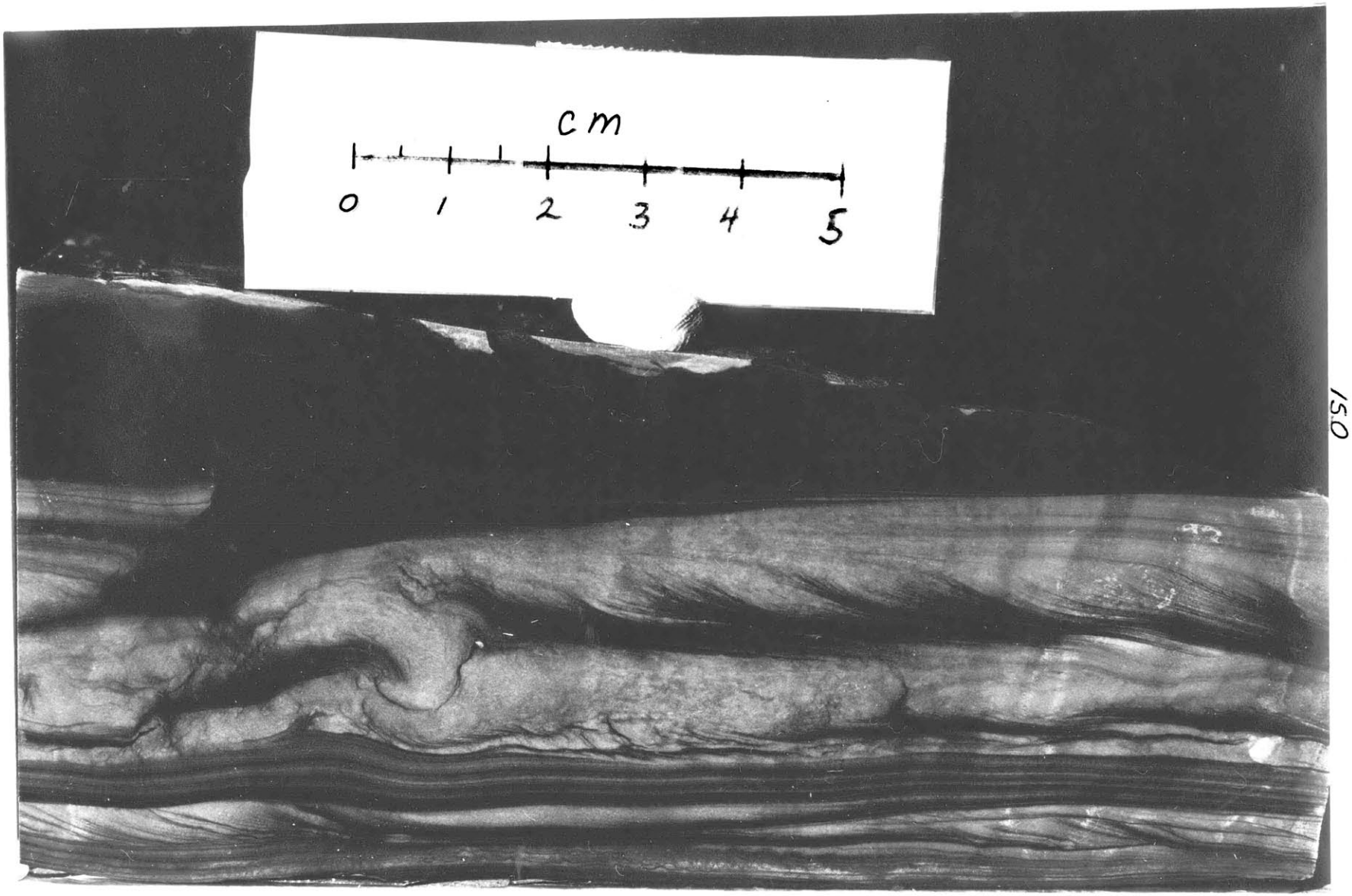
cm
0
1
2
3
4
5

Photo 29

Field Sample 2 Locality 3

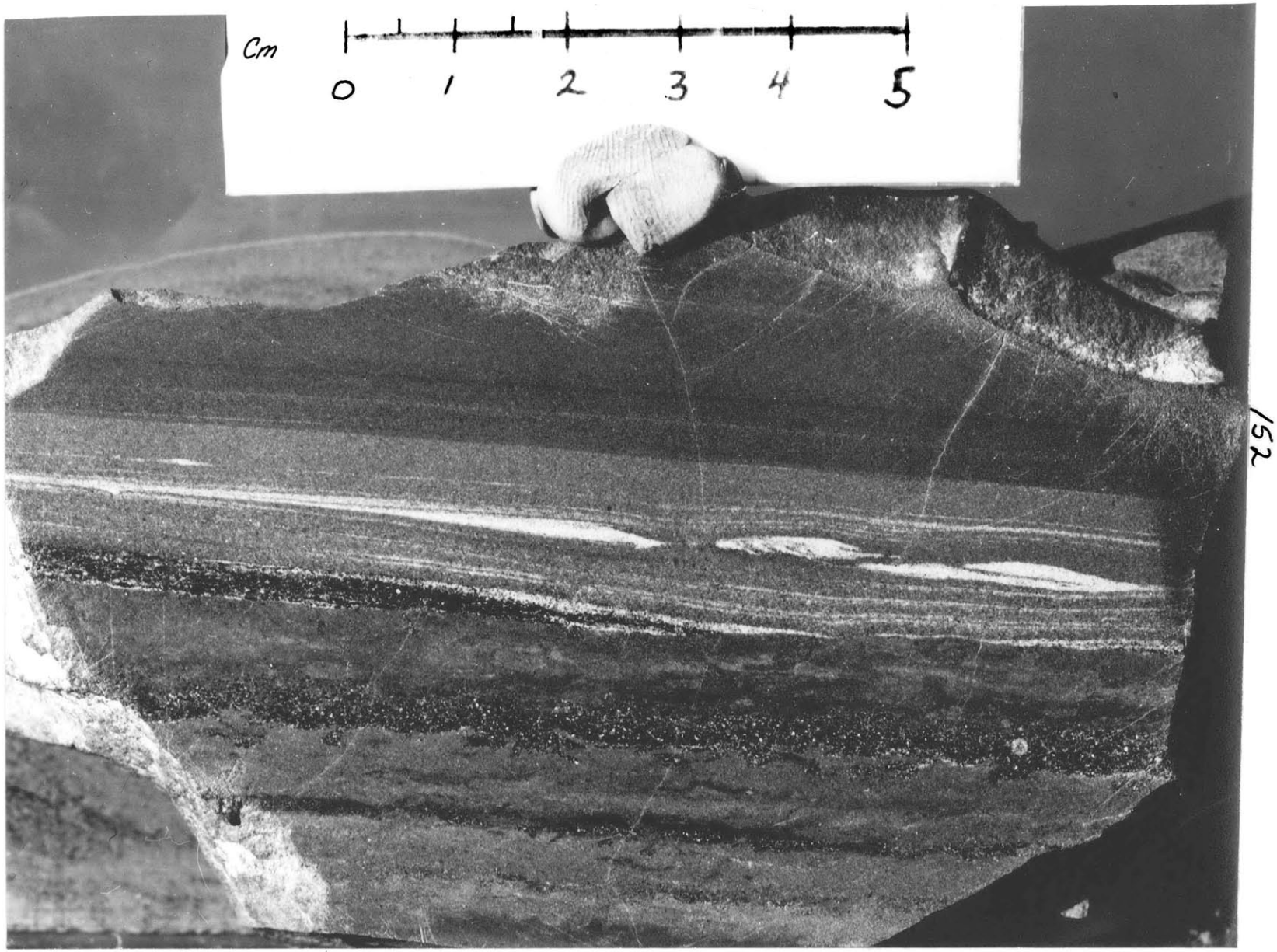

152

Photo 30

Field Sample 1 Locality 3

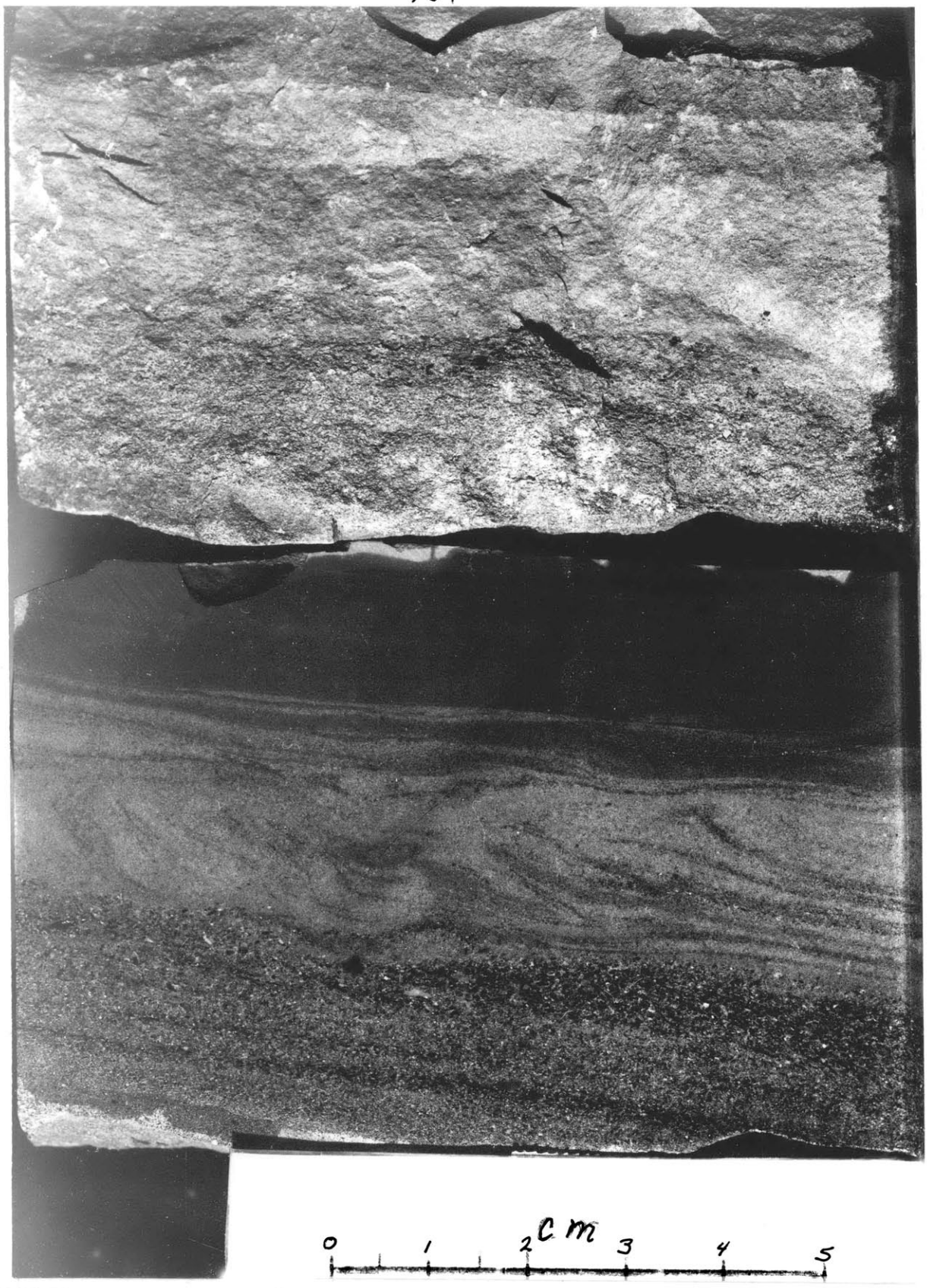
0
1
2
cm
3
4
5

Photo 31

Field Sample From Locality 4

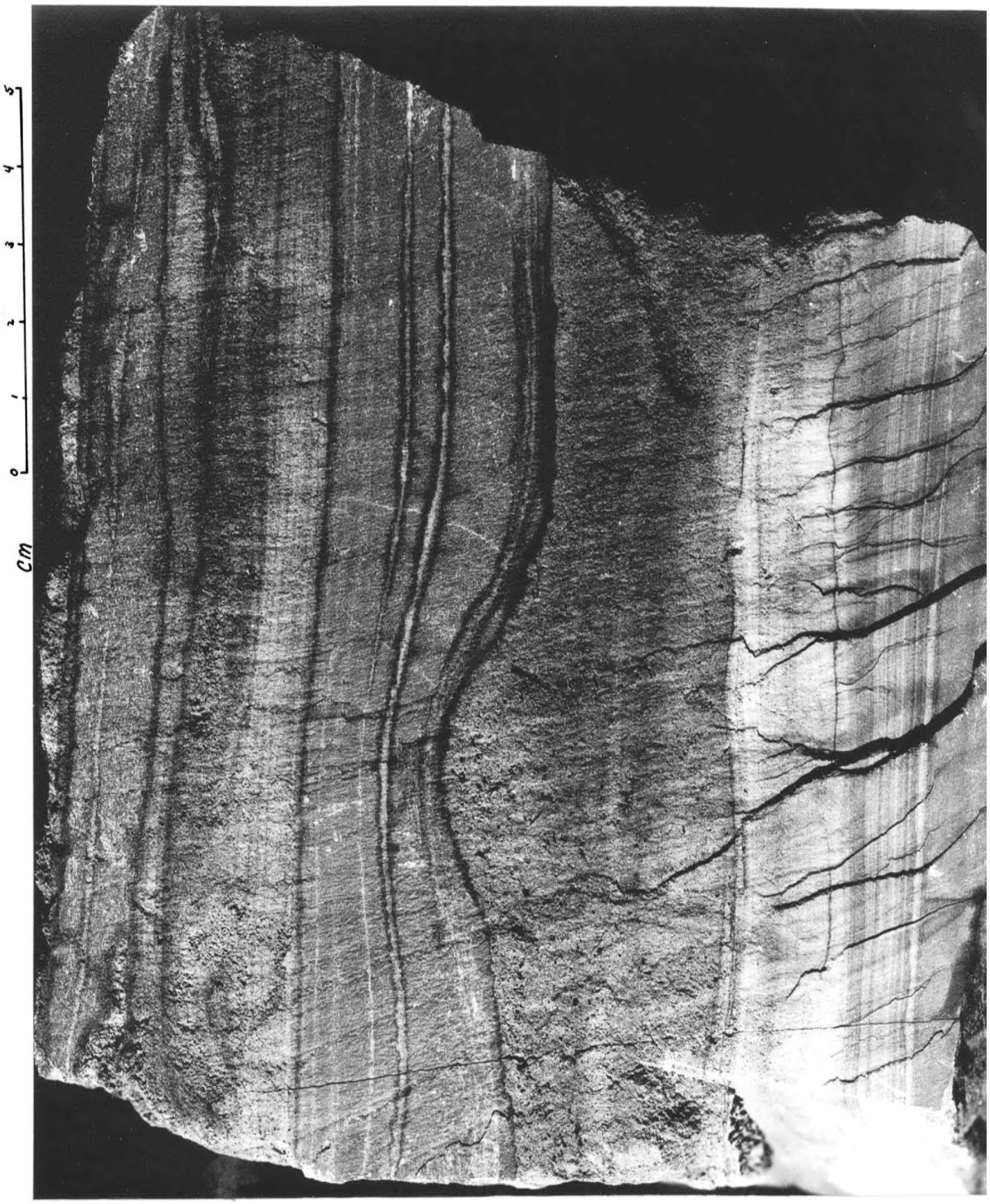
0
1
2
3
4
5
cm

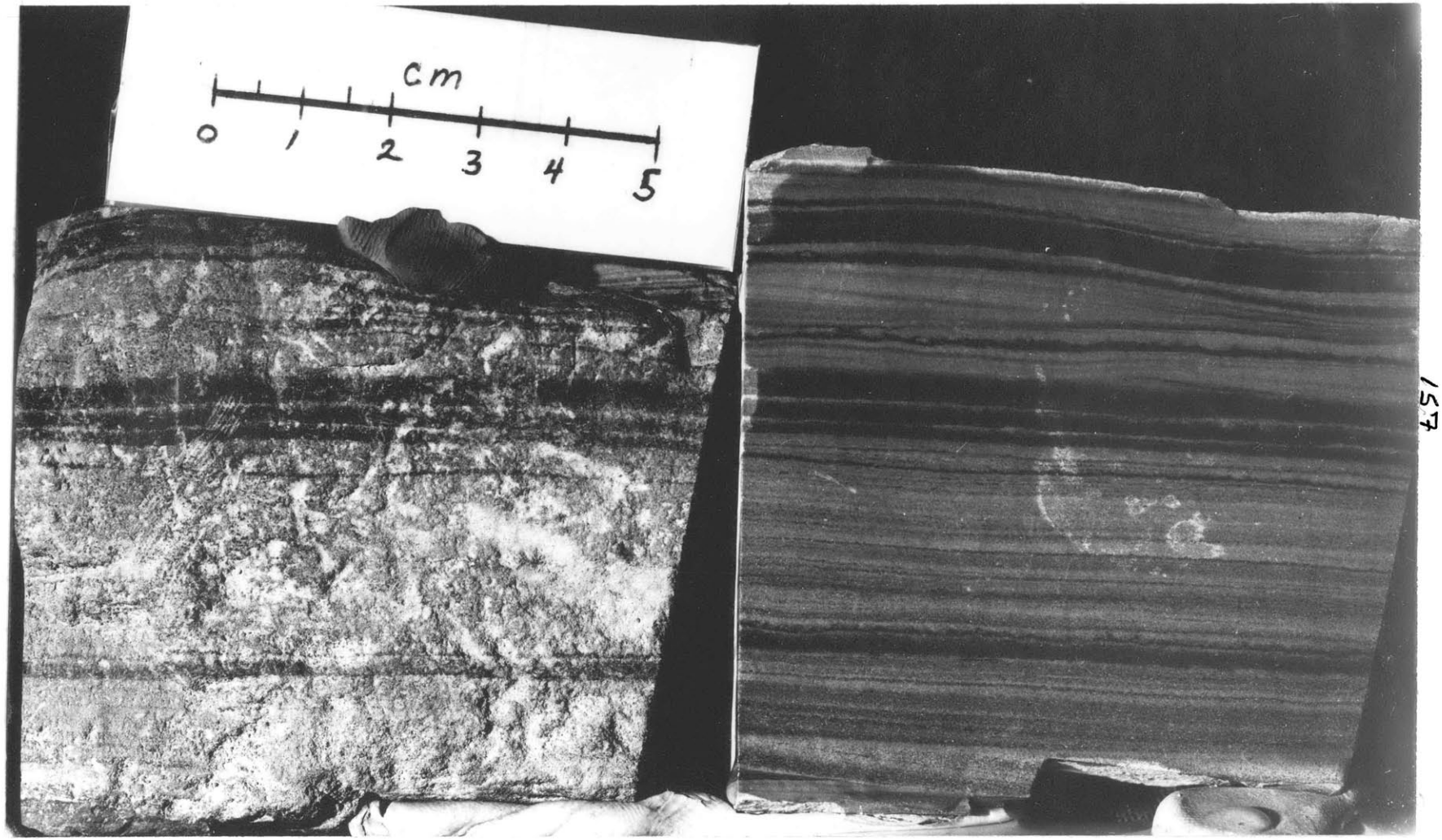

Photo 32

Field Sample From Locality 7

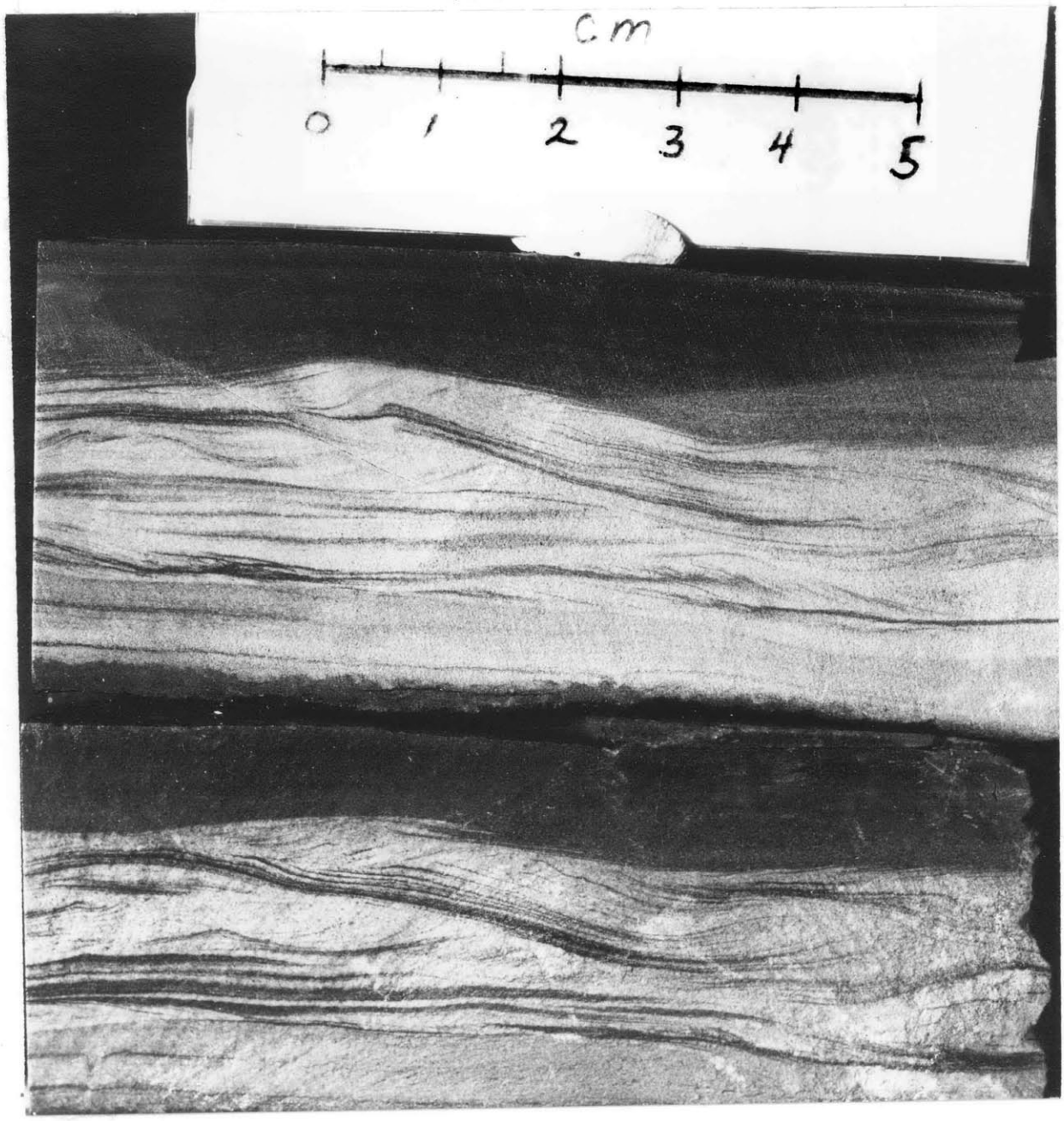

Photo 33

Field Sample 2 Locality 11

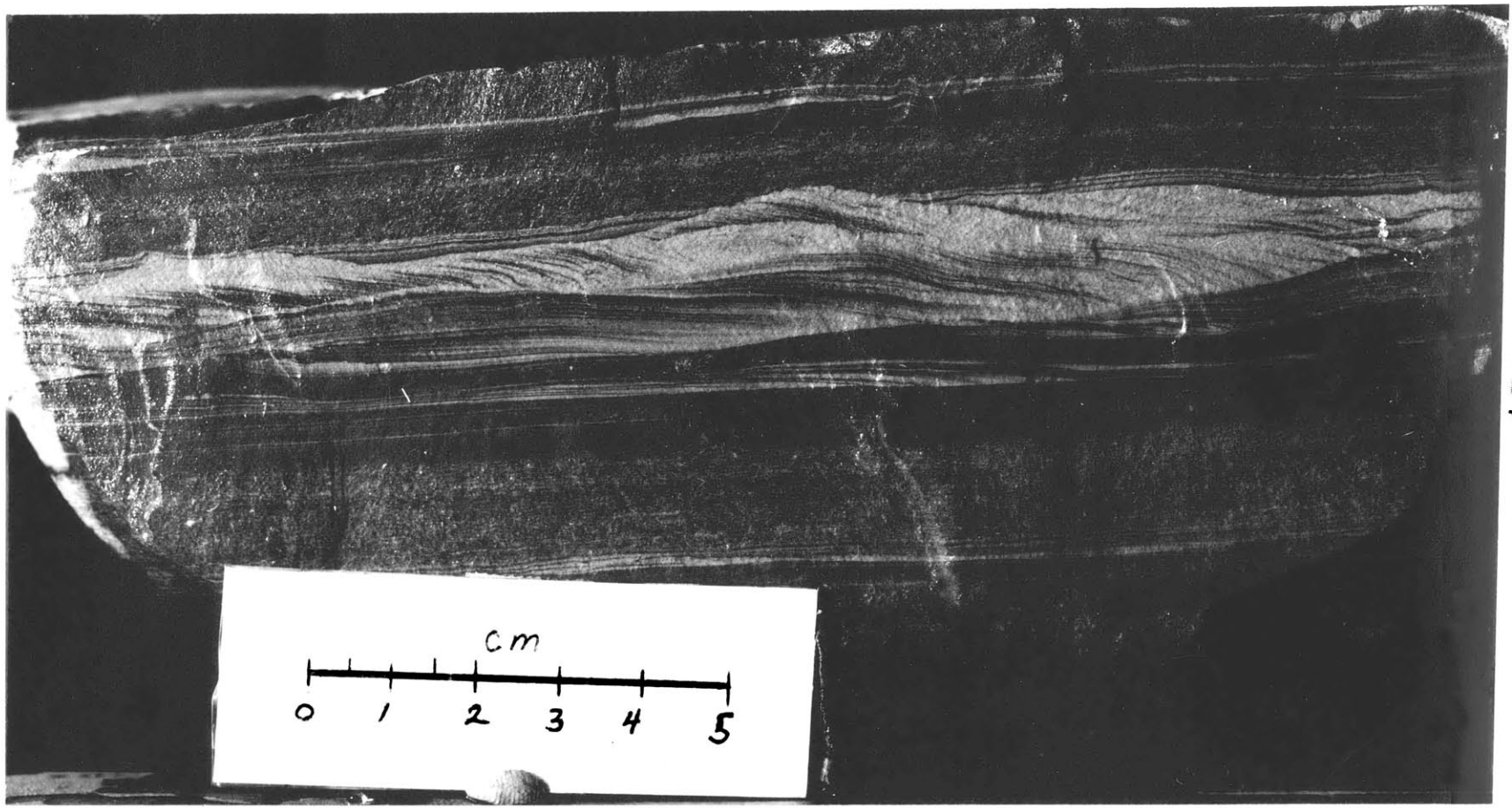

159

Photo 34

Field Sample 2 Locality 4

ACKNOWLEDGMENTS

The author wishes to thank the many people and organizations the helped make this thesis possible.

While a graduate student at M.I.T. the author received support from a part-time Research Assistantship in the Department of Earth and Planetary Sciences.

Thesis expenses were provided by The Petroleum Research Fund of the American Chemical Society, Grant No. PRF #5337-AC2.

Dr. John B. Southard suggested the subject of the investigation, provided the sediment and the laboratory, and gave much of his time in helpful discussions during the course of the work. The author, however, takes full responsibility for any errors in content or other idiocies that may occur.

Without the help of Mrs. Chris Stesky the author would have never been able to untangle his petty cash and purchase order records.

Special appreciation is expressed to Dr. David C. Roy of Boston College who suggested the various field localities visited in Maine for the gathering of samples.

Finally, the author would like to thank everyone on the 10th floor of M.I.T.'s Building 54 for tolerating an incredible amount of highly pervasive dust produced by drying silt.

###

UNITED STATES
DEPARTMENT OF THE INTERIOR
GEOLOGICAL SURVEY

STATE OF MAINE
REPRESENTED BY THE
PUBLIC UTILITIES COMMISSION

ASHLAND QUADRANGLE
MAINE - AROOSTOOK CO.
15-MINUTE SERIES (TOPOGRAPHIC)

FORT KENT 40 MI.
PORTAGE 1 MI.

(WINTERVILLE)
(PORTAGE)
(CARIBOU)

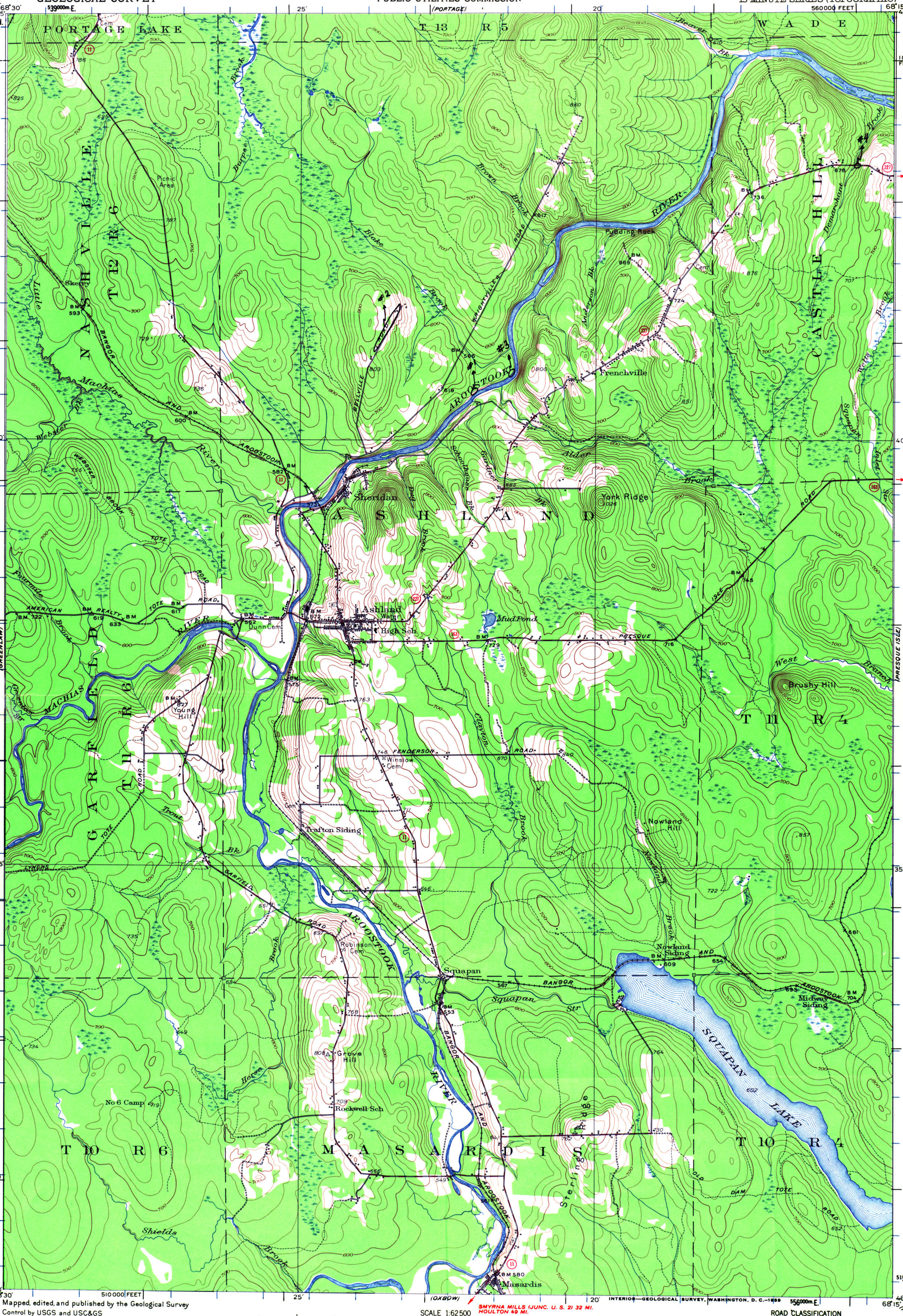

#4 Jemtland Fm. Small Rd. Cut.

#1 MADAWASKA LAKE Fm. exposure on River BANK.

#2 Jemtland Fm. exposures Along Rd.

#3 Aroostook River Fm. exposure on River BANK.

SMYRNA MILLS (JUNC. U. S. 2) 32 MI.
HOULTON 49 MI.

(GRAND LAKE SEBOEIS)
(HOWE BROOK)

INTERIOR—GEOLOGICAL SURVEY, WASHINGTON, D. C.—1959

Mapped, edited, and published by the Geological Survey
Control by USGS and USC&GS
Culture and drainage in part compiled from aerial photographs
Topography by plane-table surveys 1930-1931. Revised 1953
Polyconic projection. 1927 North American datum
10,000-foot grid based on Maine coordinate system, east zone
1000-meter Universal Transverse Mercator grid ticks, zone 19, shown in blue

APPROXIMATE MEAN DECLINATION, 1953

SCALE 1:62500

CONTOUR INTERVAL 20 FEET
DATUM IS MEAN SEA LEVEL

THIS MAP COMPLIES WITH NATIONAL MAP ACCURACY STANDARDS
FOR SALE BY U. S. GEOLOGICAL SURVEY, WASHINGTON 25, D. C.
A FOLDER DESCRIBING TOPOGRAPHIC MAPS AND SYMBOLS IS AVAILABLE ON REQUEST

QUADRANGLE LOCATION

ROAD CLASSIFICATION
Medium-duty
Light-duty
Unimproved dirt
State Route

ASHLAND, ME.
N4630-W6815/15

1953

UNITED STATES
DEPARTMENT OF THE INTERIOR
GEOLOGICAL SURVEY

STATE OF MAINE
REPRESENTED BY THE
PUBLIC UTILITIES COMMISSION

CARIBOU QUADRANGLE
MAINE—AROOSTOOK CO.
15 MINUTE SERIES (TOPOGRAPHIC)

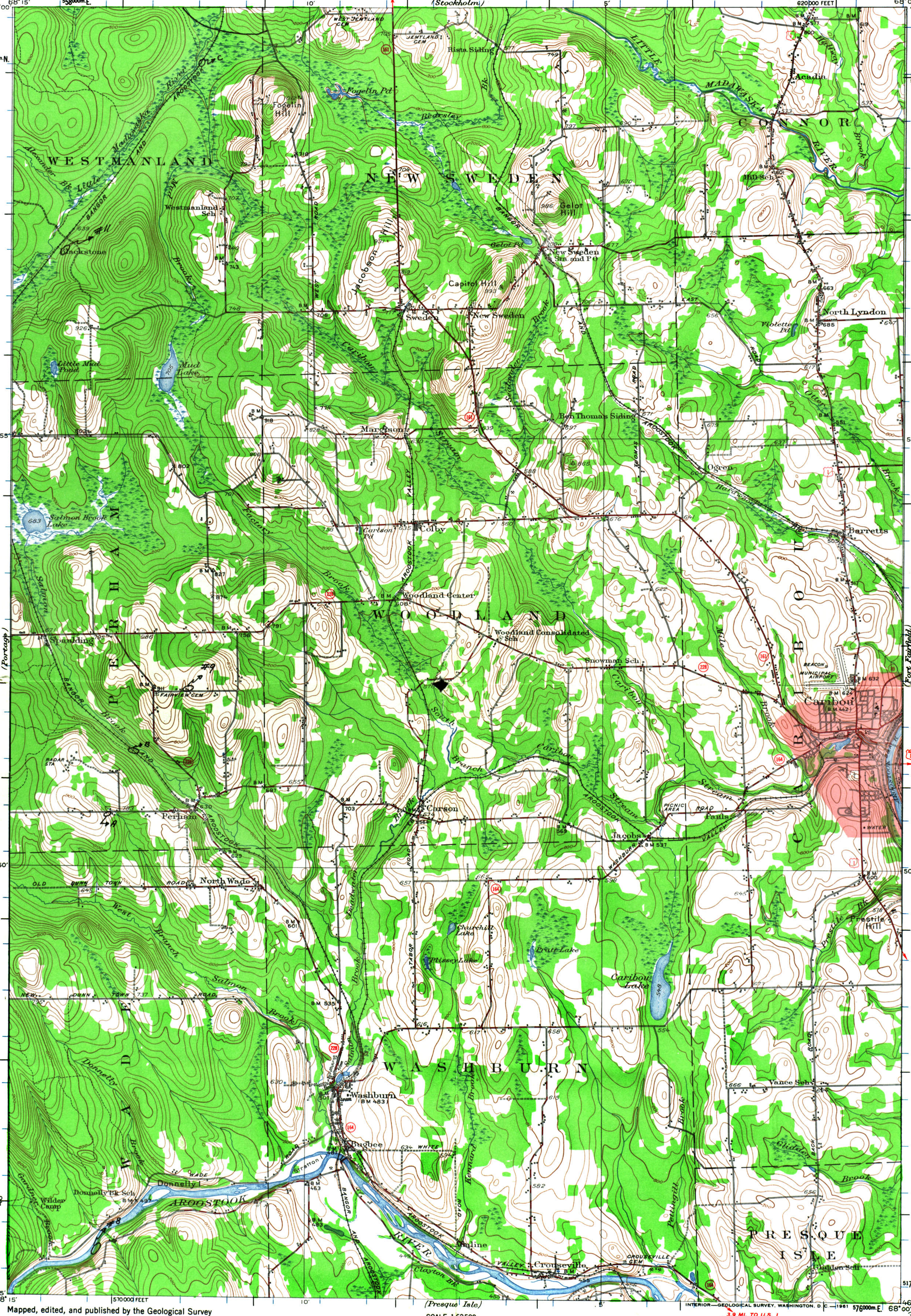

C Jemtland Fm. Exposed along RR. track

#11 Jemtland Fm. exposed in floor of quarry.

#9 Jemtland Fm. Road ditch exposures.

A Small quarry in Jemtland.

B Small RR cut exposing Jemtland Fm.

#8 Frenchville Fm. exposure along river bank

Mapped, edited, and published by the Geological Survey

Control by USGS and USC&GS

Culture and drainage in part compiled from aerial photographs
Topography by planetable surveys 1929. Revised 1953

Polyconic projection. 1927 North American datum
10,000-foot grid based on Maine coordinate system, east zone
1000-meter Universal Transverse Mercator grid ticks, zone 19, shown in blue

Red tint indicates area in which only landmark buildings are shown

APPROXIMATE MEAN DECLINATION, 1953

SCALE 1:62500

CONTOUR INTERVAL 20 FEET
DATUM IS MEAN SEA LEVEL

FOR SALE BY U. S. GEOLOGICAL SURVEY, WASHINGTON 25, D. C.
A FOLDER DESCRIBING TOPOGRAPHIC MAPS AND SYMBOLS IS AVAILABLE ON REQUEST

QUADRANGLE LOCATION

ROAD CLASSIFICATION
Heavy-duty — Light-duty
Medium-duty — Unimproved dirt
U. S. Route — State Route

CARIBOU, ME.
N4645—W6800/15
1953

UNITED STATES
DEPARTMENT OF THE INTERIOR
GEOLOGICAL SURVEY

STATE OF MAINE
REPRESENTED BY THE
PUBLIC UTILITIES COMMISSION

PORTAGE QUADRANGLE
MAINE-AROOSTOOK CO
15 MINUTE SERIES (TOPOGRAPHIC)

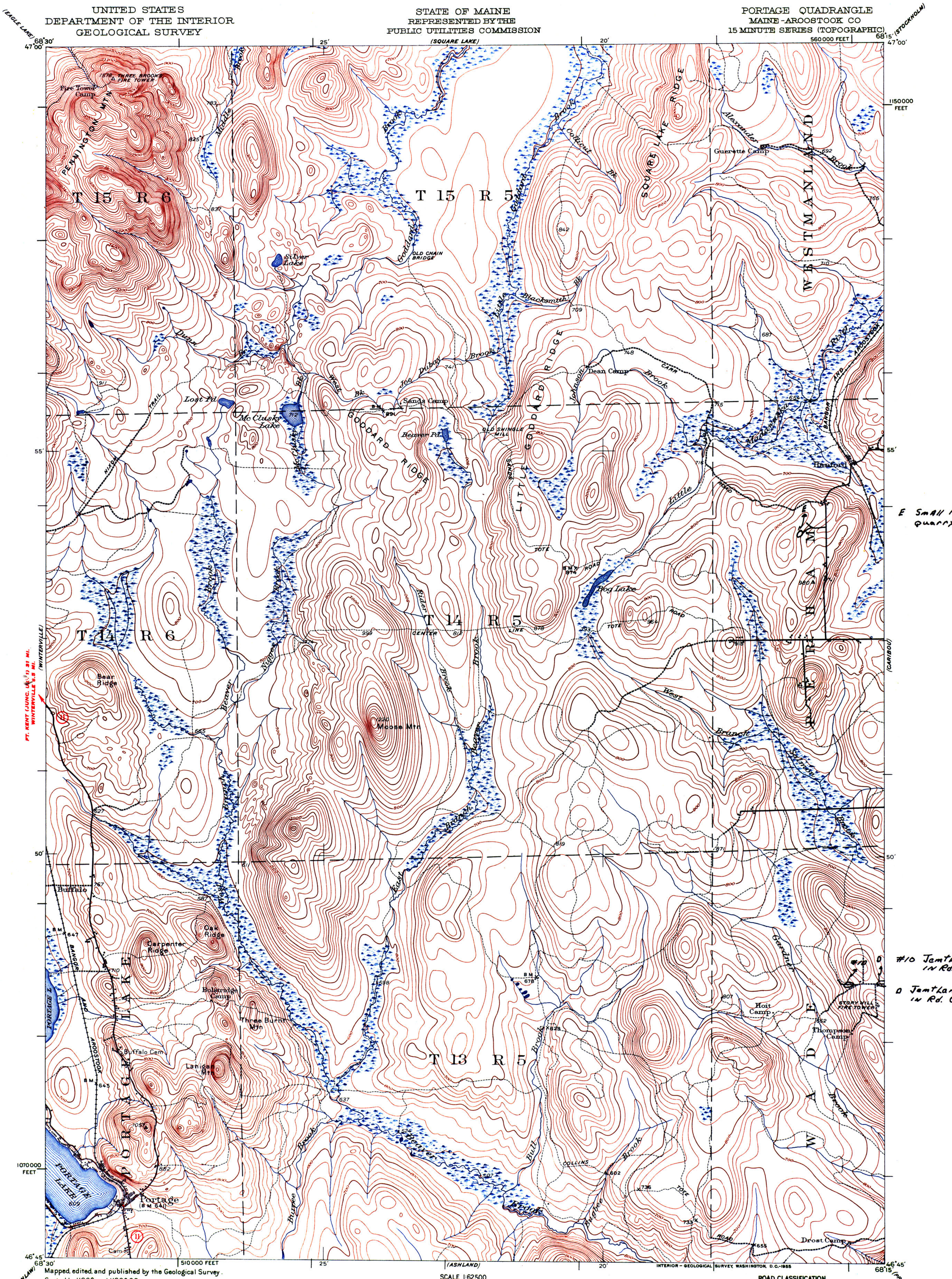

E Small Fogkin Hill Fm. quarry.

#10 Jemtland Fm. in Rd. Ditch

D Jemtland Fm in Rd. Cut.

Mapped, edited, and published by the Geological Survey.
Control by USGS and USC&GS
Topography by plane-table surveys 1929. Revised 1953
Polyconic projection. 1927 North American datum
10,000-foot grid based on Maine coordinate system, east zone

ASHLAND 10 MI.
PATTEN 59 MI.

SCALE 1:62500

1 ½ 0 1 2 3 4 MILES

3000 0 3000 6000 9000 12000 15000 18000 21000 FEET

1 .5 0 1 2 3 4 5 KILOMETERS

CONTOUR INTERVAL 20 FEET
DATUM IS MEAN SEA LEVEL

21½° TRUE NORTH MAGNETIC NORTH
APPROXIMATE MEAN DECLINATION, 1953

THIS MAP COMPLIES WITH NATIONAL MAP ACCURACY STANDARDS
FOR SALE BY U. S. GEOLOGICAL SURVEY, WASHINGTON 25, D. C.
A FOLDER DESCRIBING TOPOGRAPHIC MAPS AND SYMBOLS IS AVAILABLE ON REQUEST

ROAD CLASSIFICATION
Heavy-duty 4 LANE | 6 LANE Light-duty
Medium-duty 4 LANE | 6 LANE Unimproved dirt
U. S. Route State Route

MAINE
QUADRANGLE LOCATION

PORTAGE, ME.
N4645-W6815/15
1953

UNITED STATES
DEPARTMENT OF THE INTERIOR
GEOLOGICAL SURVEY

STATE OF MAINE
REPRESENTED BY THE
PUBLIC UTILITIES COMMISSION

PRESQUE ISLE QUADRANGLE
MAINE - AROOSTOOK CO
15 MINUTE SERIES (TOPOGRAPHIC)

#7 Jemtland Fm. Exposure on River Bank.

#5 Jemtland Fm. Rd. cut.

#6 Jemtland Fm. Small Rd. cut.

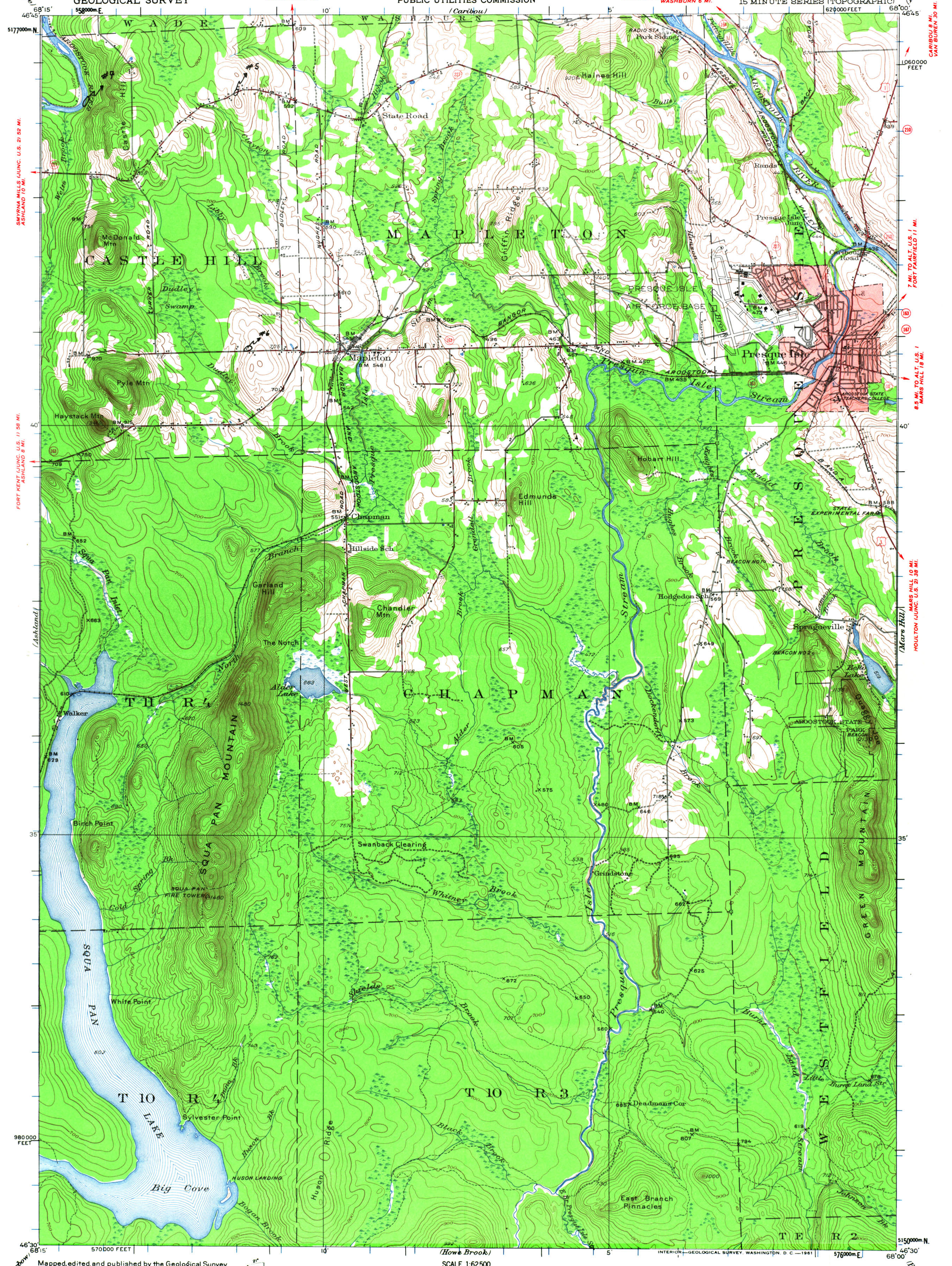

Mapped, edited, and published by the Geological Survey
Control by USGS and USC&GS

Culture and drainage in part compiled from aerial photographs
Topography by plane-table surveys 1932. Revised 1953

Polyconic projection. 1927 North American datum
10,000-foot grid based on Maine coordinate system, east zone
1000-meter Universal Transverse Mercator grid ticks, zone 19, shown in blue

Red tint indicates areas in which only landmark buildings are shown

APPROXIMATE MEAN DECLINATION, 1953 (TRUE NORTH, MAGNETIC NORTH, 21°)

SCALE 1:62500

1 ½ 0 1 2 3 4 MILES

3000 0 3000 6000 9000 12000 15000 18000 21000 FEET

1 .5 0 1 2 3 4 5 KILOMETERS

CONTOUR INTERVAL 20 FEET
DATUM IS MEAN SEA LEVEL

THIS MAP COMPLIES WITH NATIONAL MAP ACCURACY STANDARDS
FOR SALE BY U. S. GEOLOGICAL SURVEY, WASHINGTON 25, D. C.
A FOLDER DESCRIBING TOPOGRAPHIC MAPS AND SYMBOLS IS AVAILABLE ON REQUEST

MAINE
QUADRANGLE LOCATION

ROAD CLASSIFICATION

Heavy-duty
Light-duty
Medium-duty
Unimproved dirt
U. S. Route
State Route

PRESQUE ISLE, ME.
N4630-W6800/15

1953

UNITED STATES
DEPARTMENT OF THE INTERIOR
GEOLOGICAL SURVEY

STATE OF MAINE
REPRESENTED BY THE
PUBLIC UTILITIES COMMISSION

SQUARE LAKE QUADRANGLE
MAINE - AROOSTOOK CO.
15 MINUTE SERIES (TOPOGRAPHIC)

FORT KENT
SAINT AGATHA
FRENCHVILLE
MADAWASKA
LONG LAKE
MUD LAKE
CROSS LAKE
SQUARE LAKE
EAGLE LAKE
WESTMANLAND
T 17 R 5
T 17 R 4
T 16 R 6
T 16 R 5
T 16 R 4
T 15 R 6
T 15 R 5

Black Lake
Daigle Pond
Daigle
Ouellette
St Agatha
Carriveau Mill
Bickey Pond
Sinclair
Guerette
Austin Camp
Marrimony Pt
Dinah Pt
Cranberry Pt
Abraham Pt
Burnt Landing
Swede Pt
Rocky Pt
Limestone Pt
Michaud Camp
The Ledge
The Carry
Barstow Pt
Salmon Pt
Fraser Camp
Gorfinkle Camp
California Pond
Little California Pond
Harriman Pond
Carry Pond
Three Brooks Cove
Goddard Cove

O Jemtland Fm. exposed poorly on Hill.

Mapped, edited, and published by the Geological Survey

Control by USGS, USC&GS, and International Boundary Commission

Topography by plane-table surveys 1927, Revised 1953

Polyconic projection. 1927 North American datum
10,000-foot grid based on Maine coordinate system, east zone
1000-meter Universal Transverse Mercator grid ticks, zone 19, shown in blue

SCALE 1:62500

CONTOUR INTERVAL 20 FEET
DATUM IS MEAN SEA LEVEL

APPROXIMATE MEAN DECLINATION, 1953

ROAD CLASSIFICATION
Medium-duty
Light-duty
Unimproved dirt
State Route

QUADRANGLE LOCATION

THIS MAP COMPLIES WITH NATIONAL MAP ACCURACY STANDARDS
FOR SALE BY U. S. GEOLOGICAL SURVEY, WASHINGTON 25, D. C.
A FOLDER DESCRIBING TOPOGRAPHIC MAPS AND SYMBOLS IS AVAILABLE ON REQUEST

INTERIOR—GEOLOGICAL SURVEY, WASHINGTON, D. C.—1963
IMR 4328

SQUARE LAKE, ME.
N4700-W6815/15
1953

UNITED STATES
DEPARTMENT OF THE INTERIOR
GEOLOGICAL SURVEY

STATE OF MAINE
REPRESENTED BY THE
PUBLIC UTILITIES COMMISSION

STOCKHOLM QUADRANGLE
MAINE - AROOSTOOK CO
15 MINUTE SERIES (TOPOGRAPHIC)

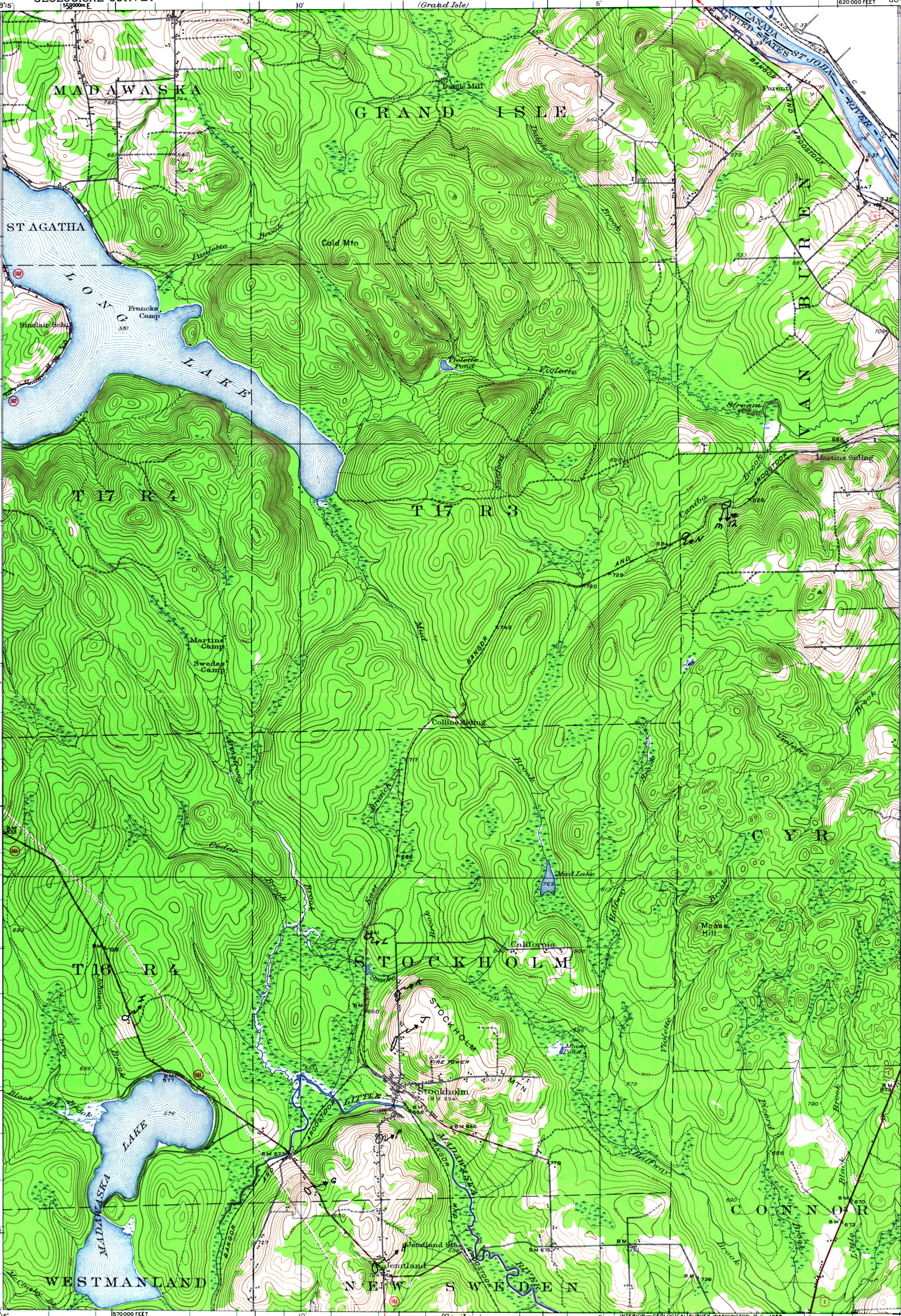

m+N } Jemtland Fm. in RR. cuts.

#12 Re-examination of m + Sample Taken

F Rd. cut Exposure of Fogelin Hill Fm.

G Quarry in Jemtland Fm.

H Jemtland Fm. Exposure.

I Madawaska Lake Fm. Exposure.

J Aquagene Tuff Turbidity current origin?

K Jemtland Fm. Road ditch Exposures

L Frenchville Fm. Exposed.

(Portage) (Ft Fairfield)

CARIBOU 15 MI.
PRESQUE ISLE 28 MI.

CARIBOU 10 MI.
PRESQUE ISLE 23 MI.

Mapped, edited, and published by the Geological Survey

Control by USGS, USC&GS, and International Boundary Commission

Topography by plane-table surveys 1927. Revised 1953

Polyconic projection. 1927 North American datum

10,000-foot grid based on Maine coordinate system, east zone

1000-meter Universal Transverse Mercator grid ticks, zone 19, shown in blue

APPROXIMATE MEAN DECLINATION, 1953

SCALE 1:62500

CONTOUR INTERVAL 20 FEET
DATUM IS MEAN SEA LEVEL

INTERIOR—GEOLOGICAL SURVEY, WASHINGTON, D. C.—1958

ROAD CLASSIFICATION

Heavy-duty — Light-duty
Medium-duty — Unimproved dirt
U. S. Route — State Route

QUADRANGLE LOCATION

THIS MAP AVAILABLE WITH OR WITHOUT SHADED RELIEF OVERPRINT
FOR SALE BY U. S. GEOLOGICAL SURVEY, WASHINGTON 25, D. C.
A FOLDER DESCRIBING TOPOGRAPHIC MAPS AND SYMBOLS IS AVAILABLE ON REQUEST

STOCKHOLM, ME.
N 4700—W 6800/15
1953

#13 Siegas Quarry - gw, cgl, distal Jemtland.

P Extensive Jemtland Fm. in Rd. Ditches.

Q Jemtland Fm. Road cuts.

UNITED STATES
DEPARTMENT OF THE INTERIOR
GEOLOGICAL SURVEY

UNITED STATES
DEPARTMENT OF THE ARMY
CORPS OF ENGINEERS

MAINE
(AROOSTOOK COUNTY)
VAN BUREN QUADRANGLE

1 240 000 FEET

Topography by W. K. Mc Kinley, W. F. Chenault, J. O. Kilmartin, S. L. Parker, and International Boundary Commission
Culture and drainage in part compiled from aerial photographs taken by Air Corps, U.S. Army
Surveyed in 1931
Revised in 1951

ROAD CLASSIFICATION

Heavy-duty — Light-duty
Medium-duty — Unimproved dirt
U. S. Route — State Route

(Caribou 7377 I)
(Stockholm) 7378 II
(Fort Fairfield) 7477 IV

SCALE 1:62500

CONTOUR INTERVAL 20 FEET
DATUM IS MEAN SEA LEVEL

Polyconic projection. 1927 North American datum
10,000-foot grid based on Maine (East) rectangular coordinate system
1000-meter Universal Transverse Mercator grid ticks, zone 19, shown in blue

UTM GRID AND 1951 MAGNETIC NORTH DECLINATION AT CENTER OF SHEET

VAN BUREN, ME.
N 4700—W 6745/15
1951
AMS 7478 III—SERIES V711

FOR SALE BY U. S. GEOLOGICAL SURVEY, WASHINGTON, D. C. 20242
A FOLDER DESCRIBING TOPOGRAPHIC MAPS AND SYMBOLS IS AVAILABLE ON REQUEST

INTERIOR—GEOLOGICAL SURVEY, WASHINGTON, D. C.—1970